

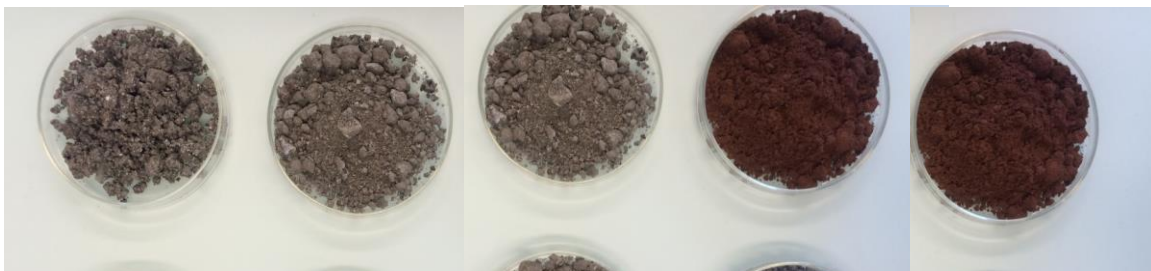


# Empa

Materials Science and Technology

## Nanomaterials in Landfills

### Module 2: Nanomaterials in landfill leachate



*Selection of municipal solid waste incineration (MSWI) residues, sludge and fly ashes collected in ZAB Deponie in Flawil, Switzerland used to prepare leachates. From left to right: Fresh MSWI bottom ash, 2 month old MSWI bottom ash, 1 year old MSWI bottom ash, sludge incineration residue and fly ash.*

Im Auftrag des Bundesamtes für Umwelt (BAFU)

St. Gallen, 4. April 2017

## **Impressum**

**Auftraggeber:** Bundesamt für Umwelt (BAFU), Abt. Abfall und Rohstoffe, CH-3003 Bern

**Auftragnehmer:** EMPA- Swiss Federal Laboratories for Materials Science and Technology  
Environmental Risk Assessment and Management Group

**Autoren:** Dr. Denise Mitrano, Prof. Dr. Bernd Nowack

EMPA- Swiss Federal Laboratories for Materials Science and Technology  
Environmental Risk Assessment and Management Group  
Lerchenfelstrasse 5  
CH-9014 St. Gallen

Xu He, Prof. Dr. Jing Wang

Advanced Analytical Technologies Laboratory  
EMPA  
Überlandstrasse 129,  
8600, Dübendorf

**Datum:** 4. April 2017

**Begleitung BAFU:** Dr. David Hiltbrunner

**Zitation** Mitrano, D.; He, X.; Wang, J.; Nowack, B. Nanomaterials in Landfills. Module 2: Nanomaterials in landfill leachate. Empa St. Gallen, 2017.

**Hinweis:** Diese Studie wurde im Auftrag des Bundesamtes für Umwelt (BAFU) verfasst. Für den Inhalt ist allein der Auftragnehmer verantwortlich.

## Table of Contents

|   |    |
|---|----|
| Zusammenfassung.....  | 4  |
| Executive Summary .....   | 7  |
| Résumé.....   | 10 |
| Publications.....   | 13 |
| Chapter 1: Mobility of metallic (nano)particles in leachates from landfills containing waste incineration residues .....  | 14 |
| Chapter 2: Aggregation and Particle Mass Distribution of nano-Au in Incineration Landfill Leachates.....  | 35 |
| Chapter 3: Agglomeration potential of TiO <sub>2</sub> in synthetic leachates made from the fly ash of different incinerated wastes .....   | 57 |
| Appendix 1: Supplemental Information: Mobility of metallic (nano)particles in leachates from landfills containing waste incineration residues .....   | 74 |
| Appendix 2: Supplemental Information: Improvements in Nanoparticle Tracking Analysis to Measure Particle Aggregation and Mass Distribution: A Case Study on Engineered Nanomaterial Stability in Incineration Landfill Leachates..... | 86 |
| Appendix 3: Supplemental Information: Agglomeration potential of TiO <sub>2</sub> in synthetic leachates made from the fly ash of different incinerated wastes .....  | 89 |

## Zusammenfassung

Die Modellierung der Massenflüsse von künstlich hergestellten Nanomaterialien (ENM) von der Produktion bis zur Entsorgung hat gezeigt, dass ein grosser Teil der Nanomaterialien schlussendlich in Deponien landet. Wie in vielen anderen Europäischen Ländern wird in der Schweiz der Siedlungsabfall verbrannt und die übrigbleibende Schlacke in speziellen Deponien abgelagert, zusammen mit Rückständen aus der Rauchgasreinigung und den Aschen aus der Klärschlammverbrennung. Die Nanomaterialien in den Siedlungsabfällen werden über die Verbrennungsrückstände in Deponien transferiert und können von dort potenziell über das Sickerwasser in die Umwelt gelangen. Während die Freisetzung von Nanomaterialien und deren Verhalten während des Gebrauchs von Produkten schon recht gut untersucht ist, wurde bis jetzt das Verhalten von Nanomaterialien am Ende des Produktzyklus, wie z.B. in der Deponie, nur wenig untersucht. Zudem gibt es bis anhin auch keine Untersuchungen über die Herkunft der Nanomaterialien in den Deponien. Das heisst dass man nicht genau weiss, welche der Nanomaterialien künstlich hergestellt wurden (ENM), welche Nanomaterialien natürlichen Ursprungs sind und welche Nanomaterialien als Nebenprodukte bei der Verbrennung entstanden. Gerade Verbrennungsprozesse sind bekannt dafür, dass eine Vielzahl von nanoskaligen Materialien entstehen, weshalb wir Nanomaterialien in Deponien auch in Abwesenheit von künstlichen Nanomaterialflüssen erwarten. Die derzeitige Situation von künstlichen Nanomaterialien und natürlichen kolloidalen Partikeln im Deponiesickerwasser muss daher in einen grösseren Zusammenhang gestellt werden um zu verstehen,

- 1) ob derzeit ein Fluss von künstlichen Nanomaterialien in Deponien und eventuell ins Sickerwasser vorhanden ist,
- 2) wie sich die Konzentration und die Charakteristika der künstlichen Nanomaterialien in Deponien von den natürlichen unterscheiden und
- 3) wie die Mobilität der Partikel sich zu möglichen Flüssen von künstlichen Nanopartikeln in die Umwelt verhält.

Um diese Fragen anzugehen, wurden drei Studien an der Empa durchgeführt. In der ersten Studie ging es darum, die kolloidalen metallischen Partikel zu untersuchen, welche derzeit von Deponien für KVA-Schlacken und Klärschlammaschen emittiert werden. Mit der Charakterisierung der partikulären Bestandteile, welche aus verschiedenen Schlacken und Aschen freigesetzt wurden und welche im Deponiesickerwasser unserer untersuchten Deponie in Flawil enthalten sind, konnten wir die chemischen und physikalischen Eigenschaften der kolloidalen und nanopartikulären Fraktion bestimmen. Weil wir Schlacken mit verschiedenem Alter verwendet haben, konnten wir geochemische Mechanismen identifizieren, welche für die Freisetzung von Partikeln während der Alterung verantwortlich sind.

Um die Stabilität von Nanopartikeln im Sickerwasser besser zu verstehen, führten wir eine separate Studie durch, in welcher wir Nanoparticle Tracking Analysis (NTA) verwendeten, um die Agglomeration der Nanopartikel im Sickerwasser zu verfolgen. Durch Messung der Stabilität eines Referenzpartikels in verschiedenen synthetischen und natürlichen Sickerwässern konnten wir Partikelgrösse, -anzahl und – Masse miteinander in Verbindung bringen und so das Verhalten von Partikeln im Sickerwasser besser verstehen.

In der dritten Studie untersuchten wir die Stabilität von nano-TiO<sub>2</sub> im Eluat von Flugasche und bestimmten so die grundlegenden Faktoren, welche Agglomeration und Sedimentation beeinflussen, mit einem speziellen Fokus auf pH und Ionenstärke.

An verschiedenen Daten wurde Sickerwasser in der Deponie Flawil gesammelt und Proben von verschieden alten Schlacken genommen. Von den Schlacken wurden im Labor Eluate gemäss Standardmethoden produziert. Messbare Konzentrationen von Partikeln wurden sowohl in den Schlackeneluat als auch im Sickerwasser gefunden, sowohl im kolloidalen (bis 1 µm) als auch im Nanobereich (bis 100 nm). Obwohl viele dieser Partikel die gleiche Zusammensetzung wie die meistverwendeten künstlichen Nanopartikel hatten (z.B. Ti, Zn, Cu, Fe, Ag, Ce), können wir nicht bestimmen, ob diese Partikel tatsächlich als künstliche Nanomaterialien in die Deponie gelangten, von Pigmenten stammen (z.B. Pigment TiO<sub>2</sub>) oder als Nebenprodukt der Verbrennung entstanden sind. Unter dem Elektronenmikroskop wurde ersichtlich, dass viele der Partikel Agglomerate von verschiedenen, metallhaltigen Partikeln sind, was darauf hindeutet, dass sie während der Verbrennung entstanden sind. Viele der Partikel waren mit einer Silikatmatrix (d.h. Glas) verbunden, welche als „Klebstoff“ für die Metalle in den Partikeln wirkte. Die Partikelkonzentrationen, welche in dieser Studie bestimmt wurden, können erste Anhaltspunkte über die Grössenordnung von nanoskaligen Partikeln im Sickerwasser von Deponien für Schlacken liefern. Über mehrere Probenahmen hinweg zeigte das Sickerwasser eine ähnliche Wasserchemie und Partikelmenge. Dagegen zeigten Schlacken verschiedenen Alters ein unterschiedliches Freisetzungsverhalten für partikuläre Metalle, was darauf hindeutet, dass sich die Mobilität der unterschiedlichen Partikel in Laufe des Verwitterungsprozesses verändert. Der sinkende pH beeinflusst die Silikatmatrix, welche der dominierende Faktor für die Metallfreisetzung und die Partikelmobilität ist.

Die Experimente über die Stabilität der Nanopartikel im Sickerwasser erlauben uns, besser zu verstehen, unter welchen Bedingungen die Partikel stabil sind. Mit der Verwendung von Goldnanopartikeln als Testsubstanz (in höherer Konzentration als unter umweltrelevanten Bedingungen) konnten wir beobachten, dass sich über einen Zeitraum von wenigen Stunden Agglomerate bildeten, welche aber in der Lösung suspendiert blieben und nicht sedimentierten. Die Interaktion der zugegebenen Nanopartikel mit den natürlichen Partikeln, welche im Sickerwasser enthalten sind, war der bestimmende Faktor für das Verhalten der Nanopartikel. Die Experimente mit TiO<sub>2</sub> Partikeln zeigten, dass unter den gewählten Bedingungen eine schnelle Agglomeration auftrat, welche die Suspension destabilisierte und zur Sedimentation der Partikel führte.

Die Abschätzung, wie der Zufluss von Nanopartikel enthaltenden Materialien im Abfallstrom die Freisetzung von metallischen Partikeln aus der Deponie beeinflussen, wird ist eine komplexe Aufgabe. Es ist sicher, dass bereits natürlicherweise eine signifikante Menge an natürlich vorhandenen metallischen Nanopartikeln und Kolloiden im Sickerwasser enthalten sind, welche während des Verbrennungsprozesses gebildet wurden.

Da eine eindeutige Identifizierung von künstlichen Nanomaterialien nicht möglich war, ist es schwierig abzuschätzen, wie sich der Eintrag von künstlichen Nanomaterialien auf deren Präsenz im Sickerwasser auswirken wird. Dazu kommt noch, dass die Nanomaterialien während der Verbrennung und in der Deponie gealtert und transformiert werden, was sie den natürlicherweise vorhandenen Partikeln ähnlicher macht. Es gibt einen publizierten Fall, in dem die Gegenwart eines Nanomaterials in einem Abfallstrom direkt mit seiner Detektion im Sickerwasser korreliert war ( $\text{TiO}_2$  in Bauabfall), doch konnte in unserer Studie kein solcher Zusammenhang bestimmt werden.

Zusammenfassend können wir feststellen, dass für viele Metalle kolloidale und nanoskalige Partikel natürlicherweise im Sickerwasser vorliegen. Diese Fraktion ist durch die geochemischen Prozesse bedingt, welche die Glasmatrix der Schlacke über die Zeit verändert und dadurch Partikel freisetzt. Die mögliche Präsenz von künstlich hergestellten Nanomaterialien in Deponiesickerwasser muss immer in diesem Zusammenhang betrachtet werden.

## Executive Summary

The modeling of the flows of engineered nanomaterials (ENM) from production and use to the end-of-life phase has shown that a large share of all ENM are expected to end up in landfills. In Switzerland, as in many other European nations, waste is incinerated and the residual ash is deposited in specially designated landfills for municipal solid waste incineration (MSWI) residue along with fly ash and incineration residues from sewage sludge. ENM can thus be transferred from consumer waste to landfills and potentially be released to the environment through landfill leachate. However, while intense study has been given to release and fate of ENM during product usage, significantly less attention has been paid to ENM enabled products at the end of life stage, such as disposal.

There has been little linkage relating the characteristics or (potential) concentrations of ENM that end up in landfills to other natural or incidental (metallic) colloidal material that already exists in the landfill. Incineration processes are known to yield a wide variety of nanoscaled materials and therefore we expect the presence of nanomaterials in landfills even in the absence of flows of ENM. The current situation of both ENM and natural colloidal particles in the landfill leachate must be put into context to understand if;

- 1) There is currently an influx of ENM into MSWI residues and eventually landfill leachate,
- 2) How the concentration and characteristics of ENM in the landfills differ from natural metallic colloids that have always to some extent been in waste material and landfill leachate and
- 3) How the mobility of these particles could relate to potential influxes of (aged) ENM or other metallic colloids into the environment.

To tackle these questions, three main study initiatives were conducted at Empa. The first of these aimed to determine the metallic colloidal material that is currently being emitted from landfills for MSWI residues and sewage incineration residues. By characterizing particulate matter that leached from a number of different ashes as well as the natural leachate from our study landfill in Flawil, we could estimate the chemical and physical characteristics of the total nano- and colloidal materials emitted. Since different aged ash was used, we could additionally suggest geo-chemical reasons for the (im)mobility of these particles as the landfill ages.

To better approximate the stability of ENM in landfill leachates we conducted a separate study that focused on using Nanoparticle Tracking Analysis (NTA) to follow the agglomeration of ENM in landfill leachates. By measuring the stability of a reference particle in various synthetic and natural leachate solutions, we could link the metrics of particle size, number and analyte mass to better understand the movement of particles in the system and suggest how stable ENM may be in the landfill. Finally, the stability of nano

TiO<sub>2</sub> was investigated in fly ash leachate to determine the governing factors of agglomeration and sedimentation of the ENM in that system, with specific focus on pH and ionic strength.

At several dates leachate was collected at the Flawil landfill and samples from the differently-aged ashes deposited at the landfill were taken. From the ashes a leachate was produced in the lab using standard procedures. There were detectable concentrations of particulate matter leached from the MSWI ash residues as well as in the natural landfill leachate in both the nano and colloidal size ranges. While a number of these particles were of the same composition than the most commonly used ENM in consumer products (e.g. Ti, Zn, Cu, Fe, Ag, Ce) we could not ascertain if these were initially ENM that were disposed of in the waste, were originating from conventional materials (e.g. pigment TiO<sub>2</sub>) or were incidental metallic particles that were formed as a byproduct of the incineration process itself. However, when imaged under TEM many of the particles were seemingly agglomerates of several different metal-containing particles, suggesting that they were formed during incineration. Silica (i.e. glass) was also found to bind many particles together acting as a “glue” for the metals contained in the particles. Nevertheless, the values determined here are the first indications of the magnitude of nano sized particles released from landfills for incineration waste. Over multiple sampling dates, the natural leachate showed similar characteristics in terms of basic water chemistry as well as particle characteristics. However, MSWI bottom ash of different ages exhibited divergent leaching behavior indicating that as a landfill ages, different particles may become mobile due to landfill weathering which includes changing pH due to carbonation. This influences the silica matrix, which is a driving factor of metal leachability and therefore particulate mobility.

The experiments about the stability of ENM in landfill leachates allow us to understand better the potential of particles to be stable under landfill conditions. ENM that were suspended in the leachate had various degrees of stability. While using Au ENM as a tracer we observed that large agglomerates were formed over the course of several hours (albeit at higher than environmentally relevant concentrations), but the agglomerates remained suspended in solution. The interaction of the added ENM with the natural particles present in the leachates was the main factor determining the ENM fate. Conversely, TiO<sub>2</sub> aggregation occurred quickly under landfill leachate conditions and were unstable in solution.

Considering how the influx of ENM containing materials into the waste stream will affect the leaching of (metallic) particles from landfills is a complex task. Certainly there already exists a significant amount of incidental metallic nano and colloidal materials in the leachate that are formed during the waste incineration process. Since we are unable to define which of these materials were initially ENM, it is difficult to determine the proportional increase of nanomaterials leaching due to an increase in ENM containing products alone. Compounding this issue, since ENM themselves will also be aged and transformed during the waste incineration process, this may make these metals more similar to other metallic components that already exist in waste and subsequently in leachate. There have been some reported cases where a large influx of a particular nanomaterial in a given waste material has been directly



evident in the leachate (e.g. TiO<sub>2</sub> ENM in building material waste), but in this study this clear distinction of ENM above the “natural” background could not be determined.

Overall we can state that for many metals a nanosized fraction is naturally present in landfill leachate. This fraction is determined by the geochemical changes that the glass matrix of the ashes undergoes during weathering at the landfill. The possible presence of ENM in landfill leachate always has to be evaluated taking this context into consideration.

## Résumé

La modélisation des flux de nanomatériaux manufacturés (NMM) depuis leur production jusqu'à leur fin de vie a montré qu'une large proportion de tous les NMM sont supposés finir en décharges. En Suisse, comme dans beaucoup d'autres nations européennes, les déchets sont incinérés et les cendres résiduelles sont enfouies dans des décharges spécifiques pour l'enfouissement des résidus d'incinération des déchets solides municipaux (DSM), des poussières des fumées et des résidus d'incinération des boues d'épuration. Ainsi, les NMM peuvent être transférés des déchets municipaux vers les décharges et émis vers l'environnement dans les lixiviats de décharges. Toutefois, bien que les émissions et le devenir des NMM aient été largement étudiés à partir de la phase d'utilisation, la phase de fin de vie des nano-produits, dont l'élimination des déchets, a fait l'objet de beaucoup moins d'attention.

Peu de liens ont été faits entre les caractéristiques ou les concentrations potentielles des NMM présents en décharge et celles des autres matériaux colloïdaux (métalliques) qui existent déjà dans les décharges. Les procédés d'incinération sont connus pour générer une grande variété de matériaux à l'échelle nanométrique. On s'attend donc à la présence de nanomatériaux dans les décharges, y compris en l'absence de flux de NMM. La situation actuelle des NMM et des particules colloïdales naturelles dans le lixiviat de décharge doit être mise en perspective pour comprendre :

- 1) S'il y a aujourd'hui un flux de NMM entrant dans les résidus d'incinération des DSM, et donc dans les lixiviats de décharge,
- 2) Dans quelle mesure la concentration et les caractéristiques des NMM dans les décharges sont différentes de celles des colloïdes métalliques naturels qui ont toujours existé dans les déchets et les lixiviats de décharge et
- 3) Comment la mobilité de ces particules pourrait être liée aux flux potentiels des NMM (altérés) ou d'autres colloïdes métalliques dans l'environnement.

Pour répondre à ces questions, trois études principales ont été menées à l'Empa. La première avait pour but de définir le matériel colloïdal métallique qui est actuellement émis depuis les décharges spécifiques aux résidus d'incinération des DSM et des boues d'épuration. En caractérisant la matière particulaire qui a été lessivée à partir de différentes cendres ainsi que le lixiviat naturel de la décharge étudiée (située à Flawil), nous avons pu estimer les caractéristiques chimiques et physiques des nanomatériaux et des colloïdes totaux émis. Grâce à l'utilisation de cendres présentant différents stades d'altération, nous avons également pu proposer des mécanismes géochimiques pour expliquer la mobilité (ou l'immobilité) de ces particules à mesure que la décharge vieillit.

Pour mieux approcher la stabilité des NMM dans les lixiviats de décharge, nous avons mené une seconde étude, ciblée sur l'utilisation de l'analyse de suivi des nanoparticules (Nanoparticle Tracking Analysis – NTA) pour suivre l'agglomération des NMM dans les lixiviats de décharges. En mesurant la stabilité d'une particule de référence dans différentes solutions de lixiviats (synthétiques et naturel) nous avons pu faire le lien entre la taille, le nombre et la masse analysée des particules pour mieux comprendre leur mouvement dans le système et évaluer la stabilité des NMM dans la décharge.

Enfin, dans une troisième étude, la stabilité des NMM a été étudiée dans le lixiviat des poussières de fumées pour déterminer les facteurs gouvernant l'agglomération et la sédimentation des NMM dans ce système, en analysant tout particulièrement l'influence du pH et de la force ionique.

Le lixiviat de décharge a été collecté à différentes dates dans la décharge de Flawil. Des échantillons de cendres déposées dans la décharge et présentant différents stades d'altération (différents âges) ont également été recueillis. Des lixiviats ont été produits en laboratoire à partir de ces cendres, en suivant une procédure standard. La matière particulaire lessivée à partir des résidus d'incinération des DSM et celle du lixiviat naturel a été détectée dans les intervalles de tailles nanométrique et colloïdal. Alors que nombre de ces particules étaient de la même composition que les NMM les plus couramment utilisés dans les produits de consommation (par exemple Ti, Zn, Cu, Fe, Ag, Ce), nous n'avons pas pu déterminer avec certitude si elles provenaient de NMM présents dans les déchets tels qu'ils avaient été jetés, si elles provenaient de matériaux conventionnels (par exemple de TiO<sub>2</sub> pigmentaire) ou si elles avaient été formées pendant le processus d'incinération. Toutefois, l'imagerie de ces particules en MET a montré que beaucoup d'entre elles apparaissaient sous la forme d'agglomérats de plusieurs particules contenant différents métaux, suggérant qu'elles ont été formées pendant l'incinération. Il a aussi été observé que de la silice (c'est-à-dire du verre) liait beaucoup de ces particules, agissant comme une « colle » pour les métaux contenus dans les particules. Néanmoins, les valeurs déterminées dans cette étude sont les premières indications de la magnitude des émissions de particules nanométriques depuis les décharges spécifiques aux résidus d'incinération. Le lixiviat naturel a montré des caractéristiques similaires à différentes dates d'échantillonnage en termes de chimie de l'eau et de caractéristiques des particules. Toutefois, les cendres résiduelles d'incinération des DMS d'âges différents ont montré des comportements de lixiviation différents, indiquant qu'à mesure que la décharge vieillit, différentes particules peuvent être mobilisées par l'altération de la décharge, qui induit entre autres des variations de pH dus à la carbonatation. Ce processus engendre des changements dans la matrice de silice, qui est un facteur important agissant sur la lixiviation et donc sur la mobilité des particules.

Les expériences menées sur la stabilité des NMM dans les lixiviats de décharges nous ont permis de mieux comprendre le potentiel de stabilité des particules dans des conditions similaires à celles d'une décharge. Les NMM qui ont été mis en suspension dans le lixiviat présentaient différents degrés de stabilité. En utilisant des NMM d'or comme traceur, nous avons vu que de gros agglomérats étaient formés au cours de plusieurs heures (bien qu'à des concentrations plus élevées que celle attendues dans l'environnement), mais

les agglomérats sont restés en suspension. L'interaction des NMM ajoutés avec les particules naturelles présentes dans les lixiviats a été le facteur principal déterminant le devenir des NMM. Inversement, l'agrégation du  $\text{TiO}_2$  s'est produite rapidement dans des conditions similaires à celles de lixiviats de décharges : ces particules étaient instables en solution.

C'est une tâche complexe que de prendre en compte la façon avec laquelle les matériaux contenant des NMM dans le flux de déchets affectent la lixiviation des particules (métalliques) depuis les décharges. Il existe très certainement dans le lixiviat une quantité significative de matériaux métalliques nanométriques et colloïdaux qui ont été formés pendant le procédé d'incinération des déchets. Comme nous sommes incapables de déterminer la part de ces matériaux qui étaient initialement des NMM, il est difficile de déterminer la part de l'augmentation du lessivage des nanomatériaux qui est due à la seule augmentation des produits contenant des NMM. De plus, l'altération et la transformation des NMM pendant le procédé d'incinération pourrait rendre ces métaux plus proches des autres composés métalliques qui existent déjà dans les déchets, et donc dans le lixiviat. Dans certains cas, le flux important d'un nanomatériau particulier dans un type de déchet donné a été directement mis en évidence dans le lixiviat (par exemple des NMM de  $\text{TiO}_2$  dans des déchets de construction), mais la présence de NMM ajoutés au fonds géochimique « naturel » n'a pas pu être clairement déterminée dans cette étude.

En général, nous pouvons établir que pour beaucoup de métaux, une fraction nanométrique est naturellement présente dans le lixiviat de décharge. Cette fraction est déterminée par les changements géochimiques que la matrice de verre des cendres subit pendant son altération dans la décharge.

## Publications

The results presented in this report are part of the following publications:

### **Chapter 1: Mobility of metallic (nano)particles in leachates from landfills containing waste incineration residue.**

Denise M. Mitrano<sup>1</sup>, Kamyar Mehrabi<sup>1</sup>, Yadira Arroyo Rojas Dasilva<sup>2</sup>, Bernd Nowack<sup>1</sup>

1. Empa, Swiss Federal Laboratories for Materials Science and Technology, Technology and Society Laboratory, Lerchenfeldstrasse 5, 9014 St. Gallen, Switzerland
2. Empa, Swiss Federal Laboratories for Materials Science and Technology, Electron Microscopy Center, Ueberlandstrasse 129, 8600 Dübendorf, Switzerland

*Environmental Science: Nano* 4: 480-492 (2017)

### **Chapter 2: Improvements in Nanoparticle Tracking Analysis to Measure Particle Aggregation and Mass Distribution: A Case Study on Engineered Nanomaterial Stability in Incineration Landfill Leachates**

Denise M. Mitrano<sup>1</sup>, Kamyar Mehrabi<sup>1</sup>, Yadira Arroyo Rojas Dasilva<sup>2</sup>, Bernd Nowack<sup>1</sup>

3. Empa, Swiss Federal Laboratories for Materials Science and Technology, Technology and Society Laboratory, Lerchenfeldstrasse 5, 9014 St. Gallen, Switzerland
4. Empa, Swiss Federal Laboratories for Materials Science and Technology, Electron Microscopy Center, Ueberlandstrasse 129, 8600 Dübendorf, Switzerland

*Environmental Science and Technology*, under revision

### **Chapter 3: Agglomeration potential of TiO<sub>2</sub> in synthetic leachates made from the fly ash of different incinerated wastes**

Xu He<sup>1,2</sup>, Denise M. Mitrano<sup>3</sup>, Bernd Nowack<sup>3</sup>, Yeonkyoung Bahk<sup>1,2</sup>, Renato Figi<sup>2</sup>, Claudia Schreiner<sup>2</sup>, Melanie Bürki<sup>2</sup>, Jing Wang<sup>\*,1,2</sup>

<sup>1</sup>Institute of Environmental Engineering, ETH Zurich, Schafmattstrasse 6, 8093, Zurich, Switzerland

<sup>2</sup>Advanced Analytical Technologies Laboratory, EMPA, Überlandstrasse 129, 8600, Dübendorf, Switzerland

<sup>3</sup>Technology and Society Laboratory, EMPA, Lerchenfeldstrasse 5, 9014, St. Gallen, Switzerland

*Environmental Pollution* 223: 616-623 (2017)

## Chapter 1

# Mobility of metallic (nano)particles in leachates from landfills containing waste incineration residues

### **Bullet points:**

- Metallic colloidal materials (including nanoparticles) are continuously emitted from landfills
- Concentration and form of particles differ depending on the type of waste residue
- Weathering of waste residues dictate release of metals over time

### **Abstract**

Incineration of municipal waste and sewage sludge is becoming an increasingly popular option for the disposal of waste materials and energy generation. The incineration process can concentrate metals in the incineration slags deposited in landfills. Emitted leachates contain a myriad of salts and metals; some of them in (nano)particulate form. In this study we collected the leachate from a Swiss landfill for municipal solid waste incineration (MSWI) residues along with the slags deposited at this site (waste incineration bottom ashes and fly ash, sewage sludge incineration bottom ash) from which simulated leachates were prepared. Basic water quality analysis (pH, DOC, TSS, major ions) and natural, incidental or engineered particles suspended in the leachate were characterized by NanoSight (for general size range), serial filtration with ICP-MS analysis for element specific particle size quantification and TEM/EDX to visualize particle morphology and composition. Special priority was given to those elements that have engineered nanoparticulate counterparts (Ti, Zn, Ag, Cu, Fe and Ce) to give an indication of 1) the current concentration and form of these particles emitted from the landfill, 2) the potential presence of engineered nanoparticles already in the samples, and 3) trends in particle size (change) in the leachate from different slags to provide an indication on particle mobility. Zn, Ag, and Cu had appreciable concentrations associated with small particulate matter (nano and 0.1 – 0.45  $\mu\text{m}$  size fractions) in natural and laboratory prepared leachates, while Ti (nano)particles were most abundant in the landfill leachate. Multiple sampling dates suggested relatively steady particulate matter in the leachate for most elements, but analysis of differently aged bottom ash slags from municipal waste revealed differences with age, indicating the influence of slag weathering in metal mobilization. MSWI residues are inherently a complex mixture of stable and unstable materials that are subject to continuous and dynamic changes over time. Therefore, in this manuscript we placed an emphasis on understanding the geochemical processes that are associated

with MSWI residue weathering and how this may dictate the likelihood of particulate metals leaching into groundwater.

## 1. Introduction

The incineration of municipal solid waste (MSW) has become an attractive option for the treatment and subsequent disposal of goods at the end of their life cycle for both the reduction of waste volume and to increase energy production. In many European countries, the main treatment for non-recyclable MSW is incineration, for example, with close to 100 % of this waste category being incinerated in Denmark and The Netherlands.<sup>1</sup> Following incineration, the volume of waste is reduced as much 90% and its weight by 75%, depending on the characteristics of the incinerated waste.<sup>2</sup> Modern MSW incinerators fitted with combined heat and power capture can utilize the energy content of the waste as electrical energy, with an average 21% of gross electricity generation and overall gross energy generation efficiencies (i.e. net electricity plus heat) can be in excess of 95%.<sup>3,4</sup> Bottom ash is the most significant by-product of the incineration process, accounting for 85-95% of all residues produced, with fly ash the other major solid output.<sup>5</sup> In Switzerland, where landfilling of biodegradable, combustible MSW and sewage sludge is practically zero, incineration was shown to have significant additional environmental benefits. This was assessed by considering a life cycle approach of waste management and taking into account direct operating emissions compared to traditional landfill operations.<sup>6</sup> Landfills for stabilized incineration residues, such as slag, solidified fly ash and air pollution control residues from MSW incinerators and vitrified treatment residues (e.g. incinerated sewage sludge), often contain a low organic content but have high concentrations of metals.<sup>7</sup> The high metal concentrations are a cause for concern due to potential groundwater contamination and subsequent aquatic toxicity. Therefore, such sites are subject to more stringent requirements than other landfills and impermeable lining systems are required to contain and facilitate the collection of landfill leachate for treatment.<sup>7</sup>

Nevertheless, leachates originating from low-organic landfills can be considered a potential pathway through which dissolved, nanoparticulate and colloidal matter may be transported to the environment. Relatively few landfill leachates have been characterized in detail to describe the physical (particulate, colloidal, dissolved) and chemical (organic complexes, inorganic complexes, free metal ions) makeup of constituent particles, and those leachates that have been characterized in such detail were from reactive (high organic) landfill sites.<sup>8</sup> Yet the studies that do exist consistently show that colloids as well as organic and inorganic complexes are important for the mobility of metals in landfill leachates, with typically less than 10% of total metal concentrations as free metal.<sup>8</sup> Hennebert et al. studied the colloidal composition of a diverse group of 25 different leachates (solid industrial and municipal waste, contaminated soil, contaminated sediments and landfill leachates) using a standardized leaching process to quantify the existence of metals in both the colloidal and dissolved fractions of the leachate.<sup>9</sup> Similar monitoring for the

existence of colloidal matter has been conducted in both active and closed reactive landfills by Matura et. al (2012), where identification of six major categories of materials were distinguished in the nanoparticulate phase: carbonates, phyllosilicates, quartz, iron oxides, organics and other salts.<sup>10</sup> In their study, the authors note that calcite colloids that formed in the landfill can bind trace inorganic contaminants (metals/metalloids) and thus immobilize them in the landfill. This may also, by extension, be applicable to inorganic nanomaterials found in landfills. In the context of toxicity and migration in aquifers, Baun et al. reviewed the concentrations of metals in MSW landfill leachates along with other water quality parameters and their impact on metal speciation and metal mobility.<sup>8</sup> Several of the references cited therein found *in situ* mobile colloids associated with metals, including As, Cd, Cr, Cu, Ni, Pb, and Zn.<sup>10-14</sup> For example, evaluating the characteristics of various size fractions of colloids emitted from a closed methanogenic landfill in the U.S., Gounaris et al. determined that a high concentration of colloids existed (most abundant in the sub-10 nm range).<sup>11</sup> The major component of these particles was organic matter but with significant associated fractions of Zn, Pb and Cr. Colloid stability, attributed to the organic coating, implied a high degree of mobility and persistence in these landfills.

The physical and chemical differences between reactive landfills, discussed above, and landfills containing incineration slag can influence (metal associated) colloidal mobility. In this manuscript the term slag can collectively refer to waste incineration bottom ashes and fly ash and sewage sludge incineration bottom ash. MSW incineration (MSWI) bottom ash mainly consists of assorted silicate-based glass phases, where the compounds embedded in the matrix (i.e. metallic inclusions) play an important role in the concentration of metals.<sup>15-17</sup> Depending on the incineration method or material (waste, sewage sludge, etc.), the mineralogical phases of the ash, their associated metal content and morphology of the inclusion can all be highly variable. The leaching behavior of major elements from MSWI bottom ash has been shown to be pH and time dependent.<sup>18</sup> Most studies are conducted at the “natural” pH of the bottom ash samples, which for fresh samples is usually alkaline (pH 10 -12) and for weathered samples approximately pH 8.<sup>19</sup> More precise details of the dominant weathering processes during landfilling of MSWI waste over time can be found in Saffarzadeh et al.<sup>20</sup> For example, Köster et al. conducted column leaching experiments of waste incineration plant residues and they showed that, depending on experimental conditions, colloids and metals can mobilize out of incineration slag.<sup>21</sup>

To date we are not aware of any studies that 1) investigate the metals associated with the colloidal fraction emitted specifically from entire landfills for incineration residues; 2) investigate the leaching potential of other incineration residues, such as MSWI fly ash or vitrified treatment residues (e.g. wastewater treatment sludge); or 3) investigate the occurrence of engineered nanomaterials (ENM) in any of these systems. Additionally, while there have been only a few studies investigating metallic (associated) colloidal material release from reactive landfills,<sup>8, 9, 11</sup> this information is absent from the MSWI bottom ash literature and there has been no distinction specifically of the nano-sized fraction.



Natural colloids are a ubiquitous component of natural water systems. Therefore, it is important to distinguish between natural, incidental and engineered analogs so that the risk assessment of ENM can be properly evaluated. By establishing a baseline of emissions of naturally occurring or incidental particles emitted from various incineration waste leachates, it is possible to identify a (potential) influx of ENM into the waste material from incineration of ENM products and subsequently detect an increase of metallic particles release from the landfill via the leachate in the future. ENM may potentially be present in any given waste stream because they are used in a wide range of consumer products.<sup>22, 23</sup> Thus they can be transported throughout the entire waste management system from municipal waste and sludge incineration to landfill.<sup>24</sup> ENM may survive through the incineration process,<sup>25, 26</sup> albeit with their original properties potentially transformed.<sup>27, 28</sup> Incinerator fly ash may also contain bulk derived nano-objects and combustion generated nano-objects (here defined as incidental particles) alongside ENM, either alone or in aggregates.<sup>29</sup> While some amount of ENM are already likely to be contained in landfills, to date there have been no studies that have directly quantified these particles in a landfill leachate. Furthermore, material flow analysis modeling studies have thus far only included landfills as a final sink for ENMs at the end of life phase because not enough information is available about further releases.<sup>30</sup>

The aim of this work was to quantify the natural, incidental and engineered particles emitted from a variety of landfill leachates, of variable compositions, derived from the incineration residues of different source materials. By completing a standardized leaching process (ISO EN 12457-2:2002) for a variety of slags and natural leachate recovered from a landfill for incineration residues in Switzerland, we had a slew of matrices to examine the differences of natural colloids and nanomaterials emitted. Abundance and distribution of small colloidal material (i.e.  $< 0.45 \mu\text{m}$ ) was investigated using NanoSight. More precise, element-specific investigations relied on serial filtration with ICP-MS analysis and STEM/EDX for morphological and chemical characterization. Through these measurements we observed the size and chemical composition of particulate matter in the solutions. While a range of elements were measured, focus was placed on those with ENM analogs that may become more dominant in landfill leachates in the coming years, such as particles including Ti, Zn, Ag, Cu, Fe, and Ce. Other basic water quality parameters for the leachates were also measured, including pH, organic matter and total suspended solids content and analysis of major ions. However, the leaching behavior of major components and trace elements from MSWI in landfills depends on typically unknown parameters such as the quantities, crystallinity and specific surface area of minerals in the bottom ash matrix. Therefore, our goal in this present work is not to suggest dissolution rates, leaching rates or define the specific morphology/chemistry of specific metallic/colloidal complexes, but rather to present the relative fraction of ENM specific metals that may be released from various incineration residues, many of which have not been previously investigated. Taken together, this data may serve as a baseline for current concentrations and compositions of (nano)particulate matter released from landfills for stabilized residues.

## 2. Materials and Methods

### 2.1 Landfill location and sampling

Samples were taken from the ZAB Deponie landfill site, located in Flawil, Switzerland. At this site, MSWI residues (bottom ash and fly ash), as well as wastewater incineration residues (sludge incineration slag), are routinely collected by the operator. After arrival on-site, the slag from the bottom ash is deposited at an intermediate location to further remove the large remaining metal pieces, such as iron and copper (i.e. descraping to retrieve the valuable metal content). Subsequently, the slags are deposited into various cells in the landfill and left in the open air until completion of the landfill cell. At the base of the landfill, an impermeable technical barrier of 20 cm thick asphalt and cobblestone layers is installed.

Solid samples were taken from different compartments of the landfill, representing different slag types and ages. The predominant waste received by this landfill is bottom ash, which consists of the ashes of MSW collected at the bottom of the incineration plant from a neighboring city. Fresh bottom ash (less than one day old), 2 month old bottom ash and one year old bottom ash were sampled by digging approximately 30 cm below the top of the respective slag piles and scooping aliquots of material into plastic bottles. Fly ash and sewage sludge incineration residues were separately sampled in the same manner from the respective compartments in the landfill. Both fly ash and sludge samples were less than 2 days old at the time of sampling.

The leachate samples were taken directly from the main outflow of the landfill, which leads into a settling basin, without prior treatment (hereafter labeled “natural leachate”). Plastic and glass bottles were used to collect the ICP-MS and DOC analysis samples, respectively. Three sampling campaigns were performed (October 13, 2015, January 8, 2016 and March 31, 2016), the first of which involved collection of leachate and all solid materials, while subsequent trips involved only the natural leachate sampling. Meteorological data (precipitation) for the week proceeding each sampling date was obtained from the Meteoswiss platform for the Flawil station, 47°25'N 9°12'E (Table S1). Further sample preparation and analysis of the natural leachate followed the same protocol as the prepared leachates from the slag material, see details in section 2.2.

### 2.2 Standardized leaching process (CEN EN 12457-2:2002)

To obtain leachates from the solid samples, a standard method from the European standard organization (CEN), a modified version of the standard protocol EN 12457-2,<sup>31</sup> was followed. This method focuses on the generation of leachate from granular waste materials and sludges. In many cases, the initial sample ashes were wet and composed of a variety of metallic parts, stones, glass and a mixture of caked slag-like materials. A brief sieving step was performed (2 mm mesh size) after the samples had been dried in air. The

major remaining portion had particle sizes below 2 mm. Photos of processed samples can be seen in Figure S1.

After the solid samples were prepared, the standardized leaching procedure was followed to acquire leachates from the various slag samples (Figure S2). Waste eluates were prepared in triplicate using a ratio of one part waste to ten parts water. Thus, 10 g of the respective waste sample was suspended in 100 mL of DI (18 megaohm) in a 250 mL polypropylene bottle. The closed bottle was then agitated with 5–10 rpm for  $24 \pm 0.5$  h at room temperature. Sedimentation of the solid waste material was allowed for  $15 \pm 5$  min, the suspension was filtered (see details below) and these aliquots were retained for further elemental analysis and basic water quality tests as described in section 2.3.

### ***2.3 Leachate solution analysis***

#### *2.3.1 Water Quality analysis*

For all (triplicate) leachates of the five slag samples and the natural leachate originating from the landfill, the pH was measured by a Metrohm 827 pH meter. Samples were prepared for dissolved organic carbon (DOC) analysis with filtration through a 0.45  $\mu\text{m}$  filter (Whatman; cellulose nitrate membrane) into glass bottles and analyzed by a commercial laboratory (Bachema AG). An initial survey of water chemistry parameters of the leachate filtered through a 0.45  $\mu\text{m}$  filter was conducted to determine which ions were present in significant concentrations by IC analysis for anions ( $\text{F}^-$ ,  $\text{Cl}^-$ ,  $\text{NO}_2^-$ ,  $\text{Br}^-$ ,  $\text{NO}_3^-$ ,  $\text{PO}_4^{3-}$  and  $\text{SO}_4^{2-}$ ) and ICP-OES analysis for cations ( $\text{Na}^+$ ,  $\text{K}^+$ ,  $\text{Mg}^{2+}$  and  $\text{Ca}^{2+}$ ). The final selection of major ions that were identified as significant contributors to the solution chemistry was measured by Bachema AG with IC measurements ( $\text{Cl}^-$  and  $\text{SO}_4^{2-}$ ) and ICP-OES analysis ( $\text{Na}^+$ ,  $\text{Ca}^{2+}$ ). To measure total suspended solids (TSS) in a selection of leachates (natural, bottom ash, fly ash and sludge), the 1.5  $\mu\text{m}$  filter samples (triplicate of 200 ml) were passed through 0.45  $\mu\text{m}$  and 0.1  $\mu\text{m}$  filters (serial filtration). The dry filters were weighed before and after the filtration to measure TSS mass. A control experiment conducted by passing DI water through the 0.45  $\mu\text{m}$  filter and measuring the mass difference with the same procedure was also conducted. This showed no significant mass change of the filter throughout the procedure.

All leachates underwent serial filtration to obtain size fractionation of metals associated with particulate matter in the leachate material. Four serial filtration steps were used: 1.5  $\mu\text{m}$  filter (Whatman, glass microfiber), 0.45  $\mu\text{m}$  filter (GE healthcare, cellulose nitrate), 0.1  $\mu\text{m}$  filter (GE healthcare, cellulose nitrate) and centrifugal microfilter (ViaSpin, 10 kDa cutoff size). Elemental composition in the leachate samples was determined by ICP-MS (Thermo Scientific Element 2). Special focus was placed on those elements that are also used in significant amounts as ENM (Ti, Zn, Ag, Cu, Fe, and Ce), but additional elemental characterization (Cd, Cr, Mn, Mo, Ni, Sb, Se, and Sn) was performed to better compare leachate composition with existing landfill leachate studies. Because of the high Ca and Si concentrations in many

samples (e.g. natural leachate), significant interferences on the measured masses of Ti was evident, leading to under or over estimation of the concentration in some instances for different filtrates. In particular, a high concentration of Ti was measured in the < 10 kDa fraction in the natural leachate samples (which is chemically/physically very unlikely) and so the measurements associated with these samples had to be entirely discarded for Ti concentrations. In other samples (e.g. bottom ash, fly ash, sludge) there was a more discernible difference in Ti concentrations between the different filtration levels and so these samples may provide a more accurate representation of Ti associated with particulate matter. Nevertheless, due to these analytical difficulties, the concentration of particulate Ti as measured by ICP-MS is not presented in the main text but is still included in the SI (Figure S4).

### *2.3.2 NanoSight Analysis*

Nanoparticle tracking analysis (NTA) is capable of sizing particles between approximately 30 to 1,000 nm, with the lower detection limit being dependent on the refractive index of the particles being measured.<sup>32</sup> To measure the distribution of natural particles in the natural landfill leachate and each of the prepared extractions, NTA measurements were performed with a NanoSight NS500 (Malvern). The software used for capturing and analyzing the data was the NTA 3.0. Samples were loaded into the sample chamber with sterile syringes by means of a syringe pump with constant rate of injection. All measurements were performed at room temperature. Each sample was measured for a total of 12 minutes. The camera level was set to 13 for every measurement to ensure standardized analysis and to eliminate possible bias induced by further adjusting parameters for each sample, but the camera focus was adjusted daily depending on the sample. Each influx of sample and video produced a histogram depicting particle size and concentration. These data were then re-plotted without further data manipulation.

### *2.3.3 Scanning Transmission Electron Microscopy (STEM) and Energy Dispersive X-ray Spectroscopy (EDX)*

Liquid suspensions of leachates filtered through a 1.5 µm filter were transferred to polypropylene vials where particles were deposited directly onto TEM grids by centrifugation using a swinging bucket rotor, with rotation speed of 45000 rpm for 2 h; conditions that enabled/ensured complete deposition of all particles > 10 nm in size onto the carbon-coated Cu TEM grid. This technique therefore concentrates particles with a low concentration onto the grid so they can be analyzed more easily opposed to drop deposition of liquid on the TEM grids. Samples were gently washed to remove residual salt by moving the grid through a drop of MilliQ water on a piece of parafilm 5 - 10 times.

Particle images were obtained via STEM combined with EDX for element detection using a JEOL 2200FS TEM/STEM operated at 200 kV. The nominal spot size of the STEM probe was 0.7 nm using a beam convergence angle of 10.8 mrad. High-angle annular dark field STEM micrographs were recorded using an inner detector angle of 100 mrad, while the bright-field STEM images were recorded with a detector angle of 15 mrad. EDX spectra of individual particles were recorded by positioning the electron probe on a selected particle.

### 3. Results

#### *Characterization of Landfill Leachates – Natural and laboratory prepared*

##### *3.1 Basic Water Chemistry Analysis*

Basic water chemistry parameters were used to characterize the natural landfill samples. All of the synthetic laboratory leachates were alkaline (pH 9 – 13), whilst the natural leachate was found to be closer to neutral (pH 7 - 8) (Table 1). The bottom ash had higher concentrations of DOC than the older slags, 2 month old and 1 year old bottom ash. The lowest values of DOC were found in the fly ash and sludge leachates, whilst the natural leachate had the highest DOC value, averaging approximately 15 mg/L across the three sampling time points. The natural landfill leachate had significantly higher ionic strength than any of the laboratory prepared leachates (Table 1). However, as expected the natural variation in total salt concentration was inversely proportional to the amount of precipitation (Figure S3). The TSS contents of all laboratory prepared leachates were approximately a third lower than that of the natural landfill leachate. In all samples, the TSS measured on the 0.1  $\mu\text{m}$  and 0.45  $\mu\text{m}$  filters were similar except for the fly ash sample, indicating that much of the particulate matter was between the 0.1  $\mu\text{m}$  and 0.45  $\mu\text{m}$  size range. For the fly ash sample, a smaller fraction of finer particles were found in solution. The pH and major ion concentrations presented here are single measurements of the solution, but are consistent with measurements that are in the historic range of values documented by the landfill operator.

**Table 1:** Water quality characterization of the natural outflow of a stabilized residue landfill in Switzerland over three sampling campaigns and five laboratory prepared leachates from various slags contained in the landfill.

| Sample Name                 | Abbreviation | pH   | DOC (mg/L) | TSS (mg/L)                |                          | Major Ions (mg/L) |                  |                 |                               |
|-----------------------------|--------------|------|------------|---------------------------|--------------------------|-------------------|------------------|-----------------|-------------------------------|
|                             |              |      |            | 0.45 $\mu\text{m}$ filter | 0.1 $\mu\text{m}$ filter | Na <sup>+</sup>   | Ca <sup>2+</sup> | Cl <sup>-</sup> | SO <sub>4</sub> <sup>2-</sup> |
| Natural Leachate Sampling 1 | Le1          | 7.5  | 15         | -----                     | -----                    | 3870              | 1210             | 8549            | 1335                          |
| Natural Leachate Sampling 2 | Le2          | 8.0  | 12         | -----                     | -----                    | 1990              | 394              | 3300            | 802                           |
| Natural Leachate Sampling 3 | Le3          | 7.9  | 19         | 26.9 $\pm$ 0.3            | 25.1 $\pm$ 0.6           | 3750              | 815              | 11900           | 2370                          |
| Bottom Ash Fresh            | BA           | 12.9 | 13         | 9.5 $\pm$ 0.4             | 8.2 $\pm$ 0.1            | 177               | 1250             | 438             | 969                           |
| Bottom Ash 2 Months Old     | B2M          | 12.5 | 13         | -----                     | -----                    | 246               | 123              | 373             | 58                            |
| Bottom Ash 1 Year Old       | B1Y          | 11.7 | 5          | -----                     | -----                    | 112               | 132              | 143             | 277                           |
| Fly Ash                     | FA           | 9.5  | 2          | 9.1 $\pm$ 1.8             | 3.3 $\pm$ 0.3            | 26                | 615              | 124             | 1485                          |
| Sewage Sludge Ash           | S            | 8.7  | 2          | 8.0 $\pm$ 1.3             | 7.4 $\pm$ 0.4            | 28                | 859              | 488             | 1525                          |

An estimate of natural background particles in the leachates can be seen in Figure 1. It is notable that no particles  $> 0.45 \mu\text{m}$  in size are observed, which corresponds well with the size cutoff of the filter used as a sample preparation step. Additionally, the relative number of particles observed by NanoSight compares well with the TSS measurements, where the natural leachate had a higher particle number. The NanoSight technique is unable to give elemental characterization of particles which are observed and in some cases may over- or underestimate particle size because of the variable light intensity reflected by particles of different composition. Nevertheless, this can serve as an interesting comparison to the other techniques that indirectly (serial filtration and ICP-MS analysis) or directly (TEM/EDX) characterize the size distribution in the leachate sample.

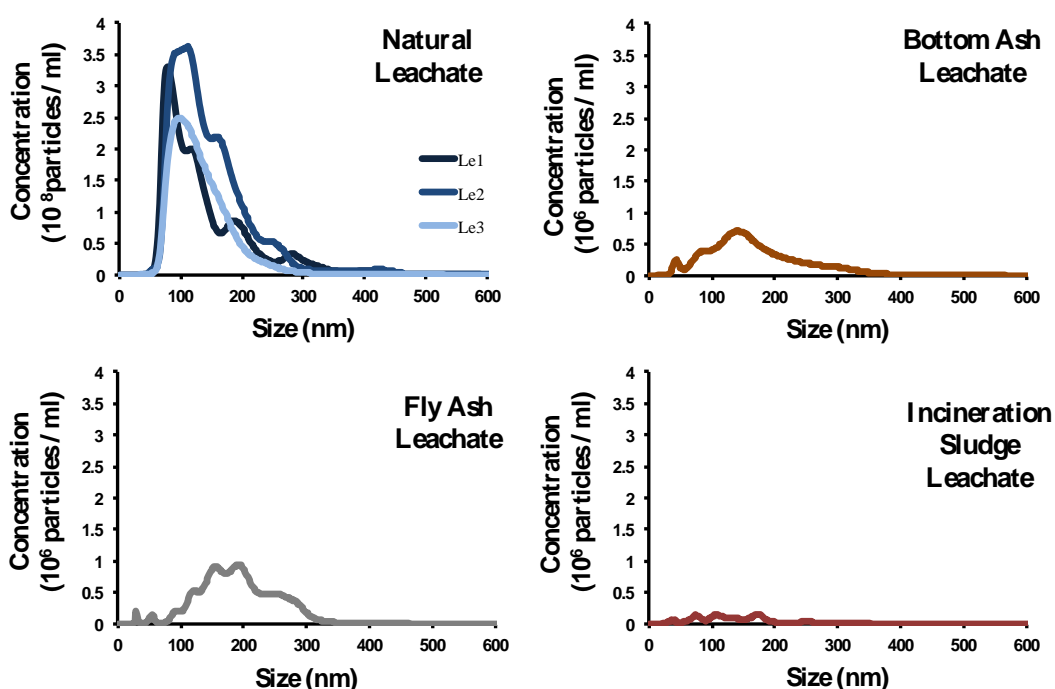


**Figure 1:** NanoSight analysis of natural particles in natural landfill leachates (sampling time points 1, 2 and 3) and laboratory prepared leachates; bottom ash, fly ash and sludge. Leachates filtered through  $0.45 \mu\text{m}$  filter prior to analysis.

### 3.2.2 Total metal analysis in serial filtration fractions

Through serial filtration of all natural and laboratory prepared leachates with subsequent ICP-MS analysis, we observed the size and chemical composition of particulate matter in four size categories (see Figure S4 for all elements measured by ICP-MS with standard deviations). While a range of elements were measured, focus was placed on those with ENM analogs which may become more dominant in landfill leachates in the

coming years, such as particles containing Ti, Zn, Ag, Cu, Fe, and Ce. Dynamic differences were observed between different landfill leachates, but within each analysis (i.e. triplicate preparations of leachate from slag samples) observed metal concentrations showed little variability. This indicates that our leaching procedure was consistent and reproducible.

Of particular note is the presence of some micro- and nano-sized Zn particles and micro-sized Fe containing particles in the leachates (Figure 2). Particles containing Zn, Ag and Cu were found in the natural leachate (Figure 2B), albeit in the low  $\mu\text{g/L}$  range. Leachates prepared in the lab from slag material released a high concentration of Zn particles, a significant fraction of which was, in the case of the leachates from bottom ash and sludge, in the nano-size range (Figure 2, panels D and H). High concentrations of particulate Fe were leached from the sludge samples (Figure 2G), an expected result considering 1) the use of Fe in the WWTP to precipitate P for subsequent recovery and 2) the red color of the slag itself. See Table S2 for full characterization of particulate matter across all elements measured.

Further analysis of the particulate matter in the natural landfill leachate over multiple sampling campaigns reveals that the concentration of each size fraction of materials remains relatively stable (Figure 3). The total metal content does not seem to be significantly influenced by rainfall events, unlike the concentration of major ions. Whilst the elements investigated here were chosen because they also make up the composition of common ENM that may leach from landfills after product disposal, it is not possible to identify any fraction of this material as natural or engineered from total metals analysis alone.

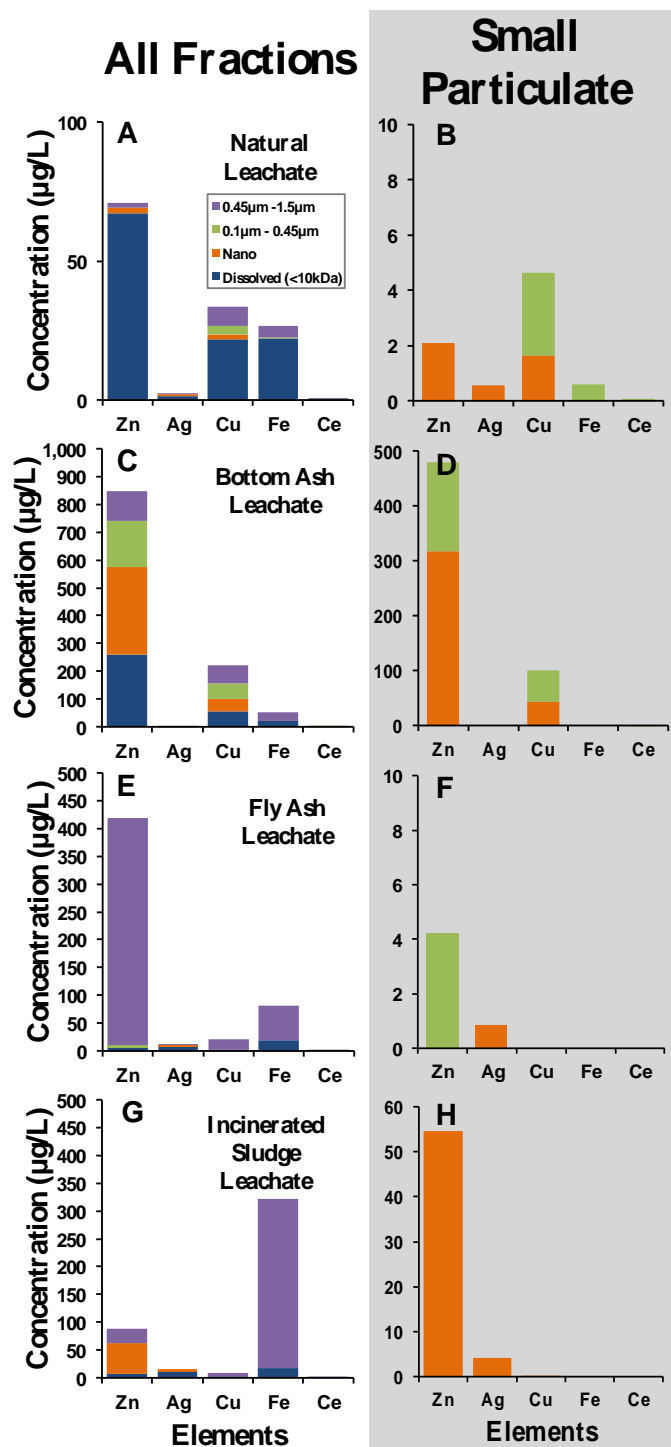


**Figure 2:** Particulate, colloidal and nanoparticulate concentrations in the leachates are presented for Zn, Ag, Cu, Fe and Ce, averaged across triplicate samples. All filtration fractions analyzed by ICP-MS are shown in the graphs on the left column, including dissolved (blue), nano (orange), 0.1 – 0.45 µm (green) and 0.45 – 1.5 µm (purple). Only the small particulate matter (nano and 0.1 - 0.45 µm fractions) is shown on the right column, shaded grey, to highlight naturally occurring particles that correspond to common ENM additives.



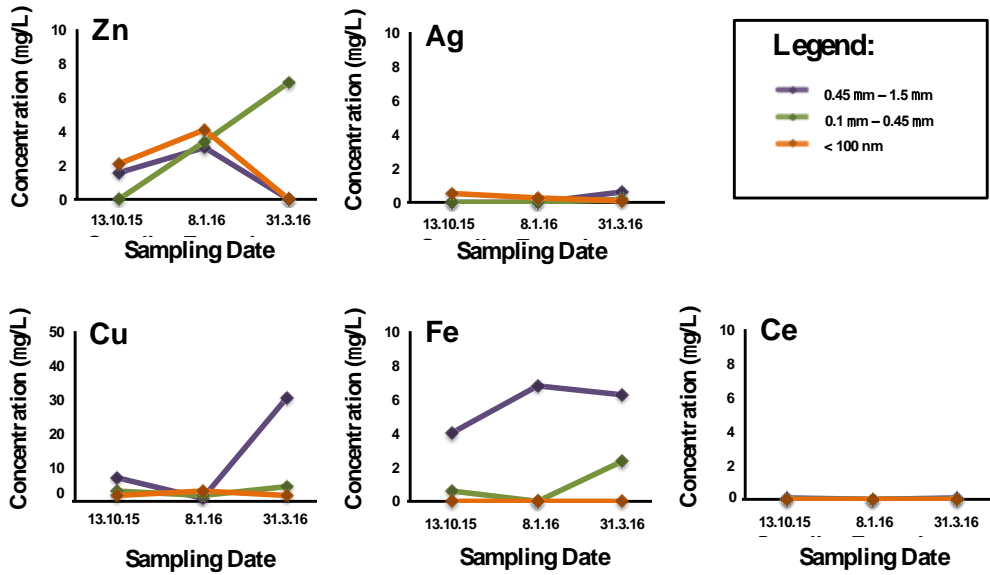


**Figure 3:** Comparison of particulate matter concentrations in natural leachate from different sampling dates at a stabilized residues landfill in Switzerland.

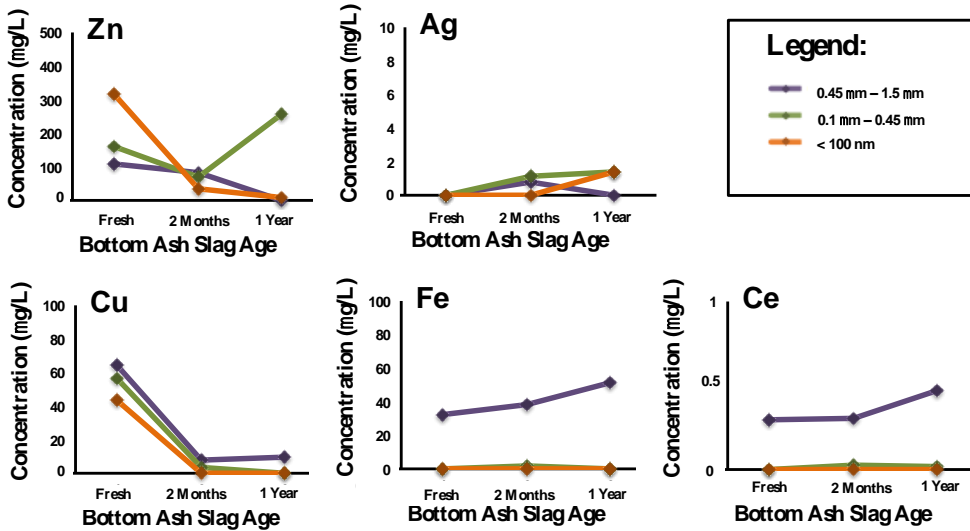


**Figure 4:** Evolution of particulate matter concentrations in laboratory prepared leachate from bottom ash slag with different age collected from a stabilized residues landfill in Switzerland.

The concentration of particulate matter that was leached from bottom ash of various ages did not vary significantly for some elements (e.g. Ag, Fe, or Ce), but the changing profiles of both Zn and Cu particulate matter can give an indication for particle size evolution and subsequent particle mobility (Figure 4). In the case of Zn, particle size increases over time. Where the nano fraction is dominant in the fresh slag, this proportion drops over the course of a year and larger sized particles (0.1  $\mu\text{m}$  – 0.45  $\mu\text{m}$ ) are predominantly

leached from slag that is one year old. While Cu particles of all size fractions are initially at a relatively high concentration (50 – 65 µg/L for each fraction), the total particulate amount drops in all fractions from the initial concentration leached from the weathered 2 month and 1 year old samples. For the largest particles, this is a five fold reduction and for the smaller particles less than 1/10 of the Cu particles are emitted from weathered bottom ash compared to the fresh bottom ash. The total mass of Cu leached from the older slags is consistent with the mass of Cu recovered from the natural leachate sampling from the landfill at each of the sampling campaigns. In comparison to the naturally collected leachate, the laboratory leaching procedure of the older slags is consistent with particle recovery for most of the elements under most conditions.

### 3.2.3 TEM/EDX Analysis of natural particles in leachates

TEM images of particles observed in the natural and laboratory prepared leachates vary in terms of particle size, metal content and morphology, both within individual samples and between various leachate compositions (Figure 5). No set number of particles were imaged per sample and so no quantitative data can be provided concerning the relative number of particles associated with each composition. However, we do provide qualitative data on which particles appeared more numerous on the sections of TEM grid that were randomly imaged or cases where only a few particles were observed in a given sample. In the natural landfill leachate samples, the most frequently identified particles were nano-sized Ti particles associated with Si. Examples of other nano-sized particles were observed in the leachate, including Cu and an Au/Ag alloy. Whilst it is not possible to determine if these particles are from anthropogenic origin from this analysis alone, the characteristics of the particles imaged (e.g. in terms of size, shape and purity) make it a possibility that these could be of anthropogenic origin. If they are from anthropogenic sources then they may be ENM, or, alternatively, they could be incidental nanomaterials formed through the high temperatures associated with waste incineration. In the MSWI bottom ash leachate, salt crystals (mainly of Ca but also with Na and K) formed a nucleolus around other particulate matter, such as Ti. This is mostly a by-product of the sample preparation (i.e. calcium carbonate crystals drying on the grid), but it hindered the observation of the particles in the leachate. Therefore, for MSWI bottom ash leachates the metals associated with each size fractionation can only be determined from the ICP-MS analysis in study.

The particles in the fly ash leachate sample were mainly conglomerates of several metals held within a Si (glass) matrix. However, these were not discrete particle shapes but rather an amorphous group of material, making individual element identification for a distinct region within the mass impossible. In other words, particles of discrete elements were not observed. As is consistent with the small particulate matter analysis from the ICP-MS serial filtration results, most particles contained some Zn and the majority of particles imaged were 100 nm in size and larger.

Particulate matter in the sludge leachate is varied, but a clear indication of the wastewater treatment process is visible in the particle leaching behavior. Specifically, the high abundance of Fe- and P-rich particles was expected, since Fe is frequently added during wastewater treatment to precipitate the P for potential future extraction. Ti particles associated with Si, in the nanometer size range but up to 200 nm, were the other predominant feature consistently and easily identified during this analysis. These particles were similar in size and morphology to those found in the natural landfill leachate. This indicates that our laboratory leaching procedure is capable of extracting particles similar to those which are found in natural samples. Finally, as with the fly ash samples, many conglomerates were found that contained a broad range of metals (e.g. see corresponding EDX results, Figure S5). This may point to particles of anthropogenic source where these conglomerates are formed during the waste incineration process. All of the previous studies on (natural) colloidal concentrations and transport in landfills have thus far not covered landfills that contain solely MSWI incineration slags nor have they investigated the leaching potential of colloids from waste residues. The novelty in this work, therefore, is to focus on the mobility and composition of metal containing colloids in the leachate of landfills for MSWI. There are significant differences between the physical and chemical characteristics of landfill leachates derived from reactive landfills, which have been surveyed more frequently, and those that contain only incineration slag. The variance in terms of pH, DOC and major ion concentrations leads to differences in (nano)particle mobility. Specifically, pH values are higher in our landfill leachates, there is a much lower concentration of TOC/DOC (up to an order of magnitude across all samples) and major ions are consistently on the higher side of the normal concentration range reported for traditional municipal sites.<sup>8, 10</sup> The decreased carbon content is expected in the waste residues studied here as this material is combusted during the incineration process.

Overall, bulk metal concentrations from previous investigations agree well with our serial filtrations of MSWI leachate, where Zn and Cu are the most concentrated metals in bottom ash.<sup>15</sup> Metals in the landfill leachates derived from incineration residues are present in both dissolved and particulate form, with the majority being dissolved. The nano fraction is a minor component of the total particulate size distribution for most samples and metals. Rather, mostly larger particles and agglomerates/aggregates/composites are found. This may partly be due to the treatment of the waste over time. The incineration process of MSW can concentrate metals in the slags and ashes, some of which are elements of environmental concern. Likewise, in all waste incineration residues inorganic ENM will likely be concentrated from the parent waste material. Modeled concentrations of engineered nano-TiO<sub>2</sub> in slag and filter ash are 395 and 543 mg/kg, respectively, for nano-Ag the values are 170 and 340 µg/kg<sup>30</sup>. Thus, the potential presence of ENM already in the samples cannot be overlooked. Nano size particles of TiO<sub>2</sub> were identified in every leachate sample and these are most likely from an anthropogenic source due to their size, purity and characteristic shape. It has been suggested that TiO<sub>2</sub> particles which have rounded edges/spherical shapes are more likely to come from anthropogenic sources and geogenic (natural) particles are more likely to have sharp-edges.<sup>33</sup> The TiO<sub>2</sub> can then either be an ENM (e.g. as used in cosmetics, etc.) or a pigment (e.g. as used in paints and in foods), with the latter case being more likely as its production volume is 100 times that of ENM.<sup>34, 35</sup>

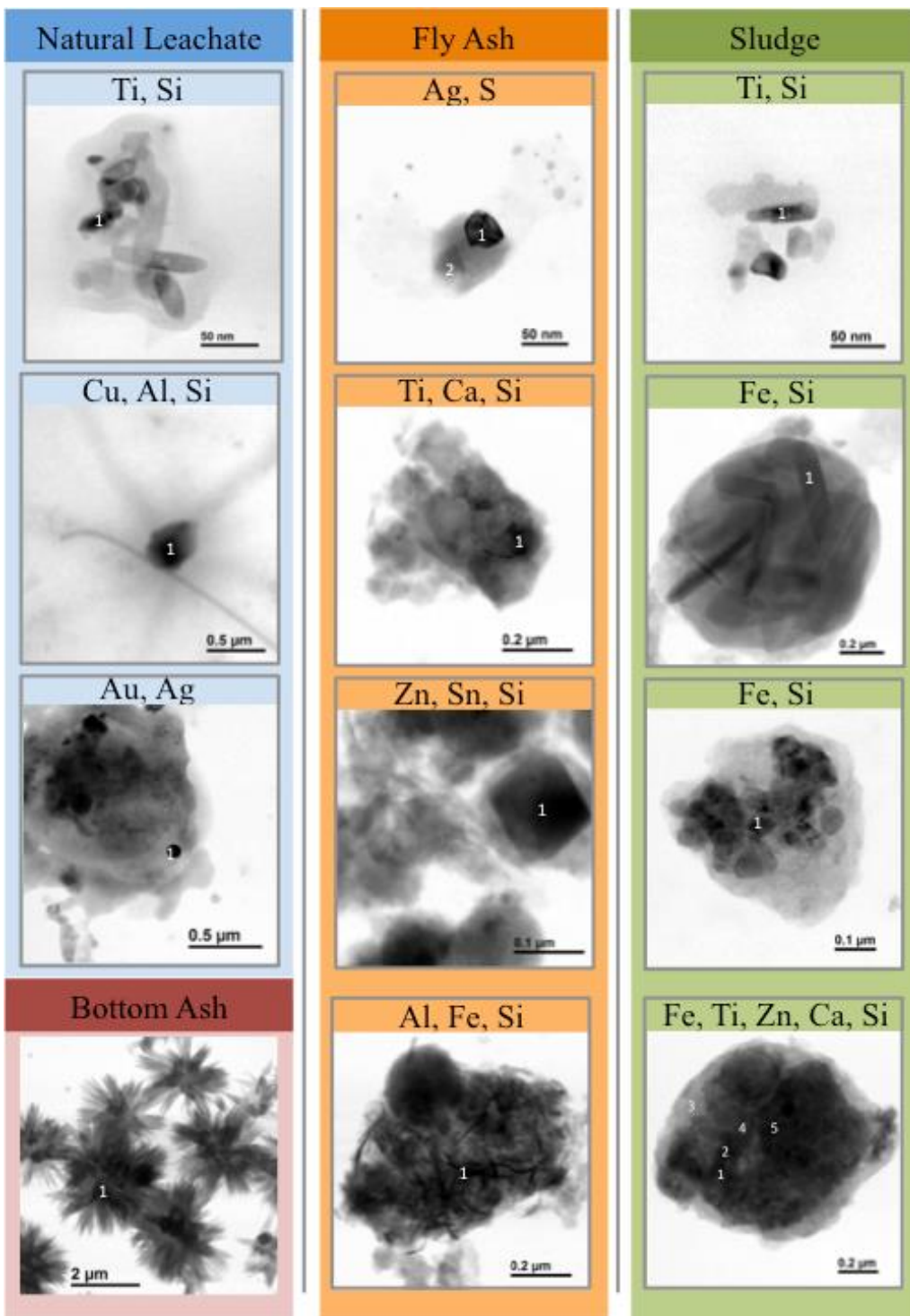


**Figure 5:** TEM images of particles observed in the natural and laboratory prepared leachates of MSWI bottom ash, MSWI fly ash and wastewater sludge incineration bottom ash. Particle size, metal content and morphology varied within individual samples and between various leachate compositions. A selection of images are presented here, which shows the diversity of (nano)particles observed. The metal content of each particle is given above the figure, with a number indicating where EDX analysis was performed (see Figure S15 for corresponding EDX analysis).

Additionally, discrete nano sized Ag/Au and Cu particles in the natural leachate were observed. However, there is no definitive evidence that these particles are directly related to ENM in the way they were imbedded in consumer products because other means of nanoparticle generation are also plausible, such as formation during the waste incineration process.<sup>36, 37</sup>

Our results indicate that, regardless of their source, quantifiable amounts of metallic particles are being leached from landfills for incineration slags, both in the colloidal and nano size ranges. The degree of mobility of metals from the glass fraction of the MSWI (which accounts for approximately 50% of the bottom ash) is largely dependent upon the pH of the percolating fluid, where a pH of  $> 9$  is necessary to dissolve the glass network consisting of Si.<sup>38</sup> This removal of the silica "glue" then results in the mobilization of particulate metal phases that have a lower solubility. Taking into account the geochemical conditions in the fresh MSWI, the landfill should be favorable for destruction of the glass matrix and thus mobility of particulate metals is possible. However, carbonation is considered a dominant process in controlling pH variation in these landfills and it is through the formation of alkaline minerals that the leachability of metals can change over time. The weathering of the MSWI material, including carbonation and glass alteration can make some elements (e.g. Zn and Cu) more stable over time, which is attributed to the decline in pH of the leachate and therefore less silica matrix dissolution.<sup>15</sup> Indeed, in our laboratory leachate tests older slags showed less mobility of these metals (Figure 4). However, the strongly alkaline MSWI residues may not be easily neutralized after landfilling, even in the long term, and so the chemical decomposition and/or the mechanical breakage of the glass may still lead to dissolution of embedded metal inclusions at every stage of the weathering process.<sup>20</sup> From the intense study of MSWI in the last three decades, it was concluded that the long-term behavior of the elevated amount of metals depends to a great extent upon the behavior of the host phases, especially the weathering rate and alteration products of silicate based glass phases (increasing mobility) and carbonate dictated pH change (decreasing mobility).

The stability of ENM in the context of landfill leachates has not been explored in detail: dissolution, aggregation, sedimentation and fate and transport processes all remain largely unknown. However, some indications of their stability may be correlated from the environmental implications of natural colloidal materials. Clay minerals were found to be efficient in binding contaminants in the landfill setting, although the efficiency to bind metals was not directly proven.<sup>8</sup> A number of studies have shown that calcite has the capacity to bind metals in landfill systems,<sup>10, 39-41</sup> with carbonates also forming metal containing aggregates.<sup>42</sup> As a result, the formation of these colloidal aggregates has the potential to limit the mobility of inorganic contaminants (i.e. metals). Additionally, natural colloids that are present are likely to play an important role in nanomaterial sedimentation (and therefore reduced mobility) in landfills, as is the case in other environmental water systems<sup>43</sup>. High salt concentrations, such as those found in the natural leachate samples, are often attributed with nanoparticle aggregation and sedimentation. Conversely, DOC is known to play an important role in ENM stability in other environmental systems, such as surface water. Hence, this may have consequences for the mobility of both naturally occurring nanomaterials and ENM that may

be contained in the system. The DOC concentration in these leachates is in the range of natural environmental waters,<sup>44</sup> where concentrations from 2 – 20 mg/L were shown to stabilize nanomaterials in aqueous solutions over an intermediate time frame.<sup>45</sup> In modeling landfill leachates, the formation of metal-DOC complexes strongly enhanced the leaching potential of some metals, particularly Cu and Pb, in MSWI bottom ash leachates.<sup>18</sup> Therefore, since the MSWI bottom ash leachates had the highest DOC concentrations of the other residues tested (fly ash, sludge), we would expect metals associated with this fraction to be potentially more mobile.

All of the waste materials considered are complex mixtures of stable and unstable minerals and thus are subject to continuous and dynamic changes throughout the weathering process, following biodegradation of organic matter and due to variations in MSWI input over the lifetime of the landfill. Therefore, it is highly unlikely that true thermodynamic equilibrium conditions will be established in short-time leaching tests performed on such complex and heterogeneous wastes. In Switzerland, all these incineration waste slags and residues are stored together in one landfill, which does not make it easy to suggest a uniform leaching behavior of metals either from these diverse materials or over the course of their weathering upon exposure to the environment. However, in the future, wastes could be separated and the leachates individually treated prior to release if there was concern that ENM (or other natural/incidental metal colloids) are especially susceptible to leach from a particular waste fraction. The suitability of this present study to simulate the metal fraction that may be released in the nano size range therefore may be best viewed individually; where each waste residue type can have a different potential natural nano and ENM release profile.

## **5. Implications**

The purpose of studying natural, incidental and ENM particles in landfill leachate solutions (either natural or laboratory prepared) is twofold. Firstly, it places any occurrence of ENM in leachates into perspective, when there are many other incidental particles (some of them metallic) existing in the leachate already. For instance, the additional risk associated with the leaching of ENM from landfills could be better contextualized if we understood whether or not this would be a large increase compared to existing natural particle concentrations. Put in another light, if the mobility of metallic particulate matter was determined to be detrimental for receiving waters, understanding this flux of material from the landfill and into the environment would be beneficial to ensure further treatment of the leachate before release was accomplished. Secondly, by better understanding particle mobility, material flow modeling for ENM can be updated. One of the main compartments that accounts for the final fate of ENM at the end of life stage identified by material flow modeling and life cycle releases, for both slag and construction wastes, was assessed to be landfills.<sup>46-49</sup> In some regards, landfills are considered to be final sinks in these models simply because almost no information on the behavior of nanomaterials in landfills is available. However, if the characteristics of landfill (leachate) can be compared to other natural water systems where fate of

ENM are assessed, this view may be updated and more realistic stance on the flow of ENM from landfills can be made, at least for the landfills for stabilized residues investigated here. As a whole, assessing the toxicity or risk of nano-objects that were leached from landfills for incineration waste was not our explicit goal and we did not perform any experiments that would implicitly justify a suggestion that there is a risk from these particles or other ENM which could be released from waste residues in the future. Since none of the tests we performed could definitely specify that the particles we observed were engineered particles, we can also not suggest if the use of ENM in products either increases the amount of ENM that will be in waste materials or that ENM will leach to a greater or lesser extent than other metallic particulate matter from landfills for incineration residues. Ultimately, regardless of particle source (i.e. natural, incidental or ENM), the mobilization of metals in the landfill is controlled by multiple complex geochemical facets dominated by solubility of the host material and carbonate buffering of the pH opposed to availability of particles put into the system or the liquid/recharge of the percolating water.

## Acknowledgements

We would like to thank ZAB Deponie in Flawil, Switzerland, the landfill operator who gave us access to collect samples on multiple occasions.

## References:

1. eurostat Municipal waste by waste operations.  
[http://appsso.eurostat.ec.europa.eu/nui/show.do?dataset=env\\_wasmun&lang=en](http://appsso.eurostat.ec.europa.eu/nui/show.do?dataset=env_wasmun&lang=en)
2. Swiss Federal Office for the Environment (FOEN) Waste disposal methods, municipal solid waste incineration <http://www.bafu.admin.ch/abfall/01495/01496/index.html?lang=en>
3. Turconi, R.; Butera, S.; Boldrin, A.; Grosso, M.; Rigamonti, L.; Astrup, T., Life cycle assessment of waste incineration in Denmark and Italy using two LCA models. *Waste Management & Research* **2011**, *0*, (0), 1-13.
4. Astrup, T. F.; Tonini, D.; Turconi, R.; Boldrin, A., Life cycle assessment of thermal waste-to-energy technologies: review and recommendations. *Waste management* **2015**, *37*, 104-115.
5. Chandler, A. J.; Eighmy, T.; Hjelmar, O.; Kosson, D.; Sawell, S.; Vehlow, J.; Van der Sloot, H.; Hartlén, J., *Municipal solid waste incinerator residues*. Elsevier: 1997; Vol. 67.
6. Herczeg, M., Municipal waste management in Switzerland. *European Environment Agency* **2013**.
7. Swiss Federal Office for the Environment (FOEN) Waste Disposal Methods, landfilling.  
<http://www.bafu.admin.ch/abfall/01495/01497/index.html?lang=en>
8. Baun, D. L.; Christensen, T. H., Speciation of heavy metals in landfill leachate: a review. *Waste management & research* **2004**, *22*, (1), 3-23.
9. Hennebert, P.; Avellan, A.; Yan, J.; Aguerre-Chariol, O., Experimental evidence of colloids and nanoparticles presence from 25 waste leachates. *Waste management* **2013**, *33*, (9), 1870-1881.
10. Matura, M.; Ettler, V.; Klementová, M., Transmission electron microscopy investigation of colloids and particles from landfill leachates. *Waste Management & Research* **2012**, *30*, (5), 530-541.

11. Gounaris, V.; Anderson, P. R.; Holsen, T. M., Characteristics and environmental significance of colloids in landfill leachate. *Environmental Science & Technology* **1993**, *27*, (7), 1381-1387.
12. Jensen, D. L.; Christensen, T. H., Colloidal and dissolved metals in leachates from four Danish landfills. *Water Research* **1999**, *33*, (9), 2139-2147.
13. Jensen, D. L.; Ledin, A.; Christensen, T. H., Speciation of heavy metals in landfill-leachate polluted groundwater. *Water Research* **1999**, *33*, (11), 2642-2650.
14. Klein, T.; Niessner, R., Characterization of heavy metal containing hydrocolloids from seepage water of a municipal waste disposal with ultrafiltration and flow field-flow fractionation. *Vom Wasser. Weinheim* **1996**, *87*, 373-385.
15. Wei, Y.; Shimaoka, T.; Saffarzadeh, A.; Takahashi, F., Mineralogical characterization of municipal solid waste incineration bottom ash with an emphasis on heavy metal-bearing phases. *Journal of Hazardous Materials* **2011**, *187*, (1), 534-543.
16. Eusden, J. D.; Eighmy, T. T.; Hockert, K.; Holland, E.; Marsella, K., Petrogenesis of municipal solid waste combustion bottom ash. *Applied Geochemistry* **1999**, *14*, (8), 1073-1091.
17. Chimenos, J.; Segarra, M.; Fernandez, M.; Espiell, F., Characterization of the bottom ash in municipal solid waste incinerator. *Journal of hazardous materials* **1999**, *64*, (3), 211-222.
18. Dijkstra, J. J.; van der Sloot, H. A.; Comans, R. N., The leaching of major and trace elements from MSWI bottom ash as a function of pH and time. *Applied Geochemistry* **2006**, *21*, (2), 335-351.
19. Meima, J. A.; Comans, R. N., The leaching of trace elements from municipal solid waste incinerator bottom ash at different stages of weathering. *Applied Geochemistry* **1999**, *14*, (2), 159-171.
20. Saffarzadeh, A.; Shimaoka, T.; Wei, Y.; Gardner, K. H.; Musselman, C. N., Impacts of natural weathering on the transformation/neof ormation processes in landfilled MSWI bottom ash: a geoenvironmental perspective. *Waste management* **2011**, *31*, (12), 2440-2454.
21. Köster, R.; Wagner, T.; Delay, M.; Frimmel, F. H., Release of Contaminants from Bottom Ashes- Colloid Facilitated Transport and Colloid Trace Analysis by Means of Laser-Induced Breakdown Detection (LIBD). In *Colloidal Transport in Porous Media*, Springer: 2007; pp 251-272.
22. Part, F.; Gressier, S.; Huber-Humer, M.; Gzásó, A. *Environmentally relevant aspects of nanomaterials at the end-of-life phase-Part II: Waste recycling and disposal*; 2015.
23. Part, F.; Zecha, G.; Causon, T.; Sinner, E.-K.; Huber-Humer, M., Current limitations and challenges in nanowaste detection, characterisation and monitoring. *Waste Management* **2015**, *43*, 407-420.
24. Mueller, N. C.; Buha, J.; Wang, J.; Ulrich, A.; Nowack, B., Modeling the flows of engineered nanomaterials during waste handling. *Environmental Science: Processes & Impacts* **2013**, *15*, (1), 251-259.
25. Walser, T.; Limbach, L. K.; Brogioli, R.; Erismann, E.; Flamigni, L.; Hattendorf, B.; Juchli, M.; Krumeich, F.; Ludwig, C.; Prikopsky, K., Persistence of engineered nanoparticles in a municipal solid-waste incineration plant. *Nature nanotechnology* **2012**, *7*, (8), 520-524.
26. Walser, T.; Gottschalk, F., Stochastic fate analysis of engineered nanoparticles in incineration plants. *Journal of Cleaner Production* **2014**, *80*, 241-251.
27. Mitrano, D. M.; Motellier, S.; Clavaguera, S.; Nowack, B., Review of nanomaterial aging and transformations through the life cycle of nano-enhanced products. *Environment international* **2015**, *77*, 132-147.
28. Roes, L.; Patel, M. K.; Worrell, E.; Ludwig, C., Preliminary evaluation of risks related to waste incineration of polymer nanocomposites. *Science of the total environment* **2012**, *417*, 76-86.
29. Buha, J.; Mueller, N.; Nowack, B.; Ulrich, A.; Losert, S.; Wang, J., Physical and chemical characterization of fly ashes from swiss waste incineration plants and determination of the ash fraction in the nanometer range. *Environmental science & technology* **2014**, *48*, (9), 4765-4773.



30. Sun, T.; Bornhöft, N. A.; Hungerbühler, K.; Nowack, B., Dynamic Probabilistic Modelling of Environmental Emissions of Engineered Nanomaterials. *Environmental Science & Technology* **2016**, *50*, (9), 4701-4711.
31. EN, B., Characterisation of Waste-Leaching-Compliance Test for Leaching of Granular Waste Materials and Sludges: Part 2. One Stage Batch Test at a Liquid to Solid Ratio of 10 L/kg for Materials with Particle Size below 4 mm (without or with Size Reduction). **2002**.
32. Filipe, V.; Hawe, A.; Jiskoot, W., Critical evaluation of Nanoparticle Tracking Analysis (NTA) by NanoSight for the measurement of nanoparticles and protein aggregates. *Pharmaceutical research* **2010**, *27*, (5), 796-810.
33. Burkhardt, M.; Sinnet, B.; Kaegi, R., Leitsubstanz für Nanopartikel im Deponiesickerwasser. *Aqua & Gas* **2015**, (12), 40-47.
34. Yang, Y.; Doudrick, K.; Bi, X.; Hristovski, K.; Herckes, P.; Westerhoff, P.; Kaegi, R., Characterization of food-grade titanium dioxide: the presence of nanosized particles. *Environmental science & technology* **2014**, *48*, (11), 6391-6400.
35. Weir, A.; Westerhoff, P.; Fabricius, L.; Hristovski, K.; von Goetz, N., Titanium dioxide nanoparticles in food and personal care products. *Environmental Science & Technology* **2012**, *46*, (4), 2242-2250.
36. Impellitteri, C. A.; Harmon, S.; Silva, R. G.; Miller, B. W.; Scheckel, K. G.; Luxton, T. P.; Schupp, D.; Panguluri, S., Transformation of Silver Nanoparticles in Fresh, Aged, and Incinerated Biosolids. *Water research* **2013**, *47*, (12), 3878-3886.
37. Meier, C.; Voegelin, A.; Pradas del Real, A.; Sarret, G.; Mueller, C. R.; Kaegi, R., Transformation of Silver Nanoparticles in Sewage Sludge during Incineration. *Environmental science & technology* **2016**, *50*, (7), 3503-3510.
38. Tanaka, N., *Safely Construction and Management of Municipal Solid Waste Landfill*. Gihodo Press: Tokyo, 2000.
39. Strnad, L.; Ettler, V.; Mihaljevic, M.; Hladil, J.; Chrastny, V., Determination of Trace Elements in Calcite Using Solution and Laser Ablation ICP-MS: Calibration to NIST SRM Glass and USGS MACS Carbonate, and Application to Real Landfill Calcite. *Geostandards and Geoanalytical Research* **2009**, *33*, (3), 347-355.
40. Ettler, V.; Matura, M.; Mihaljevič, M.; Bezdička, P., Metal speciation and attenuation in stream waters and sediments contaminated by landfill leachate. *Environmental Geology* **2006**, *49*, (4), 610-619.
41. Ettler, V.; Zelená, O.; Mihaljevič, M.; Šebek, O.; Strnad, L.; Coufal, P.; Bezdička, P., Removal of trace elements from landfill leachate by calcite precipitation. *Journal of Geochemical Exploration* **2006**, *88*, (1), 28-31.
42. Baumann, T.; Fruhstorfer, P.; Klein, T.; Niessner, R., Colloid and heavy metal transport at landfill sites in direct contact with groundwater. *Water research* **2006**, *40*, (14), 2776-2786.
43. Quik, J. T.; Stuart, M. C.; Wouterse, M.; Peijnenburg, W.; Hendriks, A. J.; van de Meent, D., Natural colloids are the dominant factor in the sedimentation of nanoparticles. *Environmental Toxicology and Chemistry* **2012**, *31*, (5), 1019-1022.
44. Ishikawa, T.; Gumiri, S., Dissolved organic carbon concentration of a natural water body and its relationship to water color in Central Kalimantan, Indonesia. *Limnology* **2006**, *7*, (2), 143-146.
45. Mitrano, D. M.; Ranville, J.; Bednar, A.; Kazor, K.; Hering, A. S.; Higgins, C., Tracking dissolution of silver nanoparticles at environmentally relevant concentrations in laboratory, natural and processed waters using single particle ICP-MS (spICP-MS). *Environmental Science: Nano* **2014**, *1*, (3), 248-259.
46. Mueller, N.; Nowack, B., Exposure modeling of engineered nanoparticles in the environment. *Environmental Science and Technology* **2008**, *42*, (12), 4447-4453.

47. Gottschalk, F.; Scholz, R.; Nowack, B., Probabilistic material flow modeling for assessing the environmental exposure to compounds: Methodology and an application to engineered nano-TiO<sub>2</sub> particles. *Environmental Modelling & Software* **2010**, *25*, (3), 320-332.
48. Sun, T. Y.; Gottschalk, F.; Hungerbühler, K.; Nowack, B., Comprehensive probabilistic modelling of environmental emissions of engineered nanomaterials. *Environmental Pollution* **2014**, *185*, 69-76.
49. Keller, A. A.; McFerran, S.; Lazareva, A.; Suh, S., Global life cycle releases of engineered nanomaterials. *Journal of Nanoparticle Research* **2013**, *15*, (6), 1-17.

## Chapter 2

# Aggregation and Particle Mass Distribution of nano-Au in Incineration Landfill Leachates

### Abstract

Numerous nanometrology techniques have been developed in recent years to determine the size, concentration and a number of other characteristics of engineered nanomaterials (ENM) in environmental matrices. Among the many available techniques, Nanoparticle Tracking Analysis (NTA) can measure individual particles to create a size distribution and measure the particle number. Therefore, we explore the possibility to use these data to calculate the particle mass distribution. Additionally, we further developed the NTA methodology to explore its suitability for analysis of ENM in complex matrices by measuring ENM agglomeration and sedimentation in municipal solid waste incineration landfill leachates over time. 100 nm Au ENM were spiked into DI H<sub>2</sub>O, synthetic and natural leachates. We present the possibility of measuring ENM in the presence of natural particles based on differences in particle refractivity indices, delineate the necessity of creating a calibration curve to adjust the given NTA particle number concentration and determined the instruments linear range under different conditions. By measuring the particle size and the particle number distribution, we were able to calculate the ENM mass remaining in suspension. By combining these metrics together with TEM analyses, we could assess the extent of both homo- and heteroagglomeration as well as particle sedimentation. Reporting both size and mass based metrics is common in atmospheric particle measurements but now the NTA can give us the possibility to apply the same approach also to aqueous samples.

### 1. Introduction

Qualitative and quantitative identification of engineered nanomaterials (ENM) is complex, as these materials have very low mass, can be highly dynamic in terms of particle agglomeration and reactivity, co-exist with ambient particles in the same size range (i.e. natural analogs) and also often coincide with molecules or macro sized counterparts of the same chemical composition.<sup>1,2</sup> Due to these difficulties, there are limited options to measure ENM size dispersions in natural samples. One of the most promising and prominent solutions which allows the user to measure individual particles at very low (ppt) concentrations

in complex samples is spICP-MS. In recent years this technique has received wide spread attention for researchers studying ENM from environmental samples, biological samples, and ENM release from products.<sup>3,4</sup> However, better understanding particle agglomeration dynamics using this technique is in its infancy.<sup>5,6</sup> Transmission electron microscopy (TEM) is another popular option to visualize particle size distribution and agglomeration with particles, even in complex media, but without being quantitative, the technique offers little in terms of being able to robustly characterize the ENM in a system of interest, though validation methods for quantifying particle number have been investigated.<sup>7</sup> Field flow fractionation, while requiring extensive method development, is another analytical option for researchers studying ENM in natural systems.<sup>8-10</sup> While not measuring particles on an individual basis like the previously mentioned techniques, the ability to provide an initial particle size distribution, ENM agglomeration and/or complexation to natural materials is possible. Conversely, some commonly used techniques, such as dynamic light scattering (DLS), can provide misleading results since the average particle size can easily be skewed by a few large particles in a mixture compared to many small particles.<sup>11</sup> In addition to this, the technique is not material specific and therefore cannot differentiate between natural particles in solution or agglomerates of natural and engineered particles.

The NanoSight (i.e. nanoparticle tracking analysis, NTA) offers advantages to measuring ENM in complex systems for its ease of use and unique measurement capabilities. The instrument differs from other light scattering techniques (e.g. DLS) in that it can measure individual particles (opposed to the entire particle population) and that an image of the particles' scattering (although not the particle itself) is recorded.<sup>12</sup> Since the optical configuration employed in NTA analysis allows NM to be simultaneously tracked and analyzed on an individual basis, the resulting data is not an intensity weighted mean but rather a high resolution particle size distribution analysis. Additionally, different materials can be distinguished through their different refractive indices and, importantly, particle concentrations can be measured.<sup>13</sup> These aspects of measurement offer a few advantages; 1) the particle size distribution will not be dominated by the larger, more intensely scattering particles as with DLS, 2) estimating the concentration of particles is possible based on the number of individual particles tracked and extrapolating from the assumed scattering volume calculated from the dimensions of the field of view and the depth of the instruments laser beam and 3) particles with varying light scattering potential can be measured separately by adjusting the camera focusing metrics (e.g. aperture, shutter, brightness, gain etc.) accordingly and analyzing the same sample over multiple runs. Each of these points are advantageous for researchers studying ENM in natural systems, where the aqueous suspensions are often complex and understanding changes in particle size and mass are important characteristics to measure. Until now, extensive method development to better understand a number of these features specifically in particle and mineral rich media has not been exploited, and so while it offers many promising features, the protocols remain to be fully validated. However, the technique does not provide details of particle morphology and there have been limited instances where the technique has been used in complex, natural systems. Some examples of where NTA was implemented in more complex matrices include the study of fullerenes in river water,<sup>14</sup> SiO<sub>2</sub> nanoparticles in biological serum,<sup>15</sup>

and Gallego-Urrea et al. reviewed the applicability of particle-tracking analysis for the suitability of nanoparticles in a range of matrices including environmental, biological and food samples.<sup>16</sup>

To test the applicability of using the NTA to study the stability of ENM in natural environments, Au ENM (used as tracers) were studied to estimate the agglomeration potential of ENM in incineration landfill leachates. Landfills were identified to be one of the predominant compartments that accounts for the final fate of ENM at the end of life stage by material flow modeling and life cycle releases.<sup>17-21</sup> In the current models, landfills are considered to be final sinks because almost no information on the behavior of nanomaterials in landfills is available.

Natural colloids are a ubiquitous component of natural water systems and are likely to affect the fate of NM, namely by heteroagglomeration and subsequent settling. In most studies investigating the effect(s) of colloids on ENM stability, ENM interaction with natural organic matter (NOM) has been the most intensely studied even though this fraction of natural colloids is relatively small compared with inorganic solids and larger biopolymers (e.g. biomass).<sup>22-24</sup> In a recent study by Mitrano et. al, the authors investigated the mobility of natural (nano)particles from landfills for municipal solid waste incineration (MSWI) residues and concluded that understanding the geochemical weathering of the landfill slag was essential in relating the type, extent and timing of particulate release from the landfill.<sup>25</sup> Therefore, landfill leachate can be considered a potential source to transport both colloidal and nanoparticulate matter into the environment when they are emitted from landfill leachate.

The overall goals of the study were twofold; firstly to improve particle quantification using the NTA to study ENM behavior in complex matrices and secondly to suggest ENM stability in landfill leachates from landfills containing MSWI residues. In terms of method development, we investigated the effects of solution chemistry on measuring particle size and particle number as well as the linear range of instrument detection in these solutions. Additionally, we transformed the NTA raw output (in terms of size and particle number) to mass of analyte to better study the agglomeration of particles over time. The stability of ENM that are deposited into landfills can be analyzed for their agglomeration potential, which in part can help to determine if the particles are likely to remain in the landfill through agglomeration and deposition or be emitted with the leachate as freely dispersed particles. This stability analysis was conducted with pristine Au ENM suspended in synthetic and natural landfill leachate solutions to help elucidate the influence of ionic composition and presence of NOM. Three types of solutions were analyzed including 1) DI water as a control, 2) leachate collected from a landfill for MSWI residues and 3) “synthetic leachate” made from only the major ions as measured in the natural leachate sample. The purpose of creating the synthetic leachate was to measure the effect of major ions on the stability of the ENM without the presence of NOM or other suspended solids found in the natural leachate sample. We then studied the stability of the particles suspended in this solution over time by following changes in particle size (distribution) and mass of analyte associated with each size category using the NTA instrument as well as visually identifying ENM aggregates and complexes using transmission electron microscopy (TEM).

## 2. Materials and Methods

### 2.1 Standards and Nanomaterials

18 M-ohm DI water was used throughout the study for ENM spiked into water and for making up the synthetic leachate solution. 100 nm citrate stabilized metallic Au (Nanocomposix) were used for calibration and in all experiments in this study. Size distributions corresponded well to TEM analysis provided by the manufacturer and NTA measurements completed in house, with average particle size being measured as  $103 \pm 11$  nm and  $103.9 \pm 0.6$  nm for each measurement, respectively (Figure S1). The hydrodynamic diameter, as measured by DLS, was  $124.7 \pm 5.6$  nm and the zeta potential was -26.mV. The Au concentration of the stock solution was given by the manufacturer but was verified via total Au analysis (ICP-MS). Given the solution concentration and particle size, we could therefore calculate the total particle number concentration in the stock solutions and make appropriate dilutions (e.g. for the calibration curve) based on this information.

### 2.2 Water Quality Analysis: Natural and Laboratory Prepared Leachate Samples

A subset of the same MSWI leachate samples used in Mitrano et. al. were also used for this current study.<sup>25</sup> Landfill samples were taken from the ZAB Deponie, located in Flawil, Switzerland. In this landfill, MSWI residues (slag from both the bottom ash and fly ash) as well as wastewater incineration residues (sludge incineration) are collected. The leachate samples were taken directly from the main outflow into the settling basin (hereafter labeled “natural leachate”). Natural leachate samples were filtered through a 0.45  $\mu$ m filter (Whatman; cellulose nitrate membrane) before spiking ENM for stability studies to remove particles too large to be measured by the NTA and that would potentially obscure ENM observation.

The pH of the natural leachate was measured by a Metrohm 827 pH meter and found to be 7.8 +/- 0.3. Samples were prepared for dissolved organic carbon (DOC) analysis with filtration through a 0.45  $\mu$ m filter (Whatman; cellulose nitrate membrane) into glass bottles and analyzed by a commercial laboratory (Bachema AG). An initial survey of water chemistry parameters of the leachate filtered through a 0.45  $\mu$ m filter was conducted to determine which ions were present in significant concentrations by IC analysis for anions ( $F^-$ ,  $Cl^-$ ,  $NO_2^-$ ,  $Br^-$ ,  $NO_3^-$ ,  $PO_4^{3-}$  and  $SO_4^{2-}$ ) and ICP-OES analysis for cations ( $Na^+$ ,  $K^+$ ,  $Mg^{2+}$  and  $Ca^{2+}$ ). Bachema AG measured the final selection of major ions that were identified as significant contributors to the solution chemistry with IC measurements ( $Cl^-$  and  $SO_4^{2-}$ ) and ICP-OES analysis ( $Na^+$ ,  $Ca^{2+}$ ). We derived a simulated leachate to examine the stability of nanoparticles consisting of the major ions existing in the natural leachate sample (e.g.  $Na^+$ ,  $Ca^{2+}$ ,  $Cl^-$  and  $SO_4^{2-}$ ). We collected the landfill leachate on three separate occasions, in order to work with “fresh” leachate so we could be assured that the particulate composition, pH, etc. was as accurate as possible without sedimentation as we were working on the method development. The freshest (third) of these samples was used as the natural leachate sample in

this study, where the final results were collected together over a short time span, but the synthetic leachate composition was derived from the first sampling time point at landfill when all of the water chemistry parameters were measured, hence the small differences between the total salts between the “natural” and “synthetic” leachate solutions. However, the overall magnitude of all the components was similar between the two leachates used in this study. See Table S1 for water chemistry of natural and synthetic leachates.

### *2.3 NanoSight (NTA) Analysis*

NTA measurements were performed with a NanoSight NS500 (NanoSight, Amesbury, United Kingdom). The samples were injected in the sample chamber with sterile syringes by means of syringe pump with a constant rate of injection. All measurements were performed at room temperature. 100 nm Au nanoparticles were analyzed first in DI water and then in the leachates. The software used for capturing and analyzing the data was NTA 3.0. Triplicate samples were measured for 4 min, with average valid particle tracks ranging from 50 to 5000 for each analysis. The camera level was set to 1 for every measurement to ensure standardized analysis and to eliminate possible bias induced by further adjusting parameters for each sample, but the camera focus was adjusted daily depending on the sample. The camera level determines the brightness of the image and thus partially is responsible for the particles that are selected to be tracked by the NTA. The levels use preset combinations of shutter and gain. For high sensitivity camera systems, the camera levels also incorporate appropriate thresholding pixel levels to improve image contrast. With these conditions, that were made constant throughout our analysis, we visually noted the same brightness of the ENM in solution across experimental sets and did not observe any additional (i.e. natural) particles during any of the measurements.

Each influx of sample and video produced a histogram depicting particle size and concentration. The information regarding individual particles were exported to an excel sheet for further data processing, but the concentration reported by the NTA was taken directly without any additional adjustment. Additionally, we calculated the total mass of analyte (particles) in each video distributing the total particle number proportionally over the particle size distribution histogram. In this way, we could determine if a mass balance was kept constant over the analysis time. Given these test conditions, we could determine if the total analyzed concentration was decreasing and particles were not being measured (e.g. from sedimentation) or simply if the NTA was recording fewer, larger particles.

### *2.4 Calibration of the NanoSight (NTA)*

The calibration of the NTA was conducted for two main reasons; 1) to define the linear range in terms of particle concentration and 2) to determine if the solution chemistry (or matrix) had an influence on the particle number measured at various concentrations. To achieve these goals, the three different

experimental solutions (DI H<sub>2</sub>O, synthetic leachate and natural leachate) were spiked with Au ENM in five particle concentrations including: a blank (i.e. no added ENM),  $0.25 \times 10^8$  particles/mL,  $0.5 \times 10^8$  particles/mL,  $1 \times 10^8$  particles/mL and  $1.5 \times 10^8$  particles/mL. In terms of mass based concentration, for 100 nm particles this equates to approximately 150 – 800  $\mu\text{g/L}$ . These concentrations were based on diluting the stock Au ENM solution (particle concentration and size given by the manufacturer and determined in house, see section 2.1) into the appropriate matrix. The samples were prepared in triplicate and analyzed directly after preparation. Two metrics were considered in this analysis, particle size (distribution) and measured concentration. Particle size evaluations were performed to ensure that the instrument was capable of successfully identifying the pristine particle size in various solution chemistries and that no agglomeration of the ENM was occurring over a very short period of time (i.e. T=0 hr measurements). The concentration measured by the NTA instrument could be compared to the expected (spiked) concentration into each solution, where any deviation from the 1:1 spiked particle number to measured particle number ratio would indicate an adjustment would need to be made to correct the concentration of particles measured by the NTA.

### *2.5 Stability of ENM in MSWI Landfill Leachates*

Stability tests were conducted at  $0.5 \times 10^8$  Au particles/mL, as this was determined to be within the appropriate linear range of particle concentrations for the NTA under our test conditions. For each of the three water chemistries investigated, triplicate samples were prepared and analyzed over a series of time points up to 24 hours. At time zero, samples were spiked with the appropriate amount of Au particles into a 50 mL polypropylene vial containing the solution of interest and shaken end-over-end by hand for 30 seconds. Using a polypropylene syringe, an aliquot of the sample was then taken 1 cm below the surface of the water/air interface and analyzed by NTA as described in Section 2.3. The vials then remained standing upright and still for all subsequent time points being sampled in the same manner for NTA analysis for each time point. This method allowed us to investigate three metrics: 1) particle size (change) over time, 2) particle number remaining in solution over time and 3) particle or particle agglomerate settling over time. The first metric was determined directly by the NTA and therefore we have simply re-plotted the size output reported from the instrument for this metric. Particle concentration was also directly measured by the NTA but this data is reported both as the raw output and as adjusted by the calculated calibration curve to correct for particle number measurement differences in varying solution chemistries; described in more detail in Section 2.6.



### 2.6 NanoSight (NTA) Data Evaluation

Individual valid track measurements (i.e. particle measurements) were exported directly from the NTA software into excel via a .csv data file. These individual particle measurements were then plotted into a histogram in excel. The particle number was measured directly by the NTA software and the number was taken directly from the report generated by the NTA without any adjustment. This particle measurement data was also used to generate the calibration curve for Au ENM suspended in the various waters at different known particle concentrations. The slope of each calibration curve was used as a “scaling factor” to adjust the particle number concentration and/or mass concentration appropriately in experimental sets. The raw number concentration and the mass concentration was multiplied by the scaling factor to adjust for instrumental differences of particles in different matrices. To calculate the mass concentration from the particle number distribution, the following steps were taken (see Equation 1): 1) make the particle size distribution histogram based on the NTA output, 2) proportionally distribute the total particle number across the particle size distribution histogram to have the number of particles in a given size range (histogram bin size, 2 nm), 3) multiply the number concentration in each bin by the associated particle diameter and transform the diameter metric into a volume metric, 4) sum all mass calculations from all bins in the histogram and finally 5) multiply by the elemental mass (in this case, Au).

$$m = \rho \sum_{i=1}^n \left( \bar{V}_{c,i} \frac{1}{6} \pi d_i^3 \right)$$

**Equation 1:** Calculations for converting the particle size distribution histogram and particle number generated from the NTA into mass of analyte measured. The diameter of particles in a particular bin  $i$  ( $d_i$ ) is multiplied by the number concentration of gold particles in a particular bin ( $\bar{V}_{c,i}$ ) and transformed from diameter to volume. This value is then summed for all bins in the histogram and multiplied by the particle density to determine the total mass of analyte in the system.

### 2.7 Transmission Electron Microscopy (TEM)

Pristine 100 nm Au nanoparticles were spiked at the same concentration as in the NanoSight analysis (i.e. approximately 1 mg/L or  $0.5 \times 10^8$  particles/mL for 100 nm Au ENM) into each of the leachate samples. Grids were prepared for the DI H<sub>2</sub>O, synthetic and natural leachate samples at  $T = 0$  hr and  $T = 4$  hr. At each time point, sample vials were vigorously shaken and 3 mL of the sample was transferred to a polypropylene vial where particles were deposited directly onto TEM grids by centrifugation using a swinging bucket rotor, with rotation speed of 45000 rpm for 1 h; conditions which completely deposited all particles  $> 10$  nm in size onto the carbon-coated Cu TEM grid. Samples were gently washed to remove residual salt by moving the grid through a drop of MilliQ water on a piece of parafilm 3 – 5 times. The centrifugation TEM grid preparation alleviates many artifacts that disrupt typical drop deposition TEM grid preparation. Therefore, this method gives us additional confidence that we can identify agglomeration of

particles in the native solution opposed to any drying effects from traditional drop deposition TEM grid preparation.

Particle images were obtained via scanning transmission electron microscopy (STEM) using a JOEL 2200FS TEM/STEM operated at 200 kV. The nominal spot size of the STEM probe was 0.7 nm using a beam convergence angle of 10.8 mrad. High-angle annular dark field STEM micrographs were recorded using an inner detector angle of 100 mrad, while the bright-field STEM images were recorded with a detector angle of 15 mrad.

### **3. Results**

#### *3.1 Measurement of ENM in the presence of natural particles*

The NTA camera settings can be set to measure particles with a lower refractivity, such as the natural particles present in landfill leachate, as shown in our previous work<sup>25</sup> and in Figure 1, panel A. In this case, the leachate was filtered through a 0.45  $\mu\text{m}$  filter and particles are visible in the solution up to that size cut off. When the settings are adjusted to those that can properly measure Au ENM (i.e. a lower camera level to capture only the brightest particles), no natural particles were observed in the same natural leachate sample when leachate samples captured at low camera level with no spiked Au ENM (Figure 1 B, red trace). However, when Au ENM are spiked into the solution, a similar distribution is observed for the main particle size distribution in both DI H<sub>2</sub>O and the landfill leachate (yellow and green traces, respectively), indicating that the additional natural particles do not disrupt the direct measurement of ENM due to the change in matrix. Neither do we observe additional particles in the Au ENM particle distribution when the particles are spiked into the natural leachate compared to DI H<sub>2</sub>O. In the case of the Au ENM spiked into the leachate, there are only some slightly larger particles observed due to Au ENM homoagglomeration between spiking the solution and analysis. This exercise confirms our ability to detect Au ENM in the presence of natural particles in our test matrices.

In all blank samples (i.e. those that did not contain any added Au ENM), including the natural leachate, the number of observed particles under typical nanoparticle analysis conditions was close to zero or zero. This indicates that our method to observe only the ENM while avoiding measurement of the natural particles in solution with a lower refractivity index was successful and therefore we do not measure a significant number of false positives (i.e. natural particles appearing as ENM in the results).

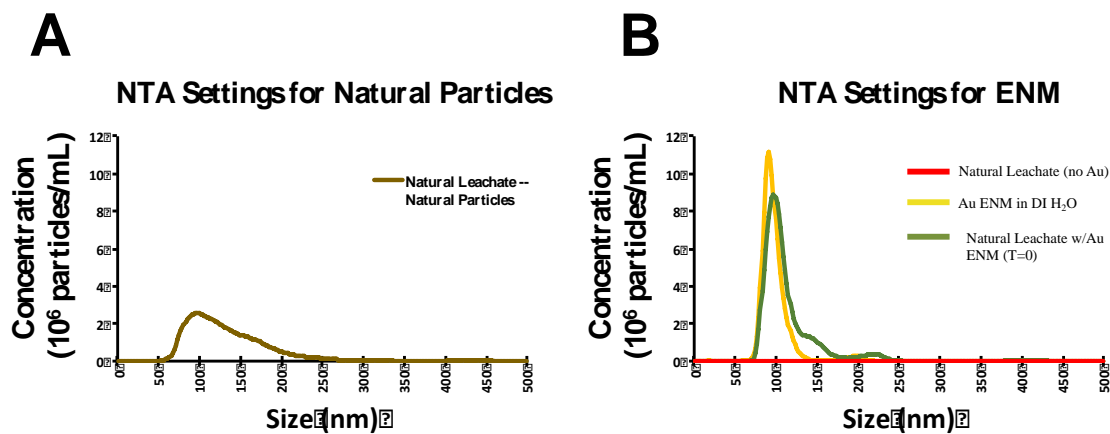


**Figure 1:** (A) NTA set to measurement conditions optimal to measure natural particles in solution, as in the natural landfill leachate from MSWI residues, filtered through a 0.45  $\mu\text{m}$  filter. (B) NTA camera level set to a lower level intend to measure bright particles (i.e. those with a high refractivity index) but still measuring the same leachate as panel A. Natural leachate with only natural particles (red trace), Au ENM spiked into DI H<sub>2</sub>O (yellow trace) and Au ENM spiked into natural leachate (green trace) are shown together. Here it is seen that natural particles in the landfill leachate are only visible on the higher camera level in Panel A, but not when the camera level is adjusted lower in panel B (red trace). However, spiked Au ENM are clearly detected in both DI H<sub>2</sub>O and the natural leachate with no interference (e.g. additional background) from the natural particles in the leachate.

### 3.2 Calibration of ENM Concentration for the NTA

The NTA calibration of ENM concentration served two purposes; 1) to determine the linear range between measured and expected concentrations of ENM in different solution compositions and 2) to identify the scaling factor of this relationship when it deviated from the expected 1:1 ratio of added particle number to measured particle number. The particle number was taken as given by the NTA 3.0 software. As shown in Figure 2A, a liner relationship is exhibited for all sample solutions with a particle concentration below  $1 \times 10^8$  particles/mL and the standard deviation between triplicate measurements was relatively small. Measured particle concentrations deviated from the linear calibration line above  $1 \times 10^8$  particles/mL.

Despite defining a linear range for particle number concentrations in each of the solutions, in every instance there was a higher measured particle concentration compared to the known particle concentration. Therefore, in every case the steeper slope exhibited by the calibration line represents an overestimation in particle number concentration and therefore the particle number measured by the NTA in the experimental samples had to be appropriately scaled to derive the correct particle number in solution by using the slope of the linear portion of the calibration curve. This scaling factor was different for each of the three solutions measured. The exaggeration in particle number was highest for the DI H<sub>2</sub>O samples (up to a factor of three) but leachate samples were also overestimated by approximately a factor of two. A similar particle number concentration was observed in both the synthetic and natural leachate samples. Overall, this indicates that the matrix can play a large role in how the NTA software ultimately calculates particle number and so a

calibration curve should be made for each new solution of interest to derive the correct scaling factor during experimental tests.

### 3.3 NTA Analysis of ENM Particle Stability in Incineration Waste Landfill Leachate

ENM stability experiments were conducted with a particle concentration of  $0.5 \times 10^8$  particles/mL since this was within the linear range identified by the calibration for all solutions of interest. The particle size distribution at each dilution point and in every water chemistry was consistent and with relatively good agreement to the average primary particle size (Figure 2 B-D). The NTA did appear to slightly overestimate the number of larger sized particles in the distribution (as evidenced by the longer whiskers for the larger particle diameters in Figure 2 B-D) even though the distribution was more Gaussian when measured by TEM (Figure S1). Nevertheless, since the measured particle size was consistent across all dilution factors and across all solutions investigated, the discrepancy in measured versus known particle number cannot simply be due to agglomeration.

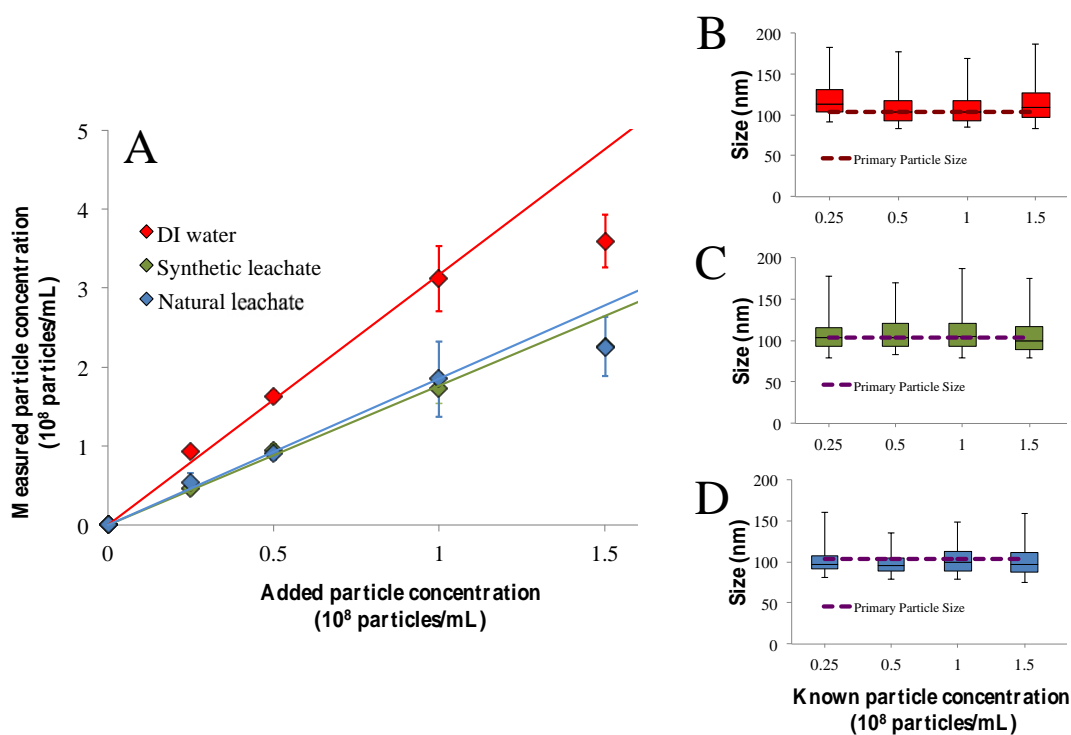


**Figure 2:** Particle number concentration calibration curves of Au nanoparticles suspended in DI H<sub>2</sub>O, synthetic and natural MSWI landfill leachates compared to the expected 1:1 know particle number to measured particle number ratio (A). A linear regression line of each of the calibration curves is presented through the linear portion of the data set (0 to  $1 \times 10^8$  particles/mL) with a predicted extension of the regression line until  $1.5 \times 10^8$  particles/mL to exemplify how these data are not in the linear range. Particle size distribution of particles measured at different dilutions in DI H<sub>2</sub>O (B), synthetic (C) and natural MSWI (D) leachates. For the box plots, 25% quantiles appear within the box plot with average particle size indicated by black line therein. Whiskers represent 95% of particle size distribution (outliers not shown). Purple dashed lines indicate Au ENM primary particle size (100 nm).

### 3.3.1 ENM Stability – Average Particle Size and Particle Size Distribution

The average particle size in DI H<sub>2</sub>O remained constant throughout the entire experimental timeline, up to 24 hr (Figure 3A). This indicates that at this concentration and with no additional salts or particulate matter, the particles are stable in solution for extended periods of time. In synthetic and natural landfill leachates (Figure 3, panels B and C), the average particle size generally increased over the course of the 24 hr experiment.

Not only did the average size increase in the leachate samples, but the size distribution became much wider as well, indicating agglomeration of the primary particles over time. Compared to the ENM distribution in DI H<sub>2</sub>O, which remains narrow and constant, the particle size distribution for synthetic and natural landfill leachates began to broaden immediately after particle spiking. The relative rate of agglomeration appeared somewhat slower in the synthetic leachate compared to the natural leachate. Differences in solution chemistry, especially differences in DOC and salt concentrations, can contribute to the stability of the particles. In the case of the synthetic leachate, since the solution is made entirely of added salt, homoagglomeration is the only possibility for the measured increase in size. However, in the natural leachate, heteroagglomeration between the Au ENM and natural material is possible. Since under the conditions we are operating the NTA only the ENM are visible, a single ENM or ENM cluster adhered to natural particles will move more slowly (increased particle size equals decreased speed of Brownian motion) and therefore be recorded as a (single) larger particle. Indeed, in the natural leachate sample the average particle size is larger than in the synthetic leachate sample. (see Figure S2 and Table S2).

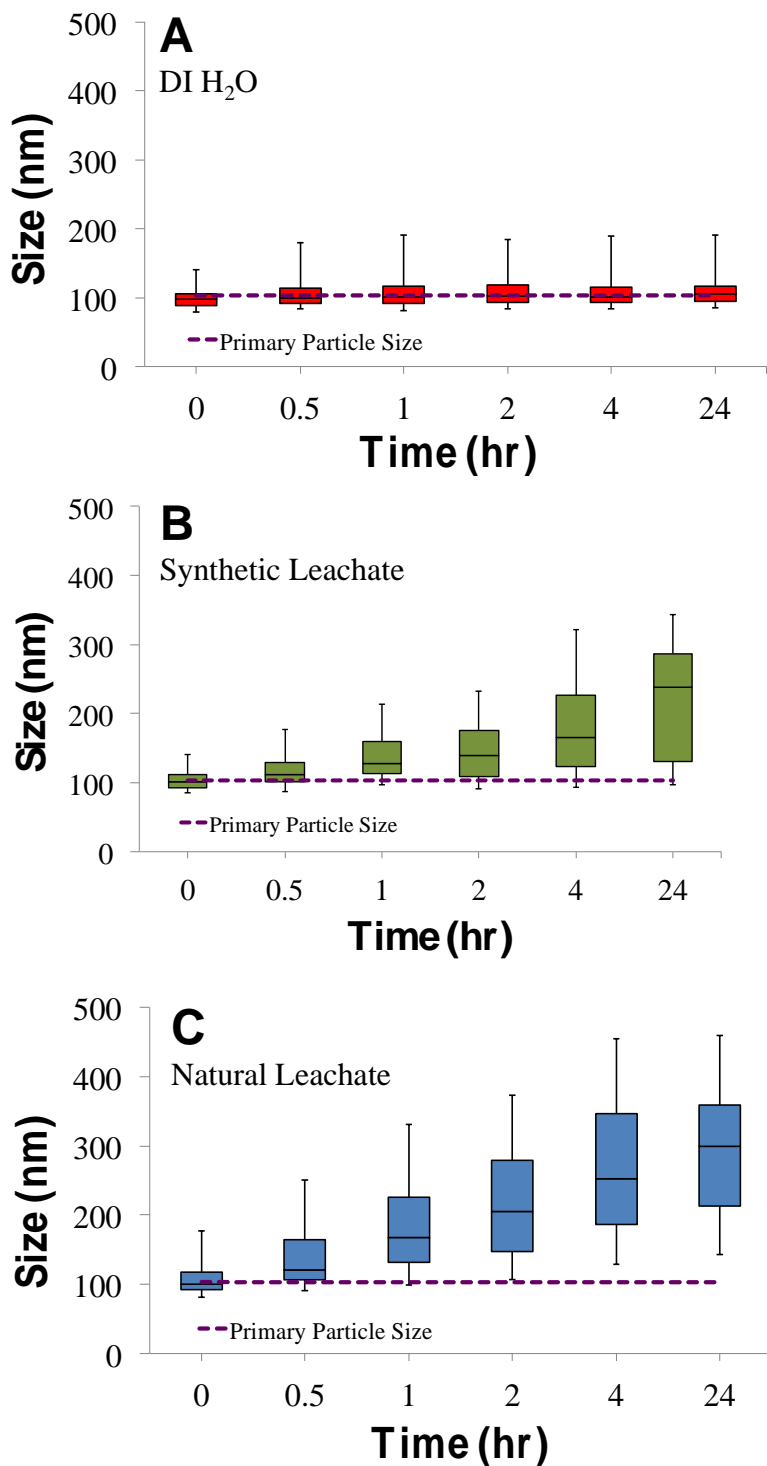


**Figure 3:** Size distribution of particle (aggregates) over time in A) DI H<sub>2</sub>O, B) synthetic landfill leachate and C) natural MSWI landfill leachate. 25% quantiles appear within the box plot with average particle size indicated by black line therein. Whiskers represent 95% of particle size distribution (outliers not shown). Purple dashed lines indicate Au ENM primary particle size (100 nm).

### 3.3.2 ENM Stability – Particle Number

The importance of calibrating the NTA for particle number in various matrices is exemplified when measuring the stability of particles over time by analyzing the change in particle number. For example, when the same concentration of Au ENM is spiked into the leachate solutions, the raw output from the NTA instrument shows a disparity in concentration between the initial particle number concentration in DI H<sub>2</sub>O, synthetic leachate and the natural leachate (Figure S3). However, when these particle numbers are corrected based on the scaling factors obtained from the calibration curve, the T = 0 hr concentrations are all very similar between the various solutions (Figure 4), albeit at a lower total particle number measured since in all instances the NTA overestimates the particle number.

The particle number concentration in DI H<sub>2</sub>O remained constant over time. Along with the particle size remaining unchanged, this further suggests that particles were stable over the 24 hr experiment and the NTA was able to consistently measure them in solution. Synthetic and natural leachates both exhibited decreases in particle number concentration over time. However, in this instance the number concentration given directly by the NTA instrument needed to be corrected by the scaling factors determined by calibrating the instrument to correctly measure the particle number in these various solutions (Figure 4). In the raw results (Figure S3), the number of particles measured in both synthetic and natural leachates appear similar and their decrease over time tracks one another. However, when scaling the particle number appropriately based on the calibration curve, it becomes evident that particles suspended in the synthetic leachate seemingly disappear from solution at a faster rate than those suspended in the natural landfill leachate solution (Figure 4). This increased stability in the natural leachate is somewhat expected because when a solution contains DOC the stability of ENM is often increased.<sup>26</sup> Since the synthetic leachate is comprised only of a salt solution that mimics the composition of the natural leachate, we can suggest that the increased stability of the ENM in the natural leachate is due to the DOC.

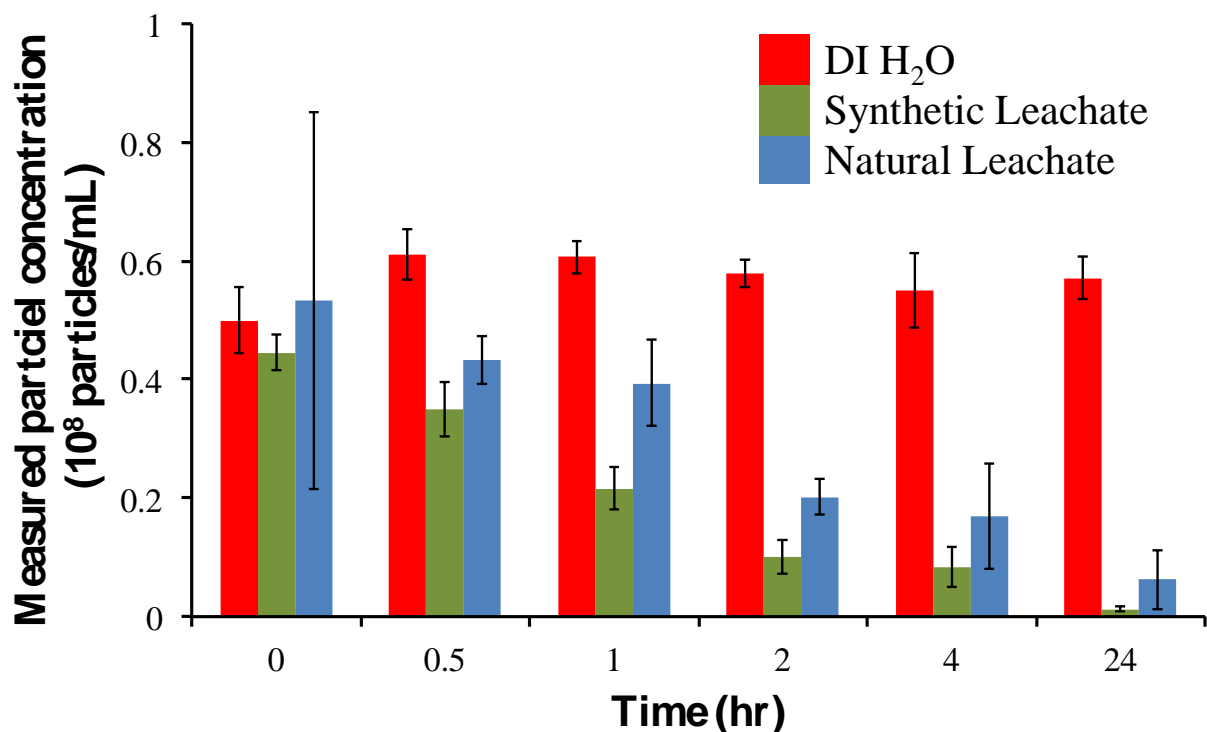


**Figure 4:** NTA measured particle number concentration of 100 nm Au particles over time in DI H<sub>2</sub>O (red bars), synthetic leachate (green bars) and natural MSWI landfill leachate (blue bars). Particle number concentration is based on the calibration curve, it is notable that the particles in the natural leachate samples appear to show an increased stability compared to the synthetic leachate solution, a result that was not visible without the correction factor applied. Error bars indicate results of triplicate experiments.

### 3.3.3 ENM Stability – Mass Evolution

However, Figure 4 only relays information about particle number but does not take into account the particle size that was measured in each solution (Figure 3). While in many studies the decrease in particle number is taken to imply removal of particles from the leachate solutions (e.g. through settling, etc.), Figure 4 simply shows that there are fewer particles in the leachate solutions. This information can be combined with the particle size distributions (Figure 3) to determine the total mass of Au remaining in the system at any given time point. If, during this analysis, the observed total Au mass in solution decreases then particles are indeed settling from solution. The total mass of the remaining ENM in solution is shown in Figure 5. The initial calculated mass of all samples was similar, at approximately 0.75 mg Au ENM/L. However the stability of ENM exhibited a different behavior over time depending on the solution they were suspended in. The total mass of Au ENMs suspended in DI H<sub>2</sub>O and synthetic leachate were relatively stable, with the mass fluctuating less than 25% on average over the course of 24 hrs. However, taken together with the particle size and particle number data (Figures 3 and 4, respectively), different conclusions can be drawn in terms of the particle behavior between these two suspensions. In DI H<sub>2</sub>O, there was little change in terms of



particle size, particle number and particle mass suggesting that the pristine particles were stable in solution with no agglomeration or settling. In contrast, in synthetic leachate, the particle size increased, the particle number decreased but the mass of particles remained steady. Increasing particle size indicates agglomeration, as does the decrease in particle number since homoagglomeration is the only possibility in this solution. However, because the particle mass remains steady over time, the entire initial mass is accounted for in solution throughout the first 4 hrs of the experiment and so little settling of the agglomerates has occurred. Because the mass decreased by the 24 hr time point, we hypothesize there is more agglomeration and subsequent settling from solution in this sample at extended time points.

Just as with the synthetic leachate solution, in the natural leachate preparation particle size was noted to increase over time while particle number decreased. Yet the behavior of Au ENM in the natural leachate is different from its more simplistic counterpart because the total calculated mass seemingly increases up to four times the initial concentration observed in the sample at time zero. While some homoagglomeration is still likely in this sample, we hypothesize that the incorrect overestimation of mass in this instance is due largely to heteroagglomeration. This can be explained by the fact that Au ENM can adhere to other larger natural material (e.g. clays, silicates, DOC, etc.) in the leachates and thus the bright ENM particles observed by the NTA are moving slower than their “free” pristine counterparts. Unlike the synthetic leachate where the total mass remains steady because homoagglomeration is the only option, heteroagglomerates of Au ENM and natural material in the natural leachate is visualized as one, larger (ENM) particle because the NTA is simply tracking the speed of the more reflective ENM adhered to the natural matter. These heteroagglomerates are then sized based on their slower diffusion speed, and thus sized larger, even if the aggregate contains a smaller ENM than the complex that is being tracked by the NTA. Therefore, when calculating the mass from particle size and number, the total mass is significantly overestimated. Furthermore, the high variability between replicates is an indication of ENM agglomeration in the sample.

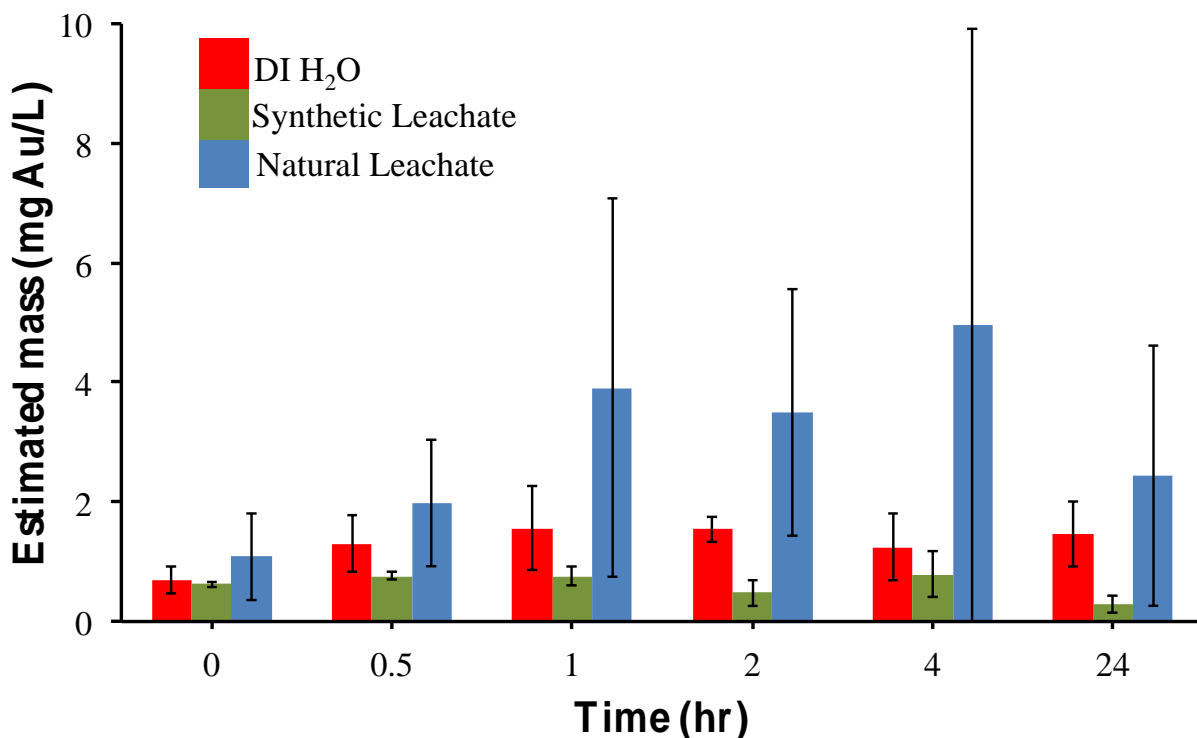


**Figure 5:** Calculated mass of Au ENM over time based on NTA measured particle size and (adjusted) particle number concentrations for DI H<sub>2</sub>O (red bars), synthetic landfill leachate (green bars) and natural leachate (blue bars). Error bars indicate triplicate experiments.

### 3.4 Visualization of Particle Aggregation with Transmission Electron Microscopy (TEM)

While often morphology and agglomeration is not studied with TEM because with drop deposition there are known artifacts when drying the sample on the grid, the technique used here to centrifuge the suspension so that particles are sedimented onto the grid directly from solution better preserves their natural state and so the extent of agglomeration can be (qualitatively) estimated. One caveat of measuring very heavy elements (i.e. the Au ENM) in the presence of natural particles (i.e. the clays, silicates and DOM of the natural leachate) is that it is difficult to image both materials simultaneously due to their different intensities in the image. Therefore in the bright field images presented here the Au ENM appear very dark but any natural material in solution appear much lighter (only applicable in the natural landfill leachate). While this may not be definitive evidence of particle behavior alone, taken together with the results from the NTA experiments a conclusion about agglomeration can begin to be drawn.

In all samples, TEM analysis shows that initially Au ENM are dispersed with little or no homoagglomeration or heteroagglomeration in the systems (Figure 6, top row of images). However, after four hours in suspension the behavior and stability of the spiked ENM begin to diverge. In the DI H<sub>2</sub>O

sample, it appears particles continue to be well dispersed as single particles. This is also what was expected given that both the particle size and particle number was measured as constant over four hours by the NTA (Figure 3, panel A and Figure 4, panel B). In the synthetic leachate sample, additional homoagglomerates of Au ENM are seen and finally in the natural leachate we can see aggregates associated with natural (light colored) material.

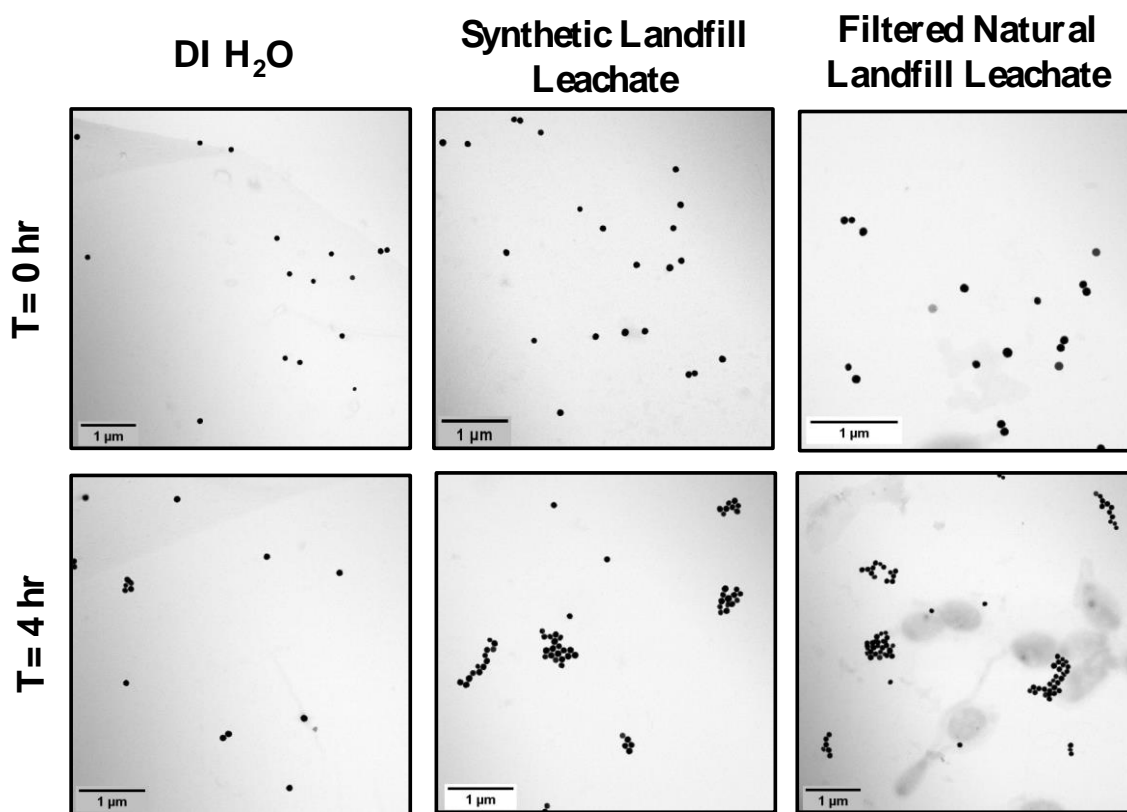


**Figure 6:** TEM images of Au ENM agglomeration state at T =0 hr and T=4 hr in DI H<sub>2</sub>O, synthetic landfill leachate and natural landfill leachate (filtered through 0.45 μm filter). Disperse, single particles are evident in all T= 0 samples and the DI H<sub>2</sub>O sample after 4 hrs, yet agglomeration is noted in both synthetic and natural landfill leachates after 4 hrs in solution. In the case of synthetic leachate, homoagglomeration (rather than heteroagglomeration) is evident; likely due to the high concentration of ENM dispersed in a solution with a relatively high salt concentration. In contrast, the ENM suspended in the natural leachate sample seemingly are affected by homoagglomeration as well as heteroagglomeration to the natural particles in the leachate.

## 4. Discussion

### 4.1 Suitability and advantages of NTA to measure ENM in complex systems

The suitability and advantages of using the NTA to measure ENM in complex systems was examined in our case study investigating the stability of ENM in landfill leachates. The feature of discerning intensely

scattering ENM in a solution of incidental particles has not yet been fully exploited but is of particular relevance in environmental ENM research. Many common and relevant ENM (e.g. Ag and Au particles) have a higher refractivity index than their natural colloidal counterparts (such as clays, silicates, etc.) and the camera settings can be adjusted to “blind” out the natural background and only track the brighter, engineered particles in solution. The relative refractive index of particles in these solutions is very important for the measurement and analysis of the ENM considering the multitude of natural particles existing in solution. In this way, we can easily detect the ENM above the natural background of incidental particles with lower refractivity index in the solution. van der Pol et al. validated a protocol to determine the refractive index of nanoparticles in suspension using NTA, specifically highlighting the usefulness of exploiting this difference in biological and clinical samples.<sup>27</sup> While the sensitivity of the method in terms of observing particles in increasingly complex media may vary depending on the test media, by making a calibration curve of known particles in the media of interest should allow one to determine the ability to measure spiked particles above a natural background with varying mineral and organic contents.

With the use of NTA, precise details of ENM stability can be investigated by obtaining multiple metrics including ENM (agglomerate) size, particle number in solution and, ultimately, relating this to the calculated mass of analyte in solution. By selecting different water chemistry variables and measuring over time, we could better monitor these trends and test the applicability of NTA to measure ENM stability in landfill leachates. In DI H<sub>2</sub>O we found that particle size, particle number and analyte mass remained constant over time. This solution therefore gave us a benefit in terms of understanding NTA analysis for “baseline” conditions. This evaluation of these reference conditions could then be compared to the results obtained when suspending ENM in assorted leachate chemistries that may induce additional particle (in)stability. Of the two experimental solutions, the synthetic leachate solution had only soluble components (i.e. ions) and pH affecting ENM stability. From the size increase, particle number decrease but overall conservation of mass in solution, we determined that the primary particles were homoagglomerating but were otherwise stable in solution. While the result of ENM homoagglomeration in a salt solution itself is not novel, the measurement techniques and metrics obtained to come to that conclusion are. Using the natural leachate, after 0.45 µm filtration, included the additional complexity of other particulate matter and DOC in the solution chemistry. It has been suggested that homoagglomeration of ENM is not as likely as heteroagglomeration between ENM and natural particles in environmental systems. In this case, we observe both homo- and heteroagglomeration but it is likely that the homoagglomeration is mainly due to the high Au ENM concentration needed for NTA detection and this is less likely to occur in a real environmental sample where the ENM concentrations are much more dilute than in the system studied here.

The difference between the measurements in synthetic and natural leachates points to another advantage of using NTA to study the behavior of ENM in these solutions which is to differentiate between homo- and heteroagglomeration. In solutions with only ENM as particles (i.e. in the DI H<sub>2</sub>O or synthetic landfill

leachate samples), homoagglomeration is the only possibility when particles are unstable and they may subsequently agglomerate and settle from solution. Conversely, in the solutions that contained additional particulate matter (i.e. the natural particles and DOC in the natural leachate), the possibility exists for ENM to aggregate with other materials (i.e. heteroagglomeration).

Despite having a lower maximum resolution of 10-30 nm and requiring a relatively high particle concentration ( $10^5$  -  $10^{10}$  particles/mL<sup>28</sup>), this technique is still useful to estimate the stability of particles in various solutions. Indeed, when the number of particles studied in this manuscript is transformed to a mass based concentration (equating to approximately 150 – 800  $\mu$ g/L), the lower end of this concentration range is within an acceptable level to study particle behavior at environmentally relevant concentrations, or is at least on par with other techniques which are commonly used and accepted as suitable for studying nanomaterial behavior at environmentally relevant concentrations. The aim of this work was not to specifically study the dynamic range of the instrument (although the upper particle number was determined), and so with additional method development it may be possible to determine particle behavior at even lower concentrations than studied here. However, the technique does not provide details of morphology and particle motion is recorded in two dimensions not three. The latter pitfall often leads to some tracks being associated with a smaller degree of motion and consequently sized (incorrectly) as larger particles.<sup>29</sup> Nevertheless, the ability to track agglomeration in real time in the native solution is a benefit of NTA that is not readily duplicated by other nanometrology techniques.

#### *4.2 Size vs. mass-based evaluation in aqueous systems*

Many experiments that focus on ENM stability, for example with DLS as the main ENM characterization technique, simply measure average particle size and estimate total concentration of particles in suspension over time. Often, based on these metrics, one comes to the conclusion that the primary particle size increases (through agglomeration) after being spiked into a solution and then when the concentration subsequently decreases, the researcher presumes the particles sediment out of suspension. However, with the additional information generated by the NTA analysis, transformation of the particle size distribution and particle number measured to mass of analyte shows that there are often more complicated metrics at play. This is exemplified by our case study on the stability of ENM in synthetic and natural landfill leachate solutions. When distributing the number of particles measured over the measured size distribution to determine the mass of particles in solution, the mischaracterization of ENM size can grossly overestimate the mass of Au in the system. Since the size of individual particles is independently tracked by the NTA, the number of particles analyzed can be spread across the particle size distribution and subsequently be converted to mass.<sup>30</sup> The mean obtained and reported from the NTA instrument is a number weighted average. However, from the (raw) distribution obtained from the NTA output; volume, mass and intensity weighted means (and histograms) can be calculated for each measurement recorded. When converting the

size-based distribution to a mass-based distribution, it becomes starkly evident that the presence of even a low number of large aggregates can represent a significant proportion of the total mass in the sample.

Reporting both size and mass based metrics is common when dealing with other particulate matter, for example in air.<sup>31,32</sup> Number- and mass-based analytical techniques are used and the results are routinely transformed from one metric into another. This is not yet the case in water but now the NTA can give us the additional information that is necessary in order to report results in both ways.

## **5. Implications**

Beyond the finite results of our case study on the stability of ENM in landfill leachates, our goal was to further investigate the advantages of using the NTA to study ENM in complex matrices. To that extent, there are several facets of the technique that are specifically (and sometimes uniquely) beneficial to detect and size ENM, along with characterizing their behavior in environmental media. Firstly, the ability to discretely measure ENM on top of the natural particle background by taking advantage of the difference in the refractivity index of the particles is particularly useful. While the NTA given particle concentration needs to be adjusted after making a calibration curve of known values, a linear range can be obtained for each solution and the different concentrations of particles did not change the measured particle size (distribution). Finally, by using the two metrics directly obtained from the NTA, the particle size distribution and the particle concentration, one can calculate the mass of analyte in solution that can provide an additional dynamic to understand the stability of particles in solution. Given the myriad of nanometrology techniques that are continually being developed and improved in recent years, the options for measurement and characterization of ENM are numerous. The benefit of measuring ENM directly in the native solution with the additional advantage of discerning ENM from natural particles suggest that NTA is a useful tool for measuring ENM in a variety of complex matrices.

## **Acknowledgements**

We would like to thank the landfill operator of the ZAB Deponie in Flawil, Switzerland, who gave us access to collect samples on multiple occasions. This study was supported by the project “Nanomaterials in Landfills” sponsored by the Swiss Federal Office for the Environment

## **Supporting Information**

Au nanoparticle size distribution measurements, natural and synthetic leachate water chemistry analysis, median size of particles measured by NTA at each time point (table and figure), measured particle number concentration in solutions without adjustment based on calibration curve.

## References

1. Lowry, G. V.; Gregory, K. B.; Apte, S. C.; Lead, J. R., Transformations of Nanomaterials in the Environment. *Environmental Science & Technology* **2012**, *46*, (13), 6893-6899.
2. Mitrano, D. M.; Nowack, B., The need for a life-cycle based aging paradigm for nanomaterials: Importance of real-world test systems to identify realistic particle transformations. *Nanotechnology* **2017**, *28*, (7), 072001.
3. Montaña, M. D.; Olesik, J. W.; Barber, A. G.; Challis, K.; Ranville, J. F., Single Particle ICP-MS: Advances toward routine analysis of nanomaterials. *Analytical and Bioanalytical Chemistry* **2016**, *408*, (19), 5053-5074.
4. Laborda, F.; Bolea, E.; Cepriá, G.; Gómez, M. T.; Jiménez, M. S.; Pérez-Arantegui, J.; Castillo, J. R., Detection, characterization and quantification of inorganic engineered nanomaterials: A review of techniques and methodological approaches for the analysis of complex samples. *Analytica chimica acta* **2016**, *904*, 10-32.
5. Kim, H.-A.; Lee, B.-T.; Na, S.-Y.; Kim, K.-W.; Ranville, J. F.; Kim, S.-O.; Jo, E.; Eom, I.-C., Characterization of silver nanoparticle aggregates using single particle-inductively coupled plasma-mass spectrometry (spICP-MS). *Chemosphere* **2017**, *171*, 468-475.
6. Mitrano, D. M.; Arroyo Rojas Dasilva, Y.; Nowack, B., Effect of Variations of Washing Solution Chemistry on Nanomaterial Physicochemical Changes in the Laundry Cycle. *Environmental Science & Technology* **2015**, *49*, (16), 9665-9673.
7. Prasad, A.; Lead, J.; Baalousha, M., An electron microscopy based method for the detection and quantification of nanomaterial number concentration in environmentally relevant media. *Science of the Total Environment* **2015**, *537*, 479-486.
8. Dubascoux, S.; Hecho, I.; Hasselöv, M.; Kammer, F.; Gautier, M.; Lespes, G., Field-flow fractionation and inductively coupled plasma mass spectrometer coupling: History, development and applications. *Journal of Analytical Atomic Spectrometry* **2010**, *25*, (5), 613-623.
9. Loeschner, K.; Navratilova, J.; Legros, S.; Wagner, S.; Grombe, R.; Snell, J.; von der Kammer, F.; Larsen, E. H., Optimization and evaluation of asymmetric flow field-flow fractionation of silver nanoparticles. *Journal of Chromatography A* **2013**, *1272*, 116-125.
10. Wagner, S.; Legros, S.; Löschner, K.; Liu, J.; Navratilova, J.; Grombe, R.; Linsinger, T.; Larsen, E.; Von Der Kammer, F.; Hofmann, T., First steps towards a generic sample preparation scheme for inorganic engineered nanoparticles in a complex matrix for detection, characterization, and quantification by asymmetric flow-field flow fractionation coupled to multi-angle light scattering and ICP-MS. *Journal of Analytical Atomic Spectrometry* **2015**, *30*, (6), 1286-1296.
11. Hasselöv, M.; Kaegi, R., *Analysis and characterization of manufactured nanoparticles in aquatic environments*. John Wiley & Sons, Inc.: United Kingdom: 2009.
12. Gillespie, C.; Halling, P.; Edwards, D., Monitoring of particle growth at a low concentration of a poorly water soluble drug using the NanoSight LM20. *Colloids and Surfaces A: Physicochemical and Engineering Aspects* **2011**, *384*, (1), 233-239.
13. Whitepaper, M., Nanoscale Material Characterization: a Review on the use of Nanoparticle Tracking Analysis (NTA). **2015**.
14. Sanchís, J.; Bosch-Orea, C.; Farré, M.; Barceló, D., Nanoparticle tracking analysis characterisation and parts-per-quadrillion determination of fullerenes in river samples from Barcelona catchment area. *Analytical and bioanalytical chemistry* **2015**, *407*, (15), 4261-4275.
15. Bartczak, D.; Vincent, P.; Goenaga-Infante, H., Determination of size-and number-based concentration of silica nanoparticles in a complex biological matrix by online techniques. *Analytical chemistry* **2015**, *87*, (11), 5482-5485.

16. Gallego-Urrea, J. A.; Tuoriniemi, J.; Hassellöv, M., Applications of particle-tracking analysis to the determination of size distributions and concentrations of nanoparticles in environmental, biological and food samples. *TrAC Trends in Analytical Chemistry* **2011**, *30*, (3), 473-483.
17. Mueller, N.; Nowack, B., Exposure modeling of engineered nanoparticles in the environment. *Environmental Science and Technology* **2008**, *42*, (12), 4447-4453.
18. Gottschalk, F.; Scholz, R.; Nowack, B., Probabilistic material flow modeling for assessing the environmental exposure to compounds: Methodology and an application to engineered nano-TiO<sub>2</sub> particles. *Environmental Modelling & Software* **2010**, *25*, (3), 320-332.
19. Sun, T. Y.; Gottschalk, F.; Hungerbühler, K.; Nowack, B., Comprehensive probabilistic modelling of environmental emissions of engineered nanomaterials. *Environmental Pollution* **2014**, *185*, 69-76.
20. Keller, A. A.; McFerran, S.; Lazareva, A.; Suh, S., Global life cycle releases of engineered nanomaterials. *Journal of Nanoparticle Research* **2013**, *15*, (6), 1-17.
21. Mitrano, D. M.; Motellier, S.; Clavaguera, S.; Nowack, B., Review of nanomaterial aging and transformations through the life cycle of nano-enhanced products. *Environment international* **2015**, *77*, 132-147.
22. Thio, B.; Montes, M. O.; Mahmoud, M.; Lee, D.; Zhou, D.; Keller, A., Mobility of Capped Silver Nanoparticles under Environmentally Relevant Conditions. *Environ Sci Technol* **2012**, *46*, (13), 6985-6991.
23. Kiser, M.; Ryu, H.; Jang, H.; Hristovski, K.; Westerhoff, P., Biosorption of nanoparticles to heterotrophic wastewater biomass. *Water Research* **2010**, *44*, 4105-4114.
24. Limbach, L. K.; Bereiter, R.; Muñáller, E.; Krebs, R.; Gañalli, R.; Stark, W. J., Removal of oxide nanoparticles in a model wastewater treatment plant: Influence of agglomeration and surfactants on clearing efficiency. *Environmental science & technology* **2008**, *42*, (15), 5828-5833.
25. Mitrano, D. M.; Mehrabi, K.; Dasilva, Y. A. R.; Nowack, B., Mobility of metallic (nano)particles in leachates from landfills containing waste incineration residues. *Environmental Science: Nano* **2017**, *4*, (2), 480-492.
26. Mitrano, D. M.; Ranville, J.; Bednar, A.; Kazor, K.; Hering, A. S.; Higgins, C., Tracking dissolution of silver nanoparticles at environmentally relevant concentrations in laboratory, natural and processed waters using single particle ICP-MS (spICP-MS). *Environmental Science: Nano* **2014**, *1*, (3), 248-259.
27. Van Der Pol, E.; Coumans, F. A.; Sturk, A.; Nieuwland, R.; van Leeuwen, T. G., Refractive index determination of nanoparticles in suspension using nanoparticle tracking analysis. *Nano letters* **2014**, *14*, (11), 6195-6201.
28. Malloy, A.; Carr, B., Nanoparticle tracking analysis—the Halo™ system. *Particle & Particle Systems Characterization* **2006**, *23*, (2), 197-204.
29. Saveyn, H.; De Baets, B.; Thas, O.; Hole, P.; Smith, J.; Van Der Meeren, P., Accurate particle size distribution determination by nanoparticle tracking analysis based on 2-D Brownian dynamics simulation. *Journal of colloid and interface science* **2010**, *352*, (2), 593-600.
30. La Rocca, A.; Di Liberto, G.; Shayler, P.; Parmenter, C.; Fay, M., Application of nanoparticle tracking analysis platform for the measurement of soot-in-oil agglomerates from automotive engines. *Tribology International* **2014**, *70*, 142-147.
31. Harrison, R. M.; Shi, J. P.; Xi, S.; Khan, A.; Mark, D.; Kinnersley, R.; Yin, J., Measurement of number, mass and size distribution of particles in the atmosphere. *Philosophical transactions of the royal society of London A: mathematical, physical and engineering sciences* **2000**, *358*, (1775), 2567-2580.
32. Anastasio, C.; Martin, S. T., Atmospheric nanoparticles. *Reviews in Mineralogy and Geochemistry* **2001**, *44*, (1), 293-349.



## Chapter 3

# Agglomeration potential of TiO<sub>2</sub> in synthetic leachates made from the fly ash of different incinerated wastes

### **Abstract**

Material flow studies have shown that a large fraction of the engineered nanoparticles used in products end up in municipal waste. In many countries, this municipal waste is incinerated before landfilling. However, the behavior of engineered nanoparticles (ENPs) in the leachates of incinerated wastes has not been investigated so far. In this study, TiO<sub>2</sub> ENPs were spiked into synthetic landfill leachates made from different types of fly ash from three waste incineration plants. The synthetic leachates were prepared by standard protocols and two types of modified procedures with much higher dilution ratios that resulted in reduced ionic strength. The pH of the synthetic leachates was adjusted in a wide range (i.e. pH 3 to 11) to understand the effects of pH on agglomeration. The experimental results indicated that agglomeration of TiO<sub>2</sub> in the synthetic landfill leachate simultaneously depend on ionic strength, ionic composition and pH. However, when the ionic strength was high, the effects of the other two factors were masked. The zeta potential of the particles was directly related to the size of the TiO<sub>2</sub> agglomerates formed. The samples with an absolute zeta potential value < 10 mV were less stable, with the size of TiO<sub>2</sub> agglomerates in excess of 1500 nm. It can be deduced from this study that TiO<sub>2</sub> ENPs deposited in the landfill may be favored to form agglomerates and ultimately settle from the water percolating through the landfill and thus remain in the landfill.

### **1. Introduction**

Nanotechnology has drawn a lot of attention from various fields such as pharmaceuticals, materials science, environmental science and electrical engineering (Hamley 2003; Heremans et al., 2013; Masciangioli and Zhang, 2003; Samad et al.,2009). Significant attention has been given to the fate of engineered nanoparticles (ENPs) in the environment and their potential risks to human health (Klaine et al., 2012; Linkov et al., 2011). ENPs can be released into the environment throughout the entire life cycle of nano-enhanced products including production, use and disposal (Gottschalk and Nowack, 2011; Mitrano et al., 2015). It has been demonstrated that commonly used ENPs, such as Ag ENPs, TiO<sub>2</sub> ENPs and carbon

nanotubes, have different levels of toxic effects on humans as well as on other organisms (Clément et al., 2013; Prabhu and Poulouse, 2012; Shvedova et al., 2012).

Several studies have indicated that landfills are one of the main final sinks for ENPs (Hincapié et al., 2015; Mueller et al., 2013; Walser and Gottschalk, 2014; Walser et al., 2012). Water (mainly from rain) passing through the landfill will be in contact with the deposited solid waste material and any ENPs remaining in the wastes. The properties of the aqueous medium evolve along its path through the landfill due to the continual attrition of organic matter and salts from the solid waste. The landfill leachate is generally defined as the liquid collected from the draining system of the landfill. ENPs are considered as emerging contaminants in landfills (Ramakrishnan et al., 2015) and a recent study has reported the presence of nanoscaled TiO<sub>2</sub> particles in construction landfills (Dietschweiler et al., 2015). In practice, landfills have barrier layers consisting of both clay and artificial membranes to prevent the leakage of landfill leachate. However, in all landfills the leachate is collected and either treated, disposed into wastewater or added directly to surface waters, depending on the composition and local regulations. It is still difficult to directly identify ENPs in landfill leachates because of limited analytical capabilities to detect ENPs in complex systems (Montaño et al., 2014) and thus not much about their presence in landfills is known.

Due to population growth and the lack of space for landfills, more attention is currently paid to alternatives to directly landfill waste. One of the most widely utilized methods, incineration of municipal waste before deposition in landfill, is a growing trend globally, especially for densely populated countries (Ji et al., 2016). In countries such as Denmark, Sweden and Japan, incineration is utilized to treat around half or more than 70% of the municipal waste, while only less than 5% of the waste is deposited directly in landfills (Ji et al., 2016; Nixon et al., 2013). In Switzerland, nearly 100% of the municipal waste and sewage sludge is incinerated before being landfilled (Mueller et al., 2013).

The stability and transport of ENPs in environmental waters is generally influenced by several factors such as the particles' intrinsic characteristics (e.g. composition, size, capping agent) and extrinsic factors such as pH, ionic strength and the concentration of natural organic matter (NOM) (Delay et al., 2011; Labille and Brant, 2010). Landfill leachates normally have more complicated and higher concentrations of ions and dissolved organic matter compared to natural waters and also their pH is elevated (Kjeldsen et al., 2002). With the increasing landfill age, the properties of landfill leachate also change, such as lower pH, and higher redox potential (Baun and Christensen, 2004; Kjeldsen et al., 2002). The behaviors of different types of ENPs such as single-walled carbon nanotubes, ZnO, Ag and TiO<sub>2</sub> in municipal landfill leachate are related to the concentration of humic acids, the composition of the waste (e.g. paper, metal, plastics, glass) in the landfill as well as the coating of the ENPs (Bolyard et al., 2013; Khan et al., 2013). NOM in the leachate may influence the stability of ENPs because NOM can be adsorbed onto the surface of ENPs and further stabilize them in solution due to repulsive steric interaction. (Delay et al., 2011; Thio et al., 2011)

Because the organic components of the municipal wastes were generally removed by incineration before they were deposited in the landfills for incinerated wastes, the properties of landfill leachate of these

landfills will be different from that of the normal landfills for mixed municipal wastes. For example, the average of Total Organic Carbon (TOC) values of the landfill leachate from a landfill for incinerated wastes in Switzerland (Landfill Pfyn) was 15 mg/L during the monitoring period of 10 years, which is much less than the TOC values of landfills for mixed municipal wastes (30 – 29000 mg/L) (Kjeldsen et al., 2002). So the behavior of ENPs in the leachates of landfills for incinerated wastes may be different from those in the leachates of landfills filled with municipal wastes without incineration.

TiO<sub>2</sub> ENPs are widely used in industrial and consumer goods such as paints, textiles, paper and cardboard and the yearly production amounts of it in EU is more than 10000 tones (Mitrano et al. 2015, Sun et al. 2014). The behaviors of TiO<sub>2</sub> ENPs in natural river water have been studied to reveal that the agglomeration of TiO<sub>2</sub> ENPs is related to the existence of electrolyte and dissolved organic matter (Adam et al., 2016; Chekli et al., 2015a). In many countries, including Switzerland, many of these products containing TiO<sub>2</sub> ENPs will be incinerated at their end of life cycle. After incineration, the acid washing process which is used to clean the flue and filter ash may affect the surface coating of TiO<sub>2</sub>, however, it cannot dissolve the particles (Mitrano et al., 2015; Mueller et al., 2013). After being disposed in the landfill, the remaining TiO<sub>2</sub> in the ashes from incineration plant will interact with the aqueous media inside of the landfill. Although TiO<sub>2</sub> ENPs have not been found directly in natural landfill leachate, batch experiments have revealed that 3% - 19% of the nano-TiO<sub>2</sub> mixed with the municipal waste can remain in the leachate under pH and ionic strength conditions which mimic landfill pore water and leachate (Dulger et al., 2016). As mentioned above, the barrier layers of the landfill may also prevent the leakage of landfill leachate as well as the possibly existing ENPs in the leachate to the environment.

Because incineration has been utilized more widely to treat the municipal wastes before the landfill and properties of the wastes change significantly after incineration, understanding the behaviors of TiO<sub>2</sub> ENPs in the leachates made from incinerated wastes is important. In this study, the agglomeration potential of TiO<sub>2</sub> ENPs spiked in different synthetic landfill leachates made from fly ashes of three different Swiss waste incineration plants was studied. For each type of fly ash, synthetic leachates were prepared based on three different protocols. In this way, the influence of pH, ionic composition and ionic strength on the agglomeration potential of TiO<sub>2</sub> ENPs were studied systematically.

## **2. Materials and methods**

### *2.1 TiO<sub>2</sub> nanoparticle suspension*

The TiO<sub>2</sub> nanoparticle suspension was prepared by dispersing commercial TiO<sub>2</sub> powder (P25, 99.5% trace metals basis, 21 nm primary particle size, Sigma-Aldrich) into deionized water (DI water), the concentration of TiO<sub>2</sub> nanoparticles in the suspension was 400 mg/L. The suspension was sonicated for 30 minutes by the Bandelin SONOREX SUPER ultrasonic baths (320 W, 100 kHz) before it was utilized for the experiments. Initial agglomeration of the TiO<sub>2</sub> agglomerates after sonication was normally between 250

nm and 300 nm. Size and zeta potential measurements of agglomerates were conducted by dynamic light scattering (DLS) (Malvern Zetasizer Nano ZS). For the DLS measurements in this study, the z-average diameter is reported to describe the mean particle size under every experimental condition.

## *2.2 Characterizations of fly ash samples*

The fly ash samples were collected from three waste incineration plants in Switzerland including: one combined municipal waste-sludge incineration plant (WaS), one municipal waste incineration plant (Wa), and one wood incineration plant (Wo). The incineration plants chosen were either medium size (incinerating 100'000 – 200'000 ton of waste per year) or large (incinerating more than 200'000 ton of waste per year) in size and the waste incinerated at these sites was representative of the major classes of waste incinerated in Switzerland. After size classification of the dry fly ash by a multiplex laboratory Zigzag classifier (model 100MZR, Alpine corporation, Germany) (Buha et al. 2014), the fine fraction with aerodynamic diameter smaller than 2  $\mu\text{m}$  was used to make the aqueous suspensions. General information about the fly ashes is listed in the supplemental information.

## *2.3 Preparation of the synthetic landfill leachate*

The first type of synthetic leachate was made according to European standard protocol EN 12457-2.(EN 2002) Briefly, the dry fly ash was dispersed into DI water with a ratio of one part waste to ten parts water (e.g. 10 g dry fly ash dispersed in 100 ml water) in a flask. The closed flask was agitated with 5-10 rpm for 24 hours at room temperature. After sedimentation of the solid ash for 15 minutes, the suspensions were filtered through a 0.45  $\mu\text{m}$  cellulosenitrat membrane filters (Satorius Stedim Biotech GmbH) and the leachate was collected. Hereafter, this leachate was abbreviated as (N). The obtained leachates made from the three types of fly ash were abbreviated as WaS(N), Wa(N) and Wo(N), respectively.

The procedure for making the second type of synthetic leachate was to put 100 mg of one type of dry fly ash dispersed into 100 ml of DI water and the suspension was stirred for 48 hours. After stirring, the fly ash suspensions were filtrated through 1.5  $\mu\text{m}$  glass microfiber filters (Whatman 934-AH) and 0.45  $\mu\text{m}$  cellulosenitrat membrane filters (Satorius Stedim Biotech GmbH) sequentially. The leachate after the sequential filtration was collected for the following experiments. The obtained leachate is further identified as (MOD). The leachates made from the three types of fly ash by this procedure were abbreviated as WaS(MOD), Wa(MOD) and Wo(MOD), respectively.

The third type of synthetic leachate was made by diluting the synthetic leachate (MOD) by 10 times. The obtained leachate was abbreviated as (MOD-D). The leachates made from the three types of fly ash were abbreviated as WaS(MOD-D), Wa(MOD-D) and Wo(MOD-D), respectively.

Conclusively, among the synthetic leachates (N), (MOD) and (MOD-D), the dilution ratio used in (MOD) (100 mg dry fly ash per 100 ml water) was 100 times higher than (N) (10 g dry fly ash per 100 ml water), and (MOD) was further diluted to obtain (MOD-D).

#### *2.4 Characterization of the synthetic landfill leachate*

pH and conductivity of the obtained leachate were measured directly in the leachate by METTLER TOLEDO InLab Expert Pro-ISM pH-electrode and an METTLER TOLEDO InLab 710 Conductivity electrode. Inductively Coupled Plasma Optical Emission Spectrometry (ICP-OES) VARIAN VISTA PRO and Ionic Chromatography (IC) METROHM IC 882 COMPACT PLUS were used to characterize the cationic and anionic components of the leachates. Certified reference materials were used for all measurements (for ICP-OES: specpure 1 g/L and 10 g/L for the elements, Alfa Aesar; for IC: Anion Mix A, Alltech).

Filtration through a 0.45  $\mu\text{m}$  filter Whatman FP 30/0.45 CA is a common approach to prepare samples for identification of dissolved cations as well as the ICP-OES measurements (Fang et al. 2009), whereas the filters with smaller cutoff sizes are also utilized in some studies focusing on colloids and better detection of the small ENPs (Baun and Christensen 2004, Bolyard et al. 2013). In this study, no further filtration was conducted and it is likely that some nano-sized particles in the fly ashes passed through the 0.45  $\mu\text{m}$  filter. The fly ash leachates from all source material were transparent after the 0.45  $\mu\text{m}$  filtration and the concentrations of residual particles therein were below the concentration threshold for reliable size measurements by DLS.

Scanning Electron Microscope with Energy-dispersive X-ray spectroscopy (SEM-EDX) was also utilized to obtain an overview of the elemental composition of particles in the leachate. The sample preparation procedures were described in the supplemental information.

#### *2.5 Agglomeration potential*

This set of experiments was designed to determine the influence of pH and zeta potential on the stability of  $\text{TiO}_2$  nanoparticles dispersed in the synthetic landfill leachates, where size changes of  $\text{TiO}_2$  agglomerates were used to reflect particle stability. The sample preparation procedures were done for all synthetic leachates.

The pH of the synthetic leachate was adjusted between 3 and 12 by adding acetic acid or sodium hydroxide<sup>23, 29</sup>. The pH range tested in the experiments covered those of the natural landfill leachates, which are normally ranged between 4.5 and 9 depending on landfill age and the deposited waste (Kjeldsen et al., 2002; Mukherjee et al. 2015). For landfill leachates from landfills of incinerated wastes, the pH is either neutral or alkaline based on our measurements of the landfills in Switzerland. In previous studies

concerning the agglomeration of TiO<sub>2</sub> ENPs in natural waters and artificial freshwaters, such as river waters and seawaters, the pH value was kept as the natural value (normally between 6 and 8) or adjusted within a relatively narrow range (e.g. between pH=4 and 8) to approximate the environmental conditions (Adam et al., 2016; Brunelli et al., 2016; Chekli et al., 2015a; Labille et al., 2015; Ottofuelling et al., 2011; von der Kammer et al., 2010). However, the pH adjustments were conducted in a wide range in this case for the leachates due to the wide variation range of pH values for different natural landfills. The significantly acidic and alkaline conditions such as pH=3 and pH=12 were not typically met in realistic landfill leachate, we tested these conditions in the interest of the understanding of the effect of pH. The pH adjustment was conducted before spiking TiO<sub>2</sub> ENPs, otherwise the agglomeration of TiO<sub>2</sub> may have happened during the pH adjustment process, which took several minutes per sample. Zeta potential measurements for the leachates without spiked TiO<sub>2</sub> were conducted after the pH adjustments and no consistent pH-zeta potential curve was obtained due to the low concentrations of the residual particles. The TiO<sub>2</sub> ENPs were added into the synthetic leachate under different pH values and the concentration of TiO<sub>2</sub> in every sample was kept constant at 40 mg/L, similar to the previous study (French et al., 2009). The samples were sonicated for two minutes and allowed to rest for additional three minutes before DLS measurements (French et al., 2009). pH values were measured again after spiking TiO<sub>2</sub> ENPs into the leachates and the values are used for the remainder of the study. For DLS measurements, three consecutive measurements were taken for each sample and at least three replicate experiments were conducted for each set of experimental conditions; where average and standard deviation of measurements are presented in the following figures and tables.

### 3. Results

#### 3.1 Characterization of fly ash particles and synthetic landfill leachates

General properties of the fly ash leachates are listed in Table 1. The ionic strength was estimated from the measured conductivity based on the linear equation: (Fang et al., 2009; Morrisson et al., 1990)

$$I = 0.0127 \times EC \quad (1),$$

where  $I$  is the ionic strength (mM) and  $EC$  is the electrical conductivity ( $\mu\text{S}/\text{cm}$ ). The equation was originally developed based on the soil solution prepared by the filtration method similar to that of this study, so the calculated ionic strengths here were only estimated values. The fly ash leachates are either nearly neutral (for WaS(N), WaS(MOD), WaS(MOD-D), and Wa(MOD-D)) or alkaline (for Wo(N), Wo(MOD), Wo(MOD-D), Wa(N), Wa(MOD)). The samples obtained through the standard protocol (N) have much higher conductivities and ionic strengths than the leachates made by the modified leachate preparation procedures (MOD). The different leachate preparation procedures between (N) and (MOD) do not influence the pH values significantly. The measured conductivities of (N) is generally within the range, while that of (MOD) is well below the range of the values of natural landfill leachate (2500 - 35000  $\mu\text{S}/\text{cm}$ )

and the leachate from land disposal of coal fly ash (2100 – 19200  $\mu\text{S}/\text{cm}$ ) reported in the literature (Due to the low solid to DI water ratio utilized to make the (MOD), the representativeness of the leachate was also checked and the results were shown in the supplemental information (S3)) (Hjelmar 1990; Kjeldsen et al., 2002). After dilution of the (MOD) leachates, the conductivity and estimated ionic strengths of the (MOD-D) leachates are higher than the general value of rain water (the average conductivity is generally smaller than 50  $\mu\text{S}/\text{cm}$ ) (Beysens et al., 2006; Topçu et al., 2002) and comparable with the value of surface waters (Chekli et al., 2015b; Rolisola et al., 2014). The (MOD-D) may represent the water (e.g. rain water) just in contact with the surface of the landfill resulting in dissolution of small amounts of salts. The (N) may represent the landfill leachate collected from the draining system. The study of Yildiz et al revealed the growing tendency of the concentration of soluble inorganic components in the landfill leachate (using chloride as the indicator) when the landfill was under operation from the year of 1984 to 1997 (Yildiz et al., 2004). It can be inferred from their study that longer percolating depth of water within the landfill results in higher ionic strength of the aquatic media. So compared with (MOD-D) and (N), (MOD) may better simulate the aqueous media formed in a certain depth within the landfill.

Table 1 also gives the ICP-OES and IC results for the concentrations of major metallic elements and anions in the (N) and (MOD) leachates after the filtration process. The compositions in the leachates of the fly ash are significantly different from those in the corresponding dry fly ash. The detailed analysis about the elemental compositions of the leachates was shown in the supplemental information.

**Table 1.** *General properties of the synthetic landfill leachates*

| Sample     | pH   | Conductivity<br>( $\mu\text{S}/\text{cm}$ ) | Ionic strength<br>(mM) | Na Ca Al Zn Cl Br $\text{SO}_4^{2-}$ |      |      |      |       |     |      |
|------------|------|---|------------------------|--------------------------------------|------|------|------|-------|-----|------|
|            |      |   |                        | (mg/l)                               |      |      |      |       |     |      |
| WaS(N)     | 6.4  | 38580                                       | 490                    | 9500                                 | 850  | <0.4 | 4230 | 21300 | 590 | 8530 |
| Wa(N)      | 9.5  | 46140                                       | 586                    | 7100                                 | 1290 | 11   | 6.7  | 17870 | 620 | 3760 |
| Wo(N)      | 13.5 | 31940                                       | 406                    | 3260                                 | 1280 | <0.4 | 3.1  | 8720  | 270 | 4620 |
| WaS(MOD)   | 7.2  | 1250  | 16                     | 100                                  | 39   | <0.4 | 43   | 220   | 6   | 160  |
| Wa(MOD)    | 9.9  | 990   | 13                     | 80                                   | 62   | 1.8  | 0.1  | 190   | 7   | 130  |
| Wo(MOD)    | 11.2 | 1020  | 13                     | 42                                   | 78   | 3.4  | 0.14 | 100   | 3   | 100  |
| WaS(MOD-D) | 6.6  | 130   | 1.6                    |                                      |      |      |      |       |     |      |
| Wa(MOD-D)  | 7.0  | 120   | 1.6                    |                                      |      |      |      |       |     |      |
| Wo(MOD-D)  | 10.0 | 140   | 1.8                    |                                      |      |      |      |       |     |      |

..

**Table 2.** Size dependence of  $TiO_2$  agglomerates on pH and zeta potential for the (N) and (MOD) leachates. Experiments were conducted at the natural pH of the leachates and in leachates adjusted to lower or higher pH.\*

| Leachate | pH             | Zeta potential (mv) | $TiO_2$ agglomerates size (nm) |
|----------|----------------|---------------------|--------------------------------|
| WaS(N)   | 3.9            | -0.4±1.3            | 2600±650                       |
|          | 6.4 (natural)  | -2.2±1.8            | 2700±740                       |
| Wa(N)    | 4.5            | 2.2±4.5             | 2400±640                       |
|          | 9.5 (natural)  | 2.9±0.5             | 2600±60                        |
|          | 11.0           | 2.9±0.1             | 3500±1380                      |
| Wo(N)    | 5.4            | -6.2±1.9            | 2400±610                       |
|          | 12.5 (natural) | -3.6±0.9            | 2600±590                       |
| WaS(MOD) | 3.6            | 9.9±0.4             | 1800±50                        |
|          | 7.2 (natural)  | 6.2±0.7             | 1900±340                       |
|          | 10.1           | -6.3±0.2            | 2100±220                       |
| Wa(MOD)  | 3.7            | 11.7±0.4            | 1900±100                       |
|          | 9.9 (natural)  | 2.8±1.2             | 2100±190                       |
| Wo(MOD)  | 4.3            | 14.3±0.8            | 1700±50                        |
|          | 11.2 (natural) | 3.9±1.3             | 2000±40                        |

\* The  $TiO_2$  particles formed large agglomerates for all the leachates under different pH values, therefore pH values were not adjusted to exactly the same values for all the leachates.

### 3.2 Agglomeration potential of $TiO_2$ ENPs in synthetic landfill leachates

The size of  $TiO_2$  agglomerates in DI water (pH = 5.75, conductivity = 25.3  $\mu$ S/cm) was  $233 \pm 27$  nm and the zeta potential of the particles were  $21.5 \pm 0.9$  mV. As a necessary step in the standard protocol, filtration of the fly ash suspensions by the 0.45  $\mu$ m filter to make the leachates also removed most of the colloids in the same size range as the agglomerates formed by  $TiO_2$  ENPs in DI water. So the interaction between  $TiO_2$  ENPs and the colloids in the leachates was eliminated prominently. The size dependence of  $TiO_2$  agglomerates on pH in the leachates made by the standard protocol (N) and modified procedures (MOD) are shown in Table 2. The zeta potential and size of  $TiO_2$  agglomerates were measured at the natural pH of the leachates and at pH adjusted to lower and higher values. For the (N) leachates, the zeta potential of the particles is always close to zero and not sensitive to any pH changes. For (MOD) leachates, the variance of zeta potential under different pH values are more evident due to the much lower ionic



strength compared with the (N) leachates. However, for both (N) and (MOD) leachates, large  $\text{TiO}_2$  agglomerates (i.e. above 1500 nm) are formed regardless of the variation in pH.

Figure 1 shows the size dependence of  $\text{TiO}_2$  agglomerates as a function of pH in DI water and (MOD-D) leachates. In DI water, the largest agglomerates are formed at pH=7. In contrast, the size of  $\text{TiO}_2$  agglomerates dispersed in (MOD-D) leachates are generally larger than 1500 nm in basic pH values without distinct maximum size, however, decreases prominently to smaller than 500 nm when pH is adjusted to less than 5. The results in Table 2 and Figure 1 indicate that  $\text{TiO}_2$  ENPs form large agglomerates under basic conditions for all types of leachates regardless of leachate dilution.

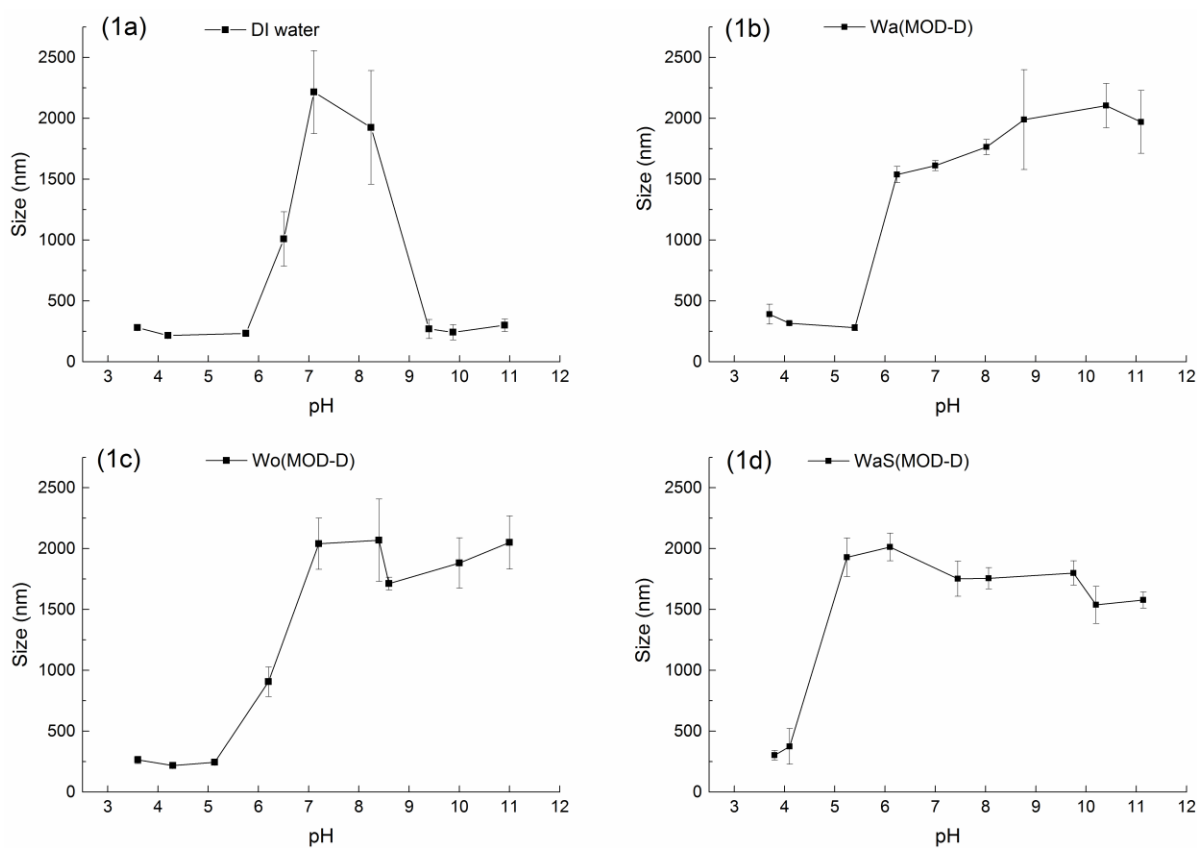


**Figure 1.** Relationship between the size of  $\text{TiO}_2$  agglomerates and pH in DI water and (MOD-D) leachates. Error bars represent standard deviation of three replicate experiments.

In addition to pH, which is one of the important environmental factors to influence the behaviors of ENPs in the leachates, zeta potential directly depicts the state of particles in terms of surface charge. Zeta potential measurements were also conducted for every experimental condition and tested pH. The interconnectivity of zeta potential and agglomeration of  $\text{TiO}_2$  ENPs in (MOD-D) leachates is shown in Figure 2. The size of  $\text{TiO}_2$  agglomerates is related to the zeta potential and varies in a wide range between 200 nm and 2500 nm under different experimental conditions. The primary particle size of dry  $\text{TiO}_2$

powder was approximately 21 nm (TEM image of the  $\text{TiO}_2$  powder was shown in the supplemental information), so every aqueous medium tested (including DI water) promoted agglomeration of  $\text{TiO}_2$  particles. The agglomeration tendency of primary  $\text{TiO}_2$  particles is mainly due to the high specific surface area of the nano-sized primary particles resulting in the high surface energy; the agglomeration is favored to achieve the thermodynamically stable state (Cerdeira et al., 2010; Needham et al., 2005). The size of the agglomerates was generally smaller than 500 nm when the absolute value of zeta potential was larger than 10 mV, and was above 1500 nm when the absolute value was smaller than 10 mV. As shown in Figure 2, when large agglomerates were formed and when the zeta potential was close to zero, more uncertainties occurred in term of both particle size and zeta potential which is reflected by the larger error bars on these samples. This is due to the unstable state of the system in which agglomeration may occur during the measuring process and the large agglomerates formed may settle to the bottom of the cuvette during analysis.

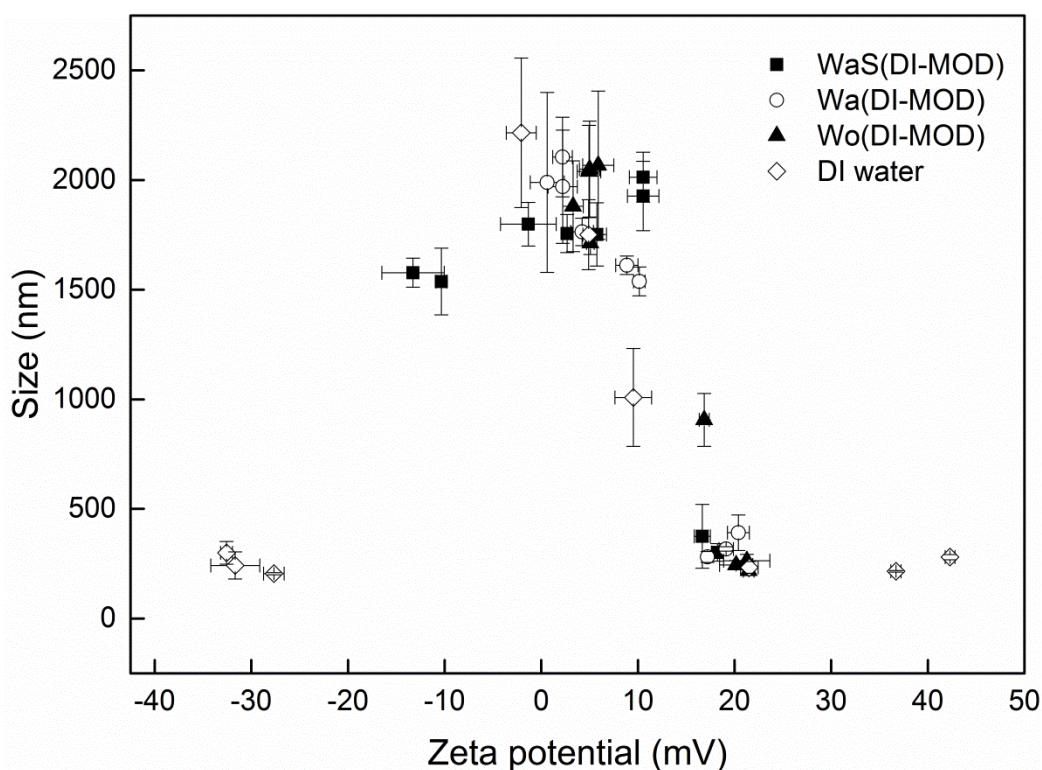


**Figure 2.** Relationship between the size of  $\text{TiO}_2$  agglomerates and zeta potential in (MOD-D) leachates. Error bars represent standard deviation of three replicate experiments.

#### 4. Discussion

To further study the influence of leachate composition on the behavior of TiO<sub>2</sub> ENPs, the pH-zeta potential relationship of the aqueous systems where TiO<sub>2</sub> ENPs were dispersed in pure DI water as well as in (MOD-D) leachates were shown in Figure 3. The results of (N) leachates given in Table 2 were also shown. The curve for the ENPs in pure DI water shows that the zeta potential is inversely proportional to pH in the range between -40 mv and 40 mv. The measured isoelectric point ( $pH_0$ ) of TiO<sub>2</sub> dispersed in DI water is approximately pH=7 in our experiments and consistent with previous studies (Dutta et al., 2004; Fernandez-Ibanez et al., 2000; French et al., 2009; Petosa et al., 2010). For (N) leachates, the zeta potential is always close to zero as discussed above. The three curves of (MOD-D) leachates are markedly different from those of the DI water, where the variance of zeta potential is smaller across the pH range resulting in overall shallower curves. This phenomenon can be attributed to the existence of electrolytes in the leachates that compresses the electrical double layer of the TiO<sub>2</sub> particles (Hunter 1981) and similar results have been reported for alumina ENPs (Jailani et al., 2008). For Wa(MOD-D) and Wo(MOD-D), when the pH is higher than 9, the zeta potential of the system remains slightly positive. This is in contrast to the negative zeta potentials with the absolute values larger than 10 mV for the samples in pure DI water and WaS(MOD-D) in the same pH range. Based on the results shown in Figure 2, the TiO<sub>2</sub> ENPs are considered to be well dispersed when the absolute value of the zeta potential is larger than 10 mV. The positive zeta potentials of Wa(MOD-D) and Wo(MOD-D) under basic pH values may be due to the uncertainties of the zeta potential measurements. In the experiments, the measurements took a longer time and had more uncertainty when the zeta potential was close to zero (in the range between -3 mv and 3 mv) due to the unstable state of the system as mentioned above. According to the Schultz-Hardy rule, the ions with higher valences are much more effective in causing the coagulation of particles. French et al found that the divalent cation (Ca<sup>2+</sup>) was more effective than monovalent cation (Na<sup>+</sup>) to promote TiO<sub>2</sub> agglomeration due to the influence of valence on Debye length (French et al., 2009). It has also been found that Al<sup>3+</sup> promoted the most agglomeration of montmorillonite among a number of ions with different valences, which could shift the zeta potential from negative to positive when the concentration of Al<sup>3+</sup> was sufficiently high (e.g. above 5×10<sup>-4</sup> M (13.5 mg/l)) (Saka and Güler, 2006). So the presence of Al<sup>3+</sup> in Wa(MOD) and Wo(MOD) as shown in Table 1 may also contribute to the differences among the zeta potentials for the various systems when pH values are larger than 9. The  $pH_0$  of WaS(MOD-D) is approximately 9 and larger than that of the pure DI water sample, which is also possible due to the existence of electrolytes in the leachate. Models specifically based on TiO<sub>2</sub> particles further revealed higher  $pH_0$  under higher electrolyte concentration for the simplified 1-1 electrolyte (Sonnefeld 2001).

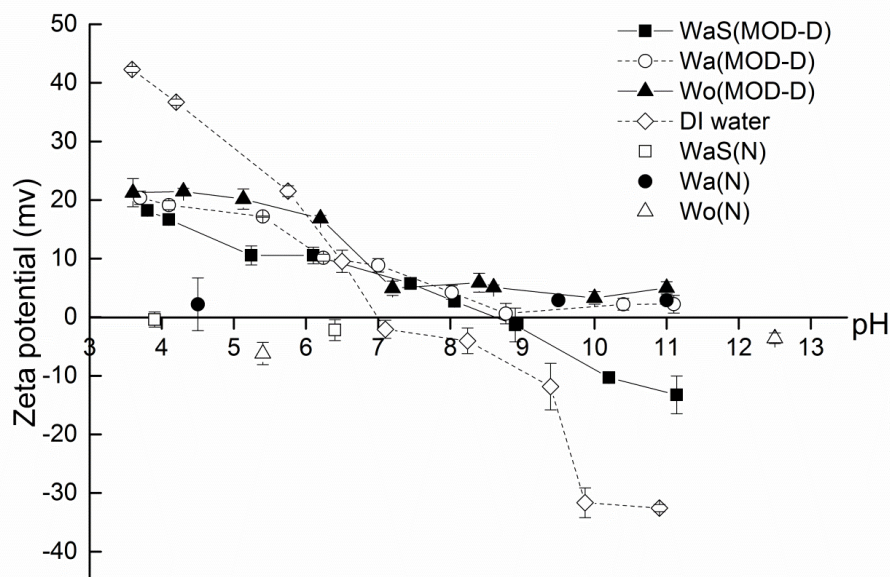


**Figure 3.** Relationship between zeta potential and pH of the  $\text{TiO}_2$  ENPs suspensions dispersed in pure DI water, (N) and (MOD-D) leachates. Error bars represent standard deviation of three replicate experiments.

Based on DLVO theory, the total interaction energy between two particles is expressed as the sum of the repulsive electrostatic interaction and the attractive interaction due to Van der Waals forces (Derjaguin 1941; Verwey et al., 1999). The  $\text{TiO}_2$  particles are most likely to agglomerate with each other and form the largest agglomerates at  $pH_0$  due to the minimum repulsive interactions. At other pH values, the agglomerates are smaller due to the non-zero zeta potential and the increasing repulsive forces. As shown in Figures 1 and 3, the results for the sample in pure DI water (Figure (1a)) confirm this mechanism well, i.e. the largest agglomerates are formed at  $pH_0$ . For the samples in Wa(MOD-D) and Wo(MOD-D) which do not have a clear  $pH_0$  in the tested pH ranges, the sizes of the agglomerates are kept at high values in a wide range of pH without distinct peaks on the curves as shown in Figure (1b) and (1c). However, for the sample of WaS(MOD-D), shown in Figure (1d), its  $pH_0$  is approximately 9, while the largest agglomerates are not formed at  $pH_0$ . The sizes of agglomerates are almost constant when pH varied from 5 to 11. For the aqueous medium containing electrolytes such as the leachates used in this study, similar findings were reported in previous research endeavors in which the pH for the formation of largest agglomerates deviated from  $pH_0$ . In addition to the DLVO theory, the deviation from  $pH_0$  was because the hydrogen bonds formed among water molecules could be either strengthened or weakened when different ions are introduced into water, which resulted in the changes of water structure around the added ions (Golikova et al., 2000; Golikova et al., 1998; Tkachenko et al., 2006).

The experimental results reveal that the agglomerate size of  $\text{TiO}_2$  in the synthetic leachates depends on ionic strength, ionic composition and pH simultaneously. When the ionic strength is low (conditions of (MOD-D) leachates), the ionic composition and pH can influence the state of  $\text{TiO}_2$  agglomerates. However, when it is high (conditions of (N) and (MOD) leachates), the effects of the other two factors may be masked. Compared with rainwater (Beysens et al., 2006; Topçu et al., 2002), the conductivity and the concentrations of ions in landfill leachate are much higher. The observation suggests that that when rainwater passes through the landfill, significant amounts of ions may dissolve in it, leading to the landfill leachate in the draining system with increased conductivity and ion concentrations.

#### **4. Conclusions**

For the synthetic leachates made from fly ash utilized in this study, the ionic strength, ionic composition and pH simultaneously influence the agglomeration behavior of  $\text{TiO}_2$ . However, solutions high in ionic strength may mask the destabilizing effects of the other two factors. In practice, rainwater is typically the main source of water entering a landfill and some ENPs may be released from the deposited waste to the aqueous media when rainwater percolates through the deposited waste. Given that the path rainwater takes through the landfill, the chemical properties will change over time and this will affect the transportation and agglomeration of ENPs as they move through the landfill. It is expected that  $\text{TiO}_2$  ENPs tend to form agglomerates in aqueous media within the landfill based on the experimental results. The settling velocity of a particle in the fluid is positively correlated to the particle size based on the Stokes's law, so ENPs released from the deposited waste are possibly settled out from the flow of leachate due to the formation of agglomerates. The interaction between ENPs and high amounts of colloids in the leachate also influence the transportation of ENPs in the landfill, so it is also possible that ENPs may leave the landfill with the leachate by heteroagglomeration with the colloids, although no solid evidence has been found for the existence of ENPs in the natural landfill leachates. In practice, tracking the transport of ENPs inside the landfills is difficult to achieve. It is possible to mimic the transport of ENPs in the simulated landfill in the laboratory although the parameters which are important for the ENPs transportation are hard to obtain and simulate in the experiments, such as the packing density of the waste. The other alternative is to utilize synthetic leachate by different types of deposited wastes such as the method employed in this study. The waste deposited in landfills is complicated and the fly ash is just one typical component. Future studies can focus on the exploration of the aqueous media made from other types of waste in landfills, which contribute to the constituents of landfill leachate. Based on these studies, understanding of the ENPs in the landfill could be advanced in the future.

## Acknowledgements

The TEM and SEM images were performed at the Electron Microscopy Center of EMPA. The authors thank Yucheng Zhang for technical support of TEM.

## References

- Adam, V., Loyaux-Lawniczak, S., Labille, J., Galindo, C., del Nero, M., Gangloff, S., Weber, T. and Quaranta, G., 2016. Aggregation behaviour of TiO<sub>2</sub> nanoparticles in natural river water. *Journal of Nanoparticle Research* 18(1), 1-11.
- Baun, D.L. and Christensen, T.H., 2004. Speciation of heavy metals in landfill leachate: a review. *Waste Management & Research* 22(1), 3-23.
- Beysens, D., Ohayon, C., Muselli, M. and Clus, O., 2006. Chemical and biological characteristics of dew and rain water in an urban coastal area (Bordeaux, France). *Atmospheric Environment* 40(20), 3710-3723.
- Bolyard, S.C., Reinhart, D.R. and Santra, S., 2013. Behavior of engineered nanoparticles in landfill leachate. *Environ Sci Technol* 47(15), 8114-8122.
- Brunelli, A., Zabeo, A., Semenzin, E., Hristozov, D. and Marcomini, A., 2016. Extrapolated long-term stability of titanium dioxide nanoparticles and multi-walled carbon nanotubes in artificial freshwater. *Journal of Nanoparticle Research* 18(5), 1-13.
- Buha, J., Mueller, N., Nowack, B., Ulrich, A., Losert, S. and Wang, J., 2014. Physical and chemical characterization of fly ashes from Swiss waste incineration plants and determination of the ash fraction in the nanometer range. *Environ Sci Technol* 48(9), 4765-4773.
- Cerdeira, A.M., Mazzotti, M. and Gander, B., 2010. Miconazole nanosuspensions: influence of formulation variables on particle size reduction and physical stability. *International journal of pharmaceutics* 396(1), 210-218.
- Cekli, L., Roy, M., Tijng, L., Donner, E., Lombi, E. and Shon, H., 2015a. Agglomeration behaviour of titanium dioxide nanoparticles in river waters: A multi-method approach combining light scattering and field-flow fractionation techniques. *Journal of Environmental Management* 159, 135-142.
- Cekli, L., Zhao, Y., Tijng, L., Phuntsho, S., Donner, E., Lombi, E., Gao, B. and Shon, H., 2015b. Aggregation behaviour of engineered nanoparticles in natural waters: characterising aggregate structure using on-line laser light scattering. *Journal of hazardous materials* 284, 190-200.
- Clément, L., Hurel, C. and Marmier, N., 2013. Toxicity of TiO<sub>2</sub> nanoparticles to cladocerans, algae, rotifers and plants—effects of size and crystalline structure. *Chemosphere* 90(3), 1083-1090.
- Delay, M., Dolt, T., Woellhaf, A., Sembritzki, R. and Frimmel, F.H., 2011. Interactions and stability of silver nanoparticles in the aqueous phase: Influence of natural organic matter (NOM) and ionic strength. *Journal of Chromatography A* 1218(27), 4206-4212.
- Derjaguin, B., 1941. Theory of the stability of strongly charged lyophobic sols and the adhesion of strongly charged particles in solutions of electrolytes. *Acta Physicochim. USSR* 14, 633-662.
- Burkhardt, M., Dietschweiler, C., Schmidt, S., Englert, A., Hemmann, J., Sinnet, B., Kägi, R., 2015. Titandioxid - Leitsubstanz für Nanopartikel in Deponie-Sickerwasser. *Aqua & Gas*, 12, 47.
- Dulger, M., Sakallioğlu, T., Temizel, I., Demirel, B., Coptu, N., Onay, T., Uyguner-Demirel, C. and Karanfil, T., 2016. Leaching potential of nano-scale titanium dioxide in fresh municipal solid waste. *Chemosphere* 144, 1567-1572.
- Dutta, P.K., Ray, A.K., Sharma, V.K. and Millero, F.J., 2004. Adsorption of arsenate and arsenite on titanium dioxide suspensions. *Journal of Colloid and Interface Science* 278(2), 270-275.

- EN, B.S. (2002) 12457-2, Characterisation of Waste–Leaching–Compliance test for leaching of granular waste materials and sludges. British Standard, UK.
- Fang, J., Shan, X.-q., Wen, B., Lin, J.-m. and Owens, G., 2009. Stability of titania nanoparticles in soil suspensions and transport in saturated homogeneous soil columns. *Environmental Pollution* 157(4), 1101-1109.
- Fernandez-Ibanez, P., De Las Nieves, F. and Malato, S., 2000. Titanium dioxide/electrolyte solution interface: electron transfer phenomena. *Journal of Colloid and Interface Science* 227(2), 510-516.
- French, R.A., Jacobson, A.R., Kim, B., Isley, S.L., Penn, R.L. and Baveye, P.C., 2009. Influence of ionic strength, pH, and cation valence on aggregation kinetics of titanium dioxide nanoparticles. *Environ Sci Technol* 43(5), 1354-1359.
- Golikova, E., Chernoberezhskii, Y.M. and Ioganson, O., 2000. On a correlation between the aggregation stability and integral electrosurface characteristics of oxide dispersions. *Colloid journal* 62(5), 532-540.
- Golikova, E., Ioganson, O., Duda, L., Osmolovskii, M., Yanklovich, A. and Chernoberezhskii, Y.M., 1998. Aggregation stability of aqueous dispersions of  $\alpha$ -Fe<sub>2</sub>O<sub>3</sub>,  $\alpha$ -FeOOH, and Cr<sub>2</sub>O<sub>3</sub> under conditions of the isoelectric state. *Colloid journal of the Russian Academy of Sciences* 60(2), 166-171.
- Gottschalk, F. and Nowack, B., 2011. The release of engineered nanomaterials to the environment. *Journal of Environmental Monitoring* 13(5), 1145-1155.
- Hamley, I., 2003. Nanotechnology with soft materials. *Angewandte Chemie International Edition* 42(15), 1692-1712.
- Heremans, J.P., Dresselhaus, M.S., Bell, L.E. and Morelli, D.T., 2013. When thermoelectrics reached the nanoscale. *Nature nanotechnology* 8(7), 471-473.
- Hincapié, I., Caballero-Guzman, A., Hiltbrunner, D. and Nowack, B., 2015. Use of engineered nanomaterials in the construction industry with specific emphasis on paints and their flows in construction and demolition waste in Switzerland. *Waste management* 43, 398-406.
- Hjelmar, O., 1990. Leachate from land disposal of coal fly ash. *Waste Management & Research* 8(1), 429-449.
- Hunter, R., 1981. *Colloid science: zeta potential in colloid science: principles and applications*, London: Academic Press.
- Jailani, S., Franks, G.V. and Healy, T.W., 2008.  $\zeta$  potential of nanoparticle suspensions: effect of electrolyte concentration, particle size, and volume fraction. *Journal of the American Ceramic Society* 91(4), 1141-1147.
- Ji, L., Lu, S., Yang, J., Du, C., Chen, Z., Buekens, A. and Yan, J., 2016. Municipal solid waste incineration in China and the issue of acidification: A review. *Waste Management & Research* 34(4), 280-297.
- Khan, I.A., Berge, N.D., Sabo-Attwood, T., Ferguson, P.L. and Saleh, N.B., 2013. Single-walled carbon nanotube transport in representative municipal solid waste landfill conditions. *Environ Sci Technol* 47(15), 8425-8433.
- Kjeldsen, P., Barlaz, M.A., Rooker, A.P., Baun, A., Ledin, A. and Christensen, T.H., 2002. Present and long-term composition of MSW landfill leachate: a review. *Critical reviews in environmental science and technology* 32(4), 297-336.
- Klaine, S.J., Koelmans, A.A., Horne, N., Carley, S., Handy, R.D., Kapustka, L., Nowack, B. and von der Kammer, F., 2012. Paradigms to assess the environmental impact of manufactured nanomaterials. *Environmental Toxicology and Chemistry* 31(1), 3-14.
- Labille, J. and Brant, J., 2010. Stability of nanoparticles in water. *Nanomedicine* 5(6), 985-998.
- Labille, J.r.m., Harns, C., Bottero, J.-Y. and Brant, J., 2015. Heteroaggregation of titanium dioxide nanoparticles with natural clay colloids. *Environ Sci Technol* 49(11), 6608-6616.

- Linkov, I., Bates, M.E., Canis, L.J., Seager, T.P. and Keisler, J.M., 2011. A decision-directed approach for prioritizing research into the impact of nanomaterials on the environment and human health. *Nature nanotechnology* 6(12), 784-787.
- Masciangioli, T. and Zhang, W.-X., 2003. Peer reviewed: environmental technologies at the nanoscale. *Environ Sci Technol* 37(5), 102A-108A.
- Mitrano, D.M., Motellier, S., Clavaguera, S. and Nowack, B., 2015. Review of nanomaterial aging and transformations through the life cycle of nano-enhanced products. *Environment international* 77, 132-147.
- Montaño, M.D., Lowry, G.V., von der Kammer, F., Blue, J. and Ranville, J.F., 2014. Current status and future direction for examining engineered nanoparticles in natural systems. *Environmental Chemistry* 11(4), 351-366.
- Morrisson, A.R., Park, J.S. and Sharp, B.L., 1990. Application of high-performance size-exclusion liquid chromatography to the study of copper speciation in waters extracted from sewage sludge treated soils. *Analyst* 115(11), 1429-1433.
- Mueller, N.C., Buha, J., Wang, J., Ulrich, A. and Nowack, B., 2013. Modeling the flows of engineered nanomaterials during waste handling. *Environmental Science: Processes & Impacts* 15(1), 251-259.
- Mukherjee, S., Mukhopadhyay, S., Hashim, M.A. and Sen Gupta, B., 2015. Contemporary environmental issues of landfill leachate: assessment and remedies. *Critical reviews in environmental science and technology* 45(5), 472-590.
- Needham, S., Wang, G. and Liu, H., 2005. Electrochemical performance of SnSb and Sn/SnSb nanosize powders as anode materials in Li-ion cells. *Journal of alloys and compounds* 400(1), 234-238.
- Nixon, J.D., Wright, D., Dey, P., Ghosh, S. and Davies, P., 2013. A comparative assessment of waste incinerators in the UK. *Waste management* 33(11), 2234-2244.
- Ottofuelling, S., Von Der Kammer, F. and Hofmann, T., 2011. Commercial titanium dioxide nanoparticles in both natural and synthetic water: comprehensive multidimensional testing and prediction of aggregation behavior. *Environ Sci Technol* 45(23), 10045-10052.
- Petosa, A.R., Jaisi, D.P., Quevedo, I.R., Elimelech, M. and Tufenkji, N., 2010. Aggregation and deposition of engineered nanomaterials in aquatic environments: role of physicochemical interactions. *Environ Sci Technol* 44(17), 6532-6549.
- Prabhu, S. and Poulouse, E.K., 2012. Silver nanoparticles: mechanism of antimicrobial action, synthesis, medical applications, and toxicity effects. *International Nano Letters* 2(1), 1-10.
- Ramakrishnan, A., Blaney, L., Kao, J., Tyagi, R., Zhang, T.C. and Surampalli, R.Y., 2015. Emerging contaminants in landfill leachate and their sustainable management. *Environmental Earth Sciences* 73(3), 1357-1368.
- Rolisola, A.M., Suárez, C.A., Menegário, A.A., Gastmans, D., Kiang, C.H., Colaço, C.D., Garcez, D.L. and Santelli, R.E., 2014. Speciation analysis of inorganic arsenic in river water by Amberlite IRA 910 resin immobilized in a polyacrylamide gel as a selective binding agent for As (v) in diffusive gradient thin film technique. *Analyst* 139(17), 4373-4380.
- Saka, E. and Güler, C., 2006. The effects of electrolyte concentration, ion species and pH on the zeta potential and electrokinetic charge density of montmorillonite. *Clay minerals* 41(4), 853-861.
- Samad, A., Alam, M.I. and Saxena, K., 2009. Dendrimers: a class of polymers in the nanotechnology for the delivery of active pharmaceuticals. *Current pharmaceutical design* 15(25), 2958-2969.
- Shvedova, A.A., Pietroiusti, A., Fadeel, B. and Kagan, V.E., 2012. Mechanisms of carbon nanotube-induced toxicity: focus on oxidative stress. *Toxicology and applied pharmacology* 261(2), 121-133.
- Sonnefeld, J., 2001. On the influence of background electrolyte concentration on the position of the isoelectric point and the point of zero charge. *Colloids and Surfaces A: Physicochemical and Engineering Aspects* 190(1), 179-183.



Sun, T.Y., Gottschalk, F., Hungerbühler, K. and Nowack, B., 2014. Comprehensive probabilistic modelling of environmental emissions of engineered nanomaterials. *Environmental Pollution* 185, 69-76.

Thio, B.J.R., Zhou, D. and Keller, A.A., 2011. Influence of natural organic matter on the aggregation and deposition of titanium dioxide nanoparticles. *Journal of hazardous materials* 189(1), 556-563.

Tkachenko, N.H., Yaremko, Z.M. and Bellmann, C., 2006. Effect of 1-1-charged ions on aggregative stability and electrical surface properties of aqueous suspensions of titanium dioxide. *Colloids and Surfaces A: Physicochemical and Engineering Aspects* 279(1), 10-19.

Topçu, S., Incecik, S. and Atımtay, A.T., 2002. Chemical composition of rainwater at EMEP station in Ankara, Turkey. *Atmospheric Research* 65(1), 77-92.

Verwey, E.J.W., Overbeek, J.T.G. and Overbeek, J.T.G., 1999. *Theory of the stability of lyophobic colloids*, Courier Corporation.

von der Kammer, F., Ottofuelling, S. and Hofmann, T., 2010. Assessment of the physico-chemical behavior of titanium dioxide nanoparticles in aquatic environments using multi-dimensional parameter testing. *Environmental Pollution* 158(12), 3472-3481.

Walser, T. and Gottschalk, F., 2014. Stochastic fate analysis of engineered nanoparticles in incineration plants. *Journal of Cleaner Production* 80, 241-251.

Walser, T., Limbach, L.K., Brogioli, R., Erismann, E., Flamigni, L., Hattendorf, B., Juchli, M., Krumeich, F., Ludwig, C. and Prikopsky, K., 2012. Persistence of engineered nanoparticles in a municipal solid-waste incineration plant. *Nature nanotechnology* 7(8), 520-524.

Yildiz, E.D., Ünlü, K. and Rowe, R.K., 2004. Modelling leachate quality and quantity in municipal solid waste landfills. *Waste Management & Research* 22(2), 78-92.

## Appendix 1

### Supplemental Information: Mobility of metallic (nano)particles in leachates from landfills containing waste incineration residues

**Table S1:** *Precipitation recorded at the Flawil weather station by Meteoswiss in the week before each sampling campaign.*

| <b>Date</b>                       | <b>Precipitation<br/>(mm)</b> |
|-----------------------------------|-------------------------------|
| 2015.10.07                        | 1.0                           |
| 2015.10.08                        | 0.0                           |
| 2015.10.09                        | 0.0                           |
| 2015.10.10                        | 0.0                           |
| 2015.10.11                        | 0.0                           |
| 2015.10.12                        | 0.0                           |
| 2015.10.13 (first<br>collection)  | 10.5                          |
| 2016.01.02                        | 11.1                          |
| 2016.01.03                        | 0.3                           |
| 2016.01.04                        | 16.5                          |
| 2016.01.05                        | 1.0                           |
| 2016.01.06                        | 0.5                           |
| 2016.01.07                        | 11                            |
| 2016.01.08 (second<br>collection) | 14.8                          |
| 2016.03.25                        | 3.7                           |
| 2016.03.26                        | 0.4                           |
| 2016.03.27                        | 0.6                           |
| 2016.03.28                        | 0.0                           |
| 2016.03.29                        | 2.1                           |
| 2016.03.30                        | 0                             |
| 2016.03.31 (third<br>collection)  | 0                             |

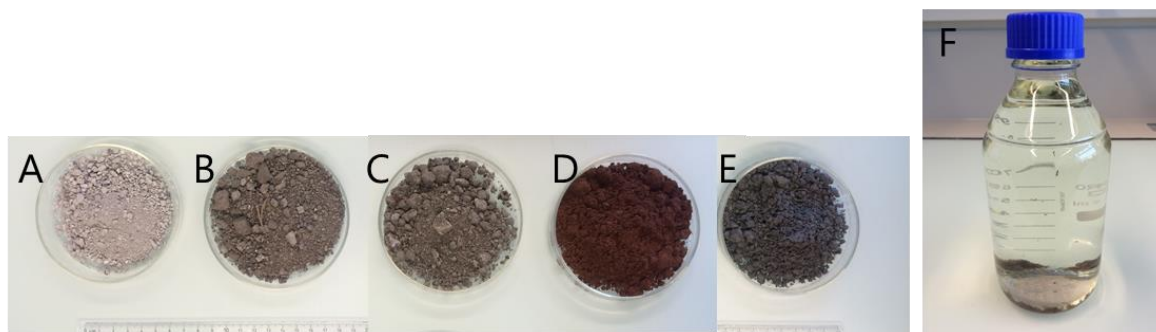


**Figure S1:** Samples collected from the landfill: bottom ash a) fresh, b) 2 months old, C) 6 months to 1 year old; D) Sludge incineration, E) fly ash and F) natural leachate.

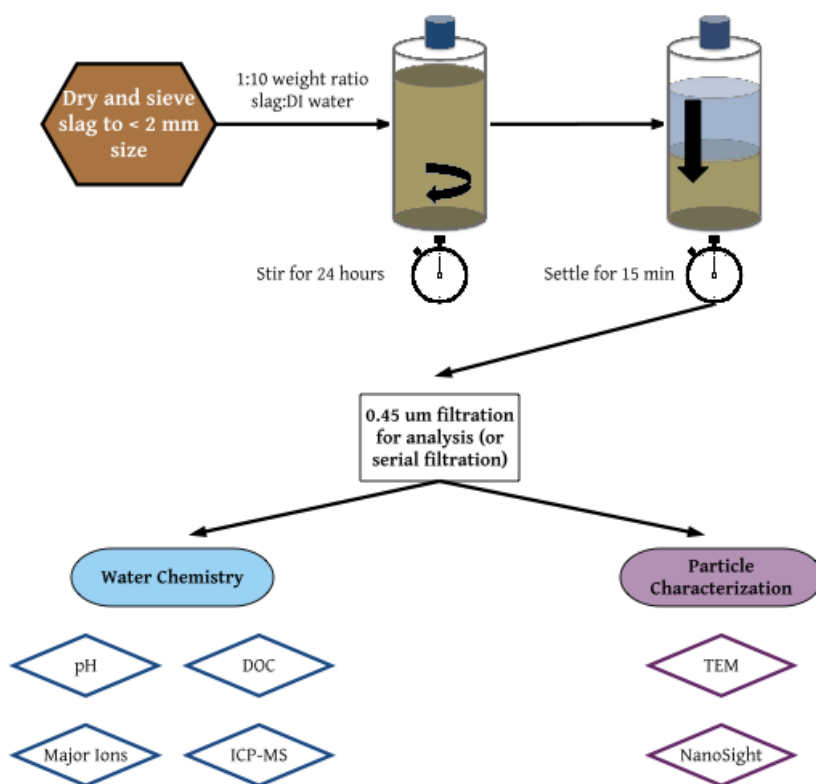


**Figure S2:** Leaching process of various slags recovered from the landfill and further processing of leachate for chemical and physical characterization.

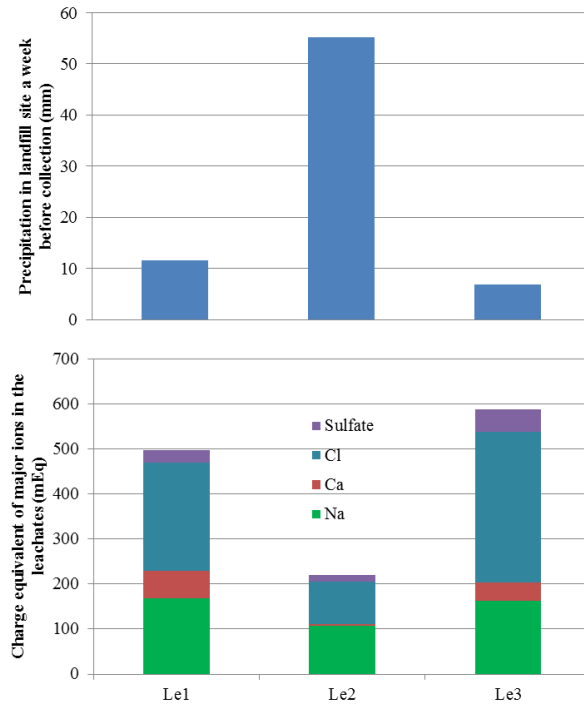


**Figure S3:** Precipitation a week before sample collection (top graph) and charge equivalent of major ions measured by IC and ICP-OES (bottom graph). The salt concentration in the natural leachate is inversely proportional to the amount of rainfall in the week prior to sampling in each case. Le1, Le2, and Le3 correspond to the 1<sup>st</sup>, 2<sup>nd</sup>, and 3<sup>rd</sup> sampling campaigns.

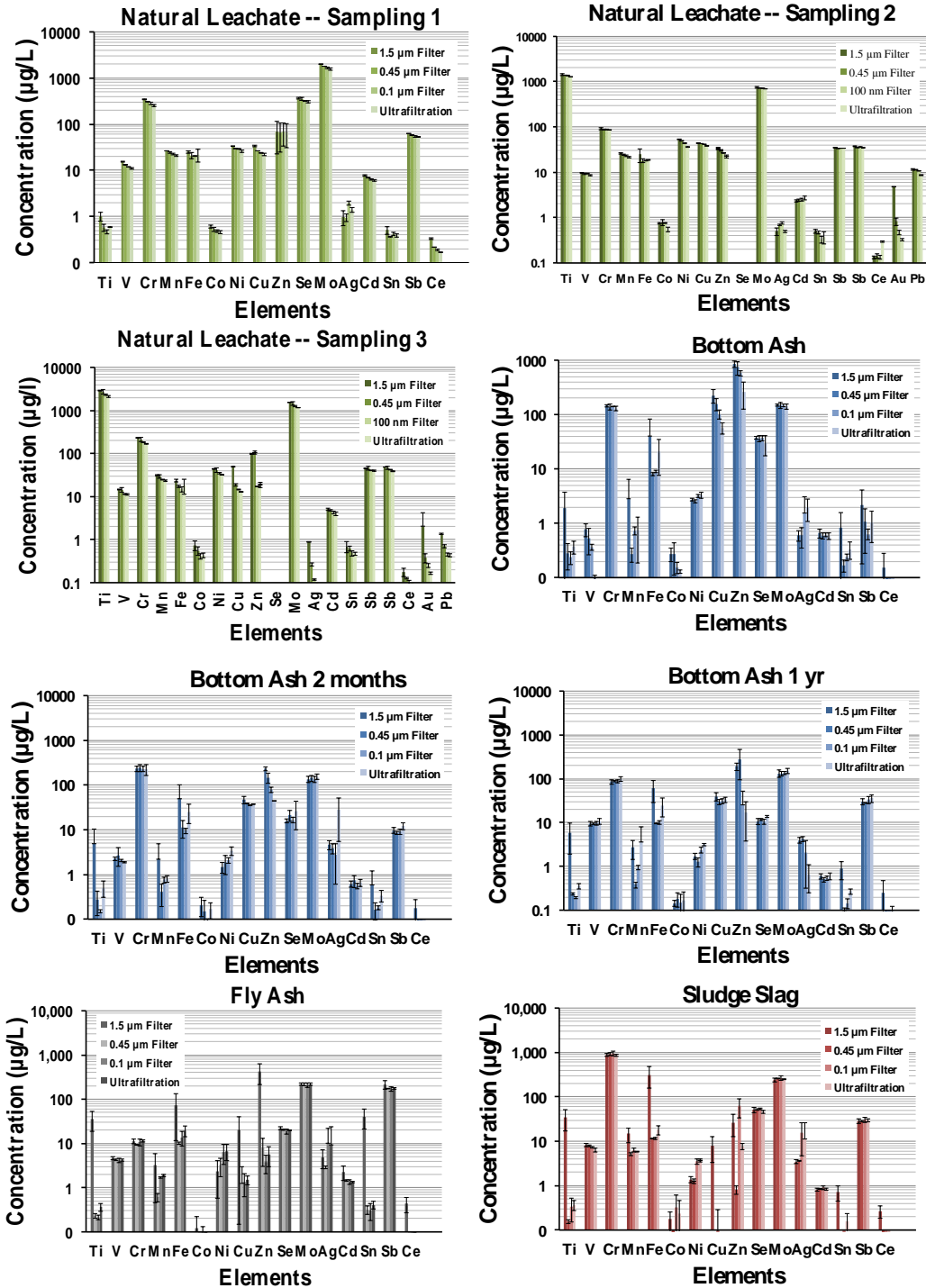


**Figure S4:** Full ICP-MS elemental analysis of the leachates in serial filtration studies. Average of triplicate leachates shown with standard deviation between replicates. Ultrafiltration depicts the analysis of metal < 10 kDa. Please note the logarithmic scale of the graphs.



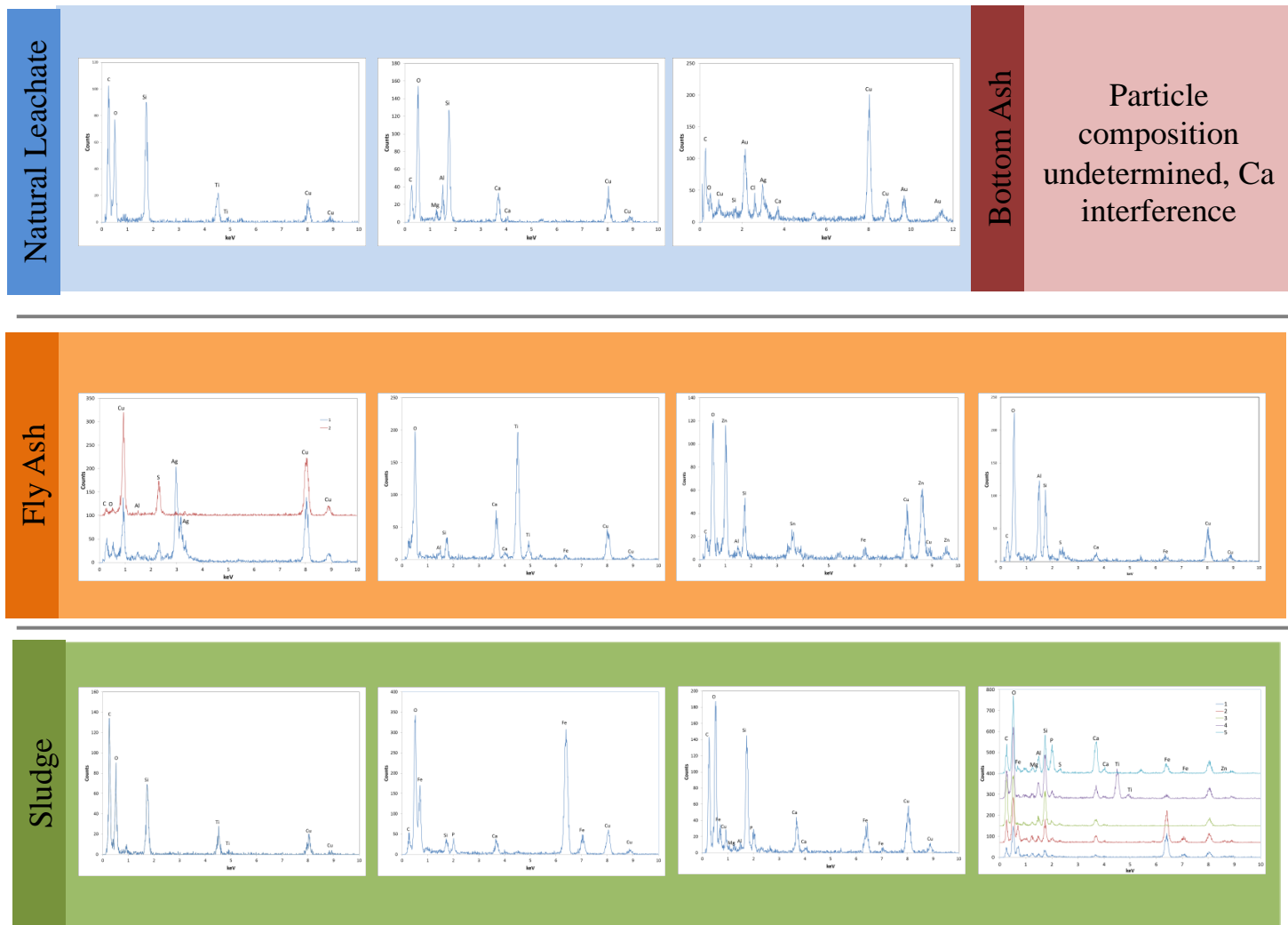
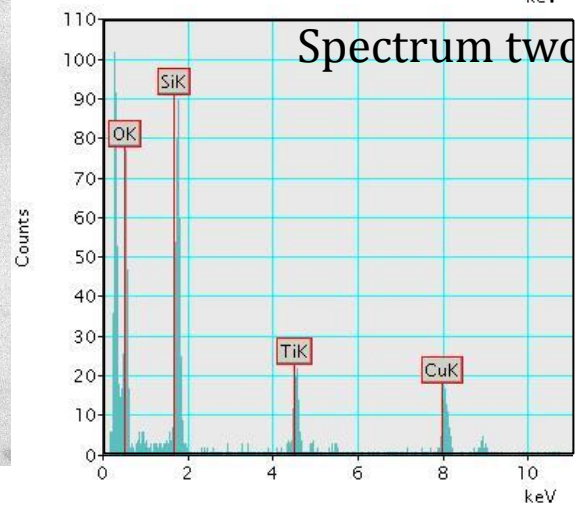
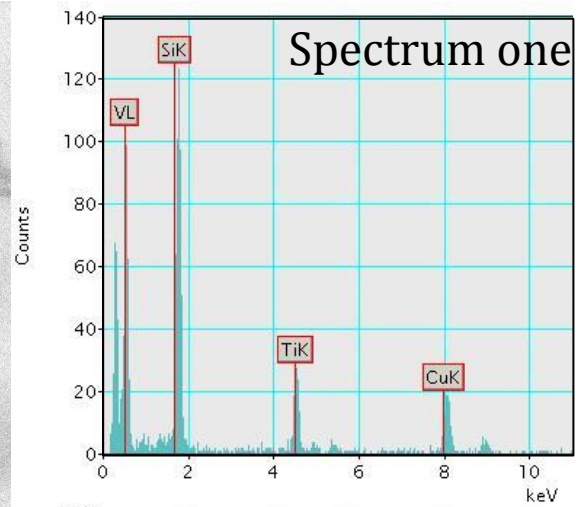
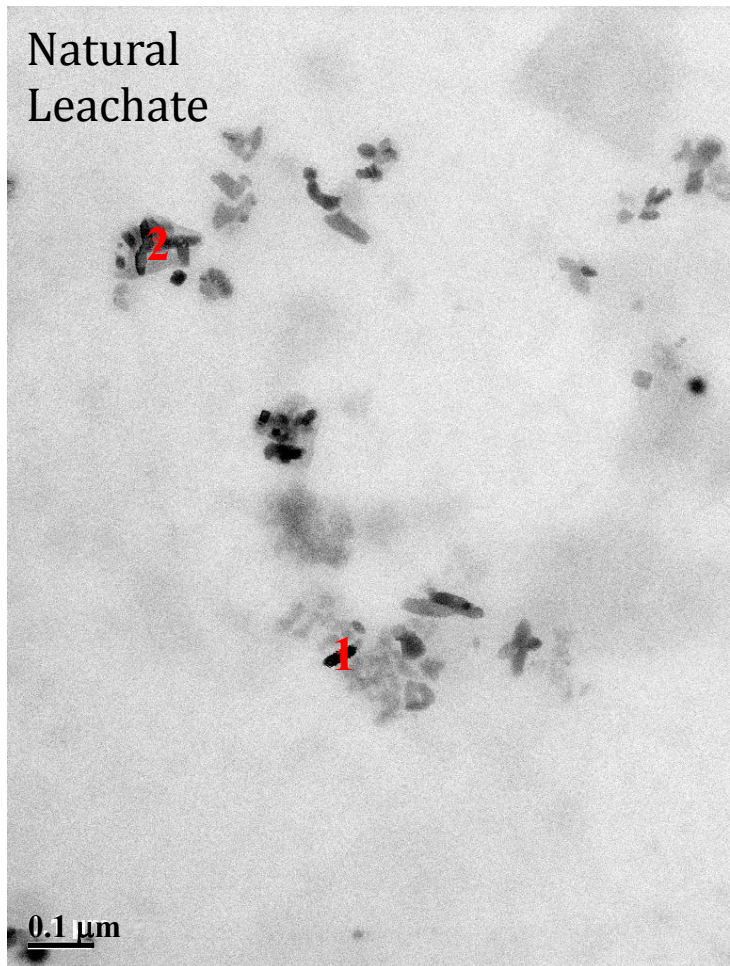
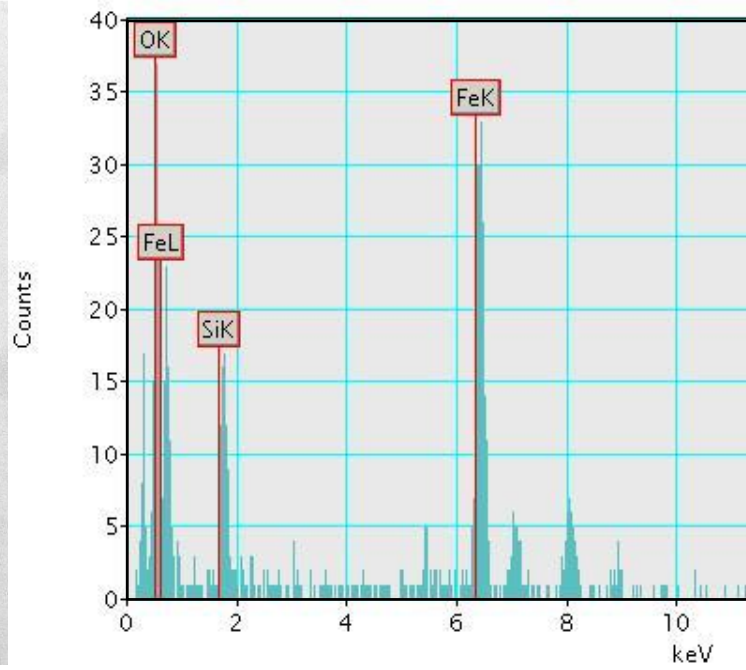
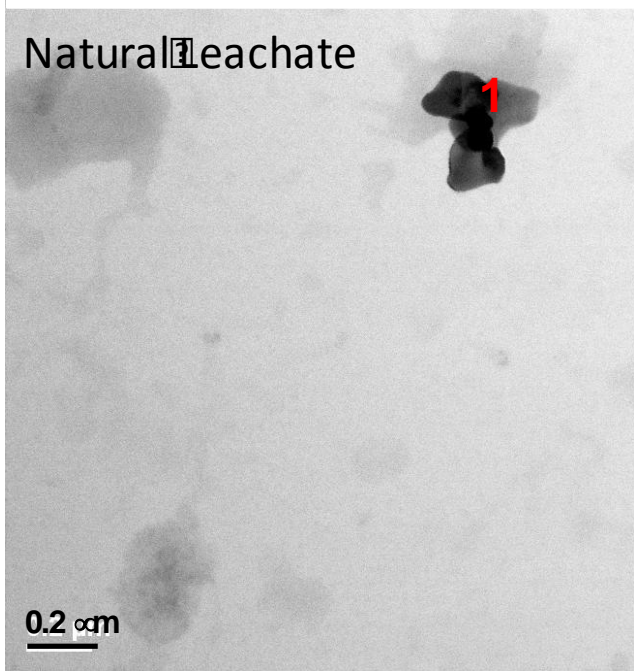
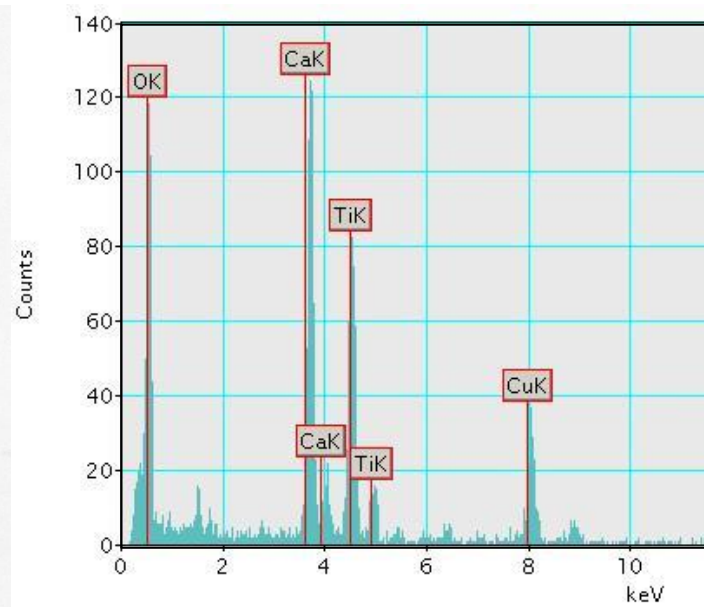
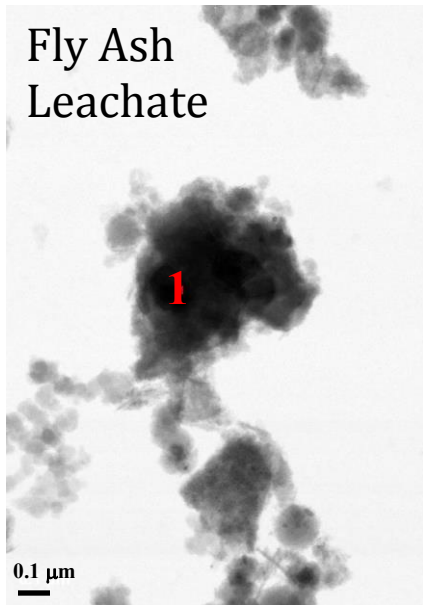


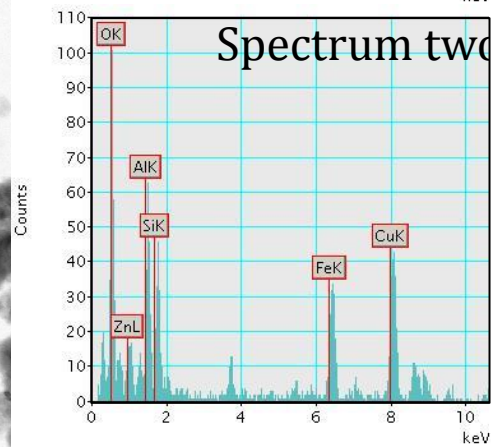
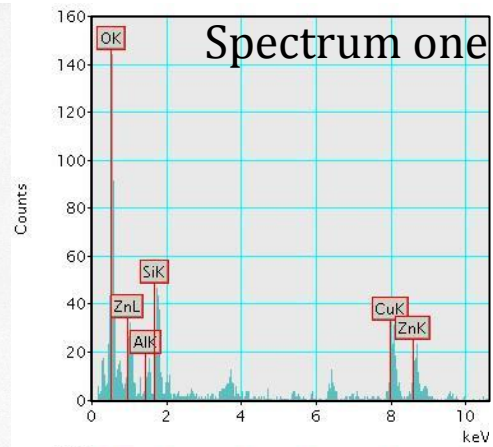
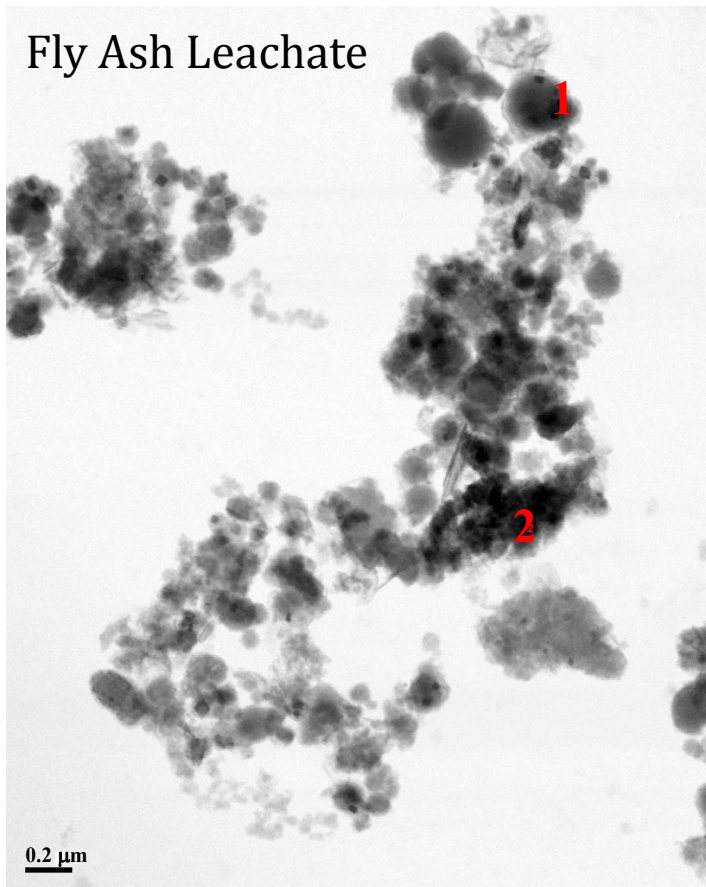
Figure S5: EDX analysis corresponding to TEM images presented in Figure 5 of the main manuscript

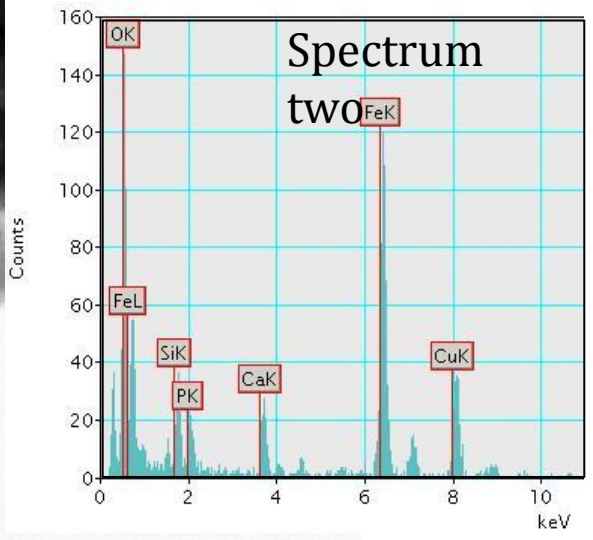
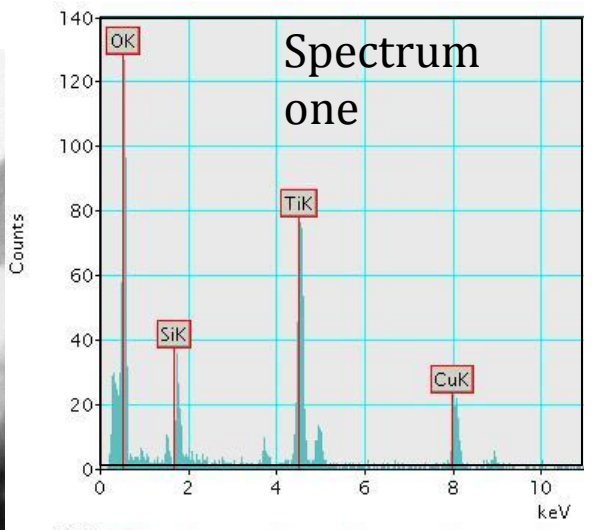
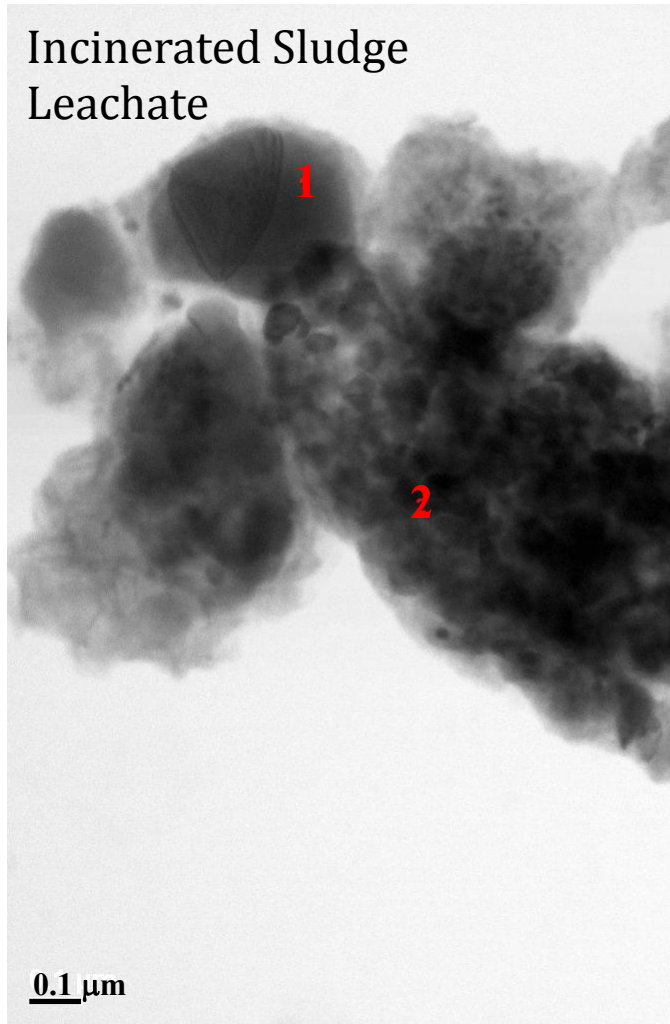












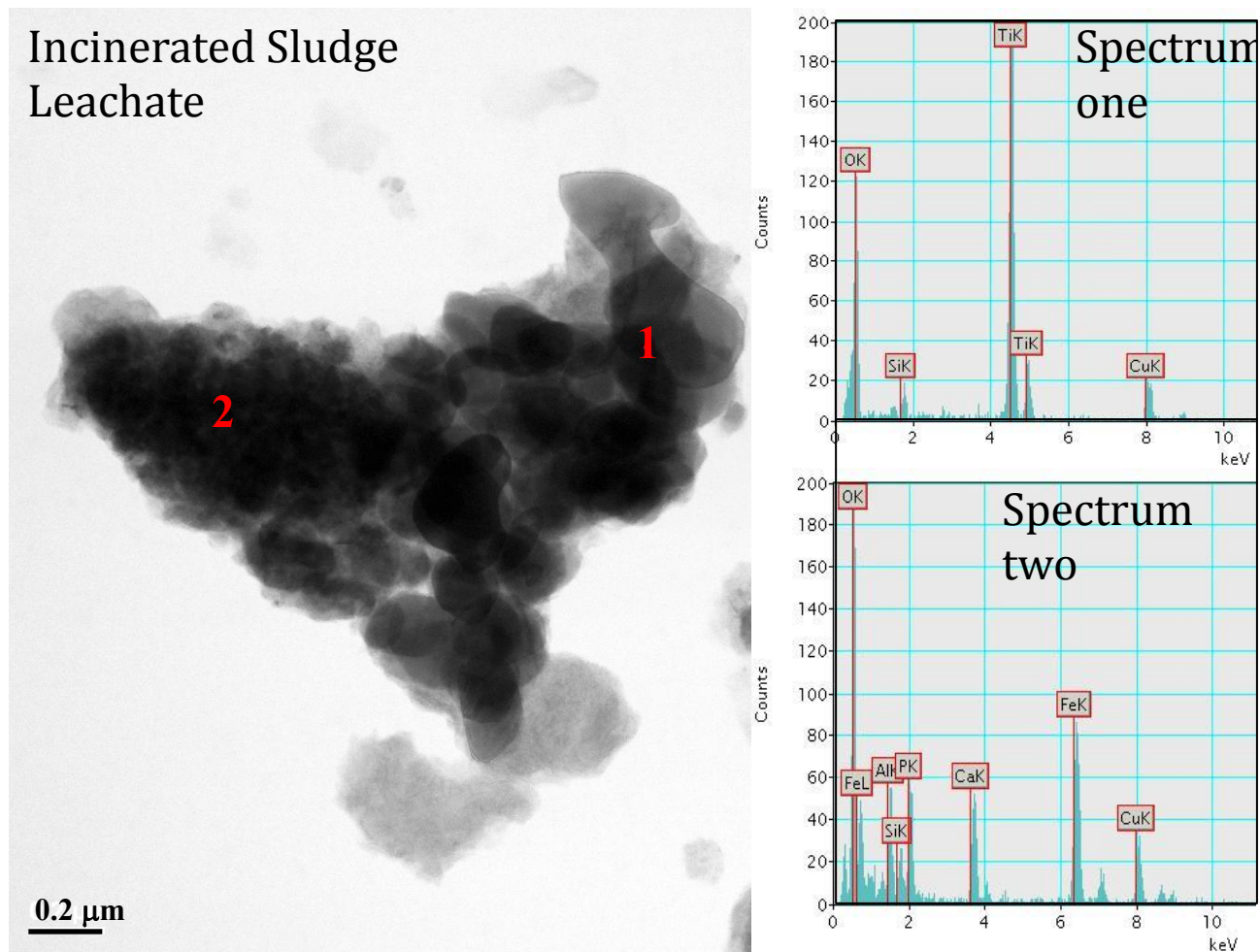
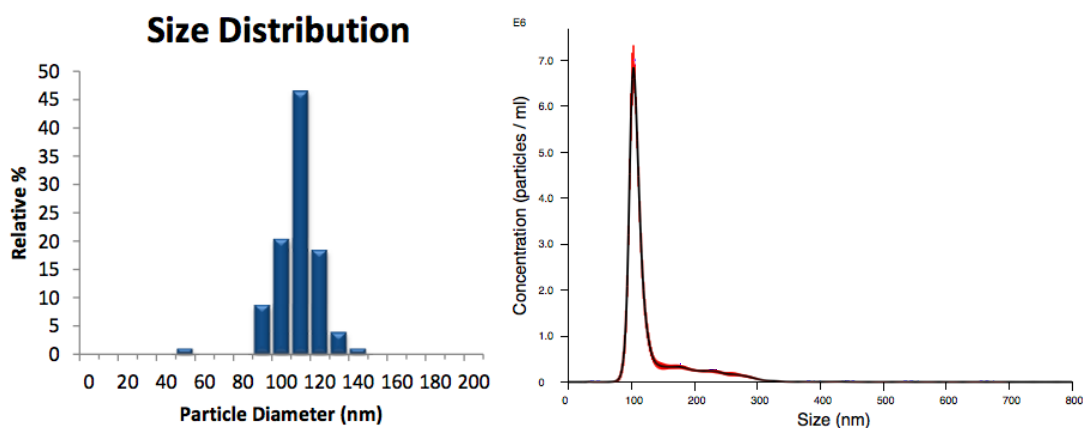


Figure SIU6: TEM images of particles observed in the natural and laboratory prepared leachates of MSWI bottom ash, MSWI fly ash and wastewater sludge incineration bottom ash. EDX analysis corresponding to TEM images is shown on the right.

## Appendix 2

### Supplemental Information: Improvements in Nanoparticle Tracking Analysis to Measure Particle Aggregation and Mass Distribution: A Case Study on Engineered Nanomaterial Stability in Incineration Landfill Leachates



**Figure S1:** 100 nm Au particle size distribution provided by the manufacturer from TEM images (left image) and by in house characterization of particles in DI H<sub>2</sub>O using the NTA (right image) .

**Table S1:** Major water chemistry parameters for MSWI landfill leachate collected in Flawil, Switzerland (i.e. natural leachate) and laboratory prepared synthetic leachate.

|                               | Natural leachate (pH 8.5) |       | Synthetic leachate (pH 7) |       |
|-------------------------------|---------------------------|-------|---------------------------|-------|
|                               | mg/L                      | mEq/L | mg/L                      | mEq/L |
| Na <sup>+</sup>               | 3750                      | 163   | 4324                      | 188   |
| Ca <sup>2+</sup>              | 815                       | 41    | 1203                      | 60    |
| Cl <sup>-</sup>               | 11900                     | 335   | 7810                      | 220   |
| SO <sub>4</sub> <sup>2-</sup> | 2370                      | 49    | 1344                      | 28    |
| DOC                           | 19                        | ----  | ----                      | ----  |

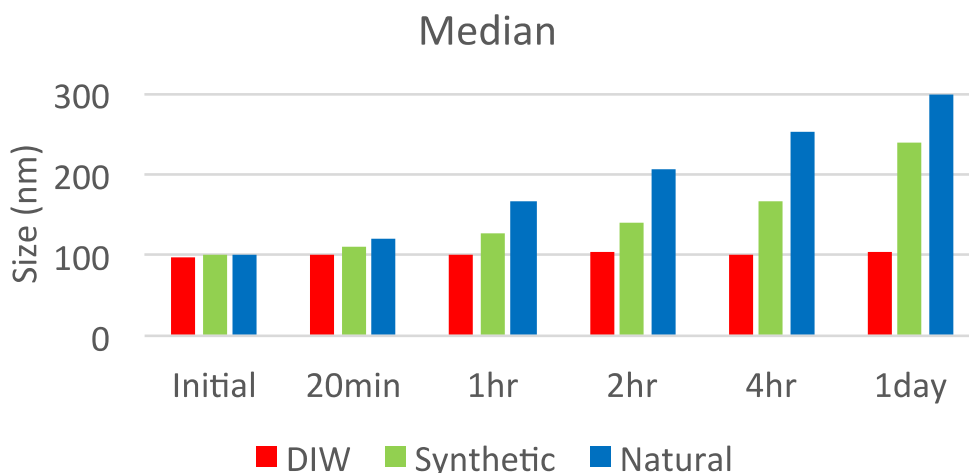


**Figure S2:** Median size measured by NTA in each solution and at each time point.

**Table S2:** Median size measured by NTA in each solution and at each time point.

|           |        | Initial | 20min | 1hr | 2hr | 4hr | 1day |
|-----------|--------|---------|-------|-----|-----|-----|------|
| DIW       | 5%     | 79      | 83    | 81  | 83  | 83  | 85   |
|           | Q1     | 89      | 91    | 91  | 93  | 93  | 95   |
|           | Median | 97      | 99    | 101 | 103 | 101 | 105  |
|           | Q3     | 105     | 113   | 117 | 119 | 115 | 117  |
|           | 95%    | 141     | 179   | 191 | 185 | 189 | 191  |
| Natural   | 5%     | 81      | 91    | 99  | 107 | 129 | 143  |
|           | Q1     | 93      | 107   | 131 | 147 | 187 | 213  |
|           | Median | 101     | 121   | 167 | 205 | 253 | 299  |
|           | Q3     | 117     | 165   | 225 | 279 | 347 | 359  |
|           | 95%    | 177     | 251   | 331 | 373 | 455 | 459  |
| Synthetic | 5%     | 85      | 87    | 97  | 91  | 93  | 97   |
|           | Q1     | 93      | 101   | 113 | 109 | 123 | 131  |
|           | Median | 101     | 111   | 127 | 139 | 165 | 239  |
|           | Q3     | 111     | 129   | 159 | 175 | 227 | 287  |
|           | 95%    | 141     | 177   | 213 | 233 | 321 | 343  |

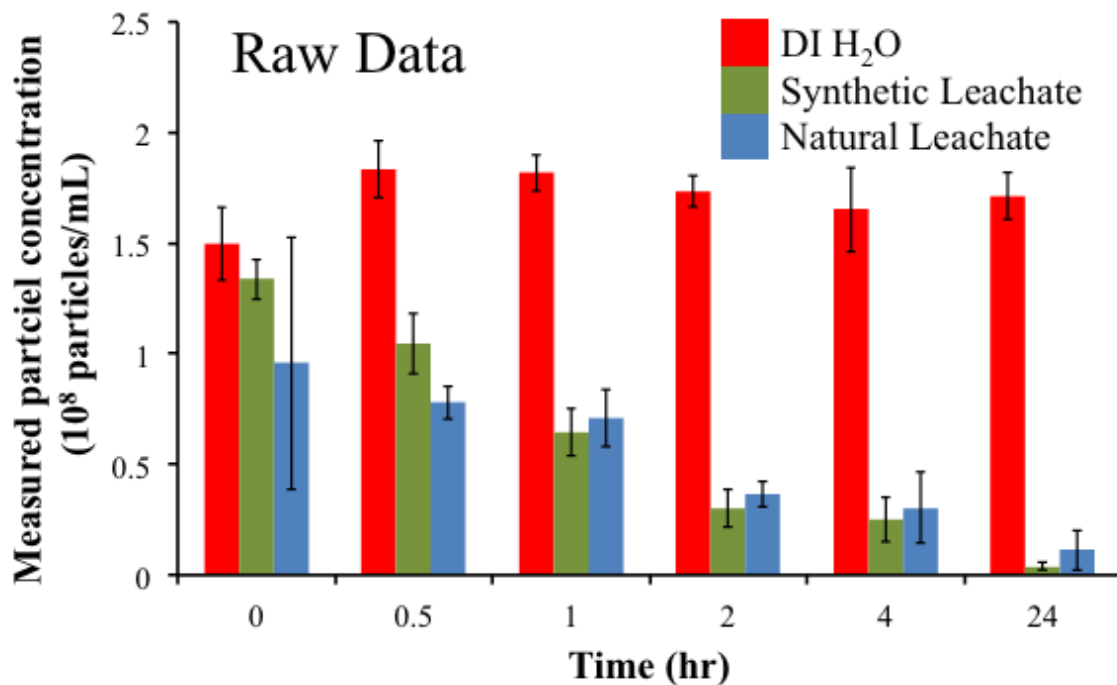


**Figure S3:** NanoSight measured particle number concentration of 100 nm Au particles over time in DI H<sub>2</sub>O (red bars), synthetic leachate (green bars) and natural landfill leachate (blue bars). Raw depicts the raw data as obtained directly from the NTA instrument and is the complement to Figure 4 in the main text which shows the same data after scaling the values based on calibrating the NTA instrument.



## Appendix 3

### Supplemental Information: Agglomeration potential of TiO<sub>2</sub> in synthetic leachates made from the fly ash of different incinerated wastes

#### **Supplemental Information**

- S1: TEM image of the TiO<sub>2</sub> powder
- S2: Overview of dry fly ash properties
- S3: representativeness of the leachates (MOD)
- S4: SEM-EDX images
- S5: Analysis of the elemental compositions of the leachates

**S1. TEM image of the TiO<sub>2</sub> powder**

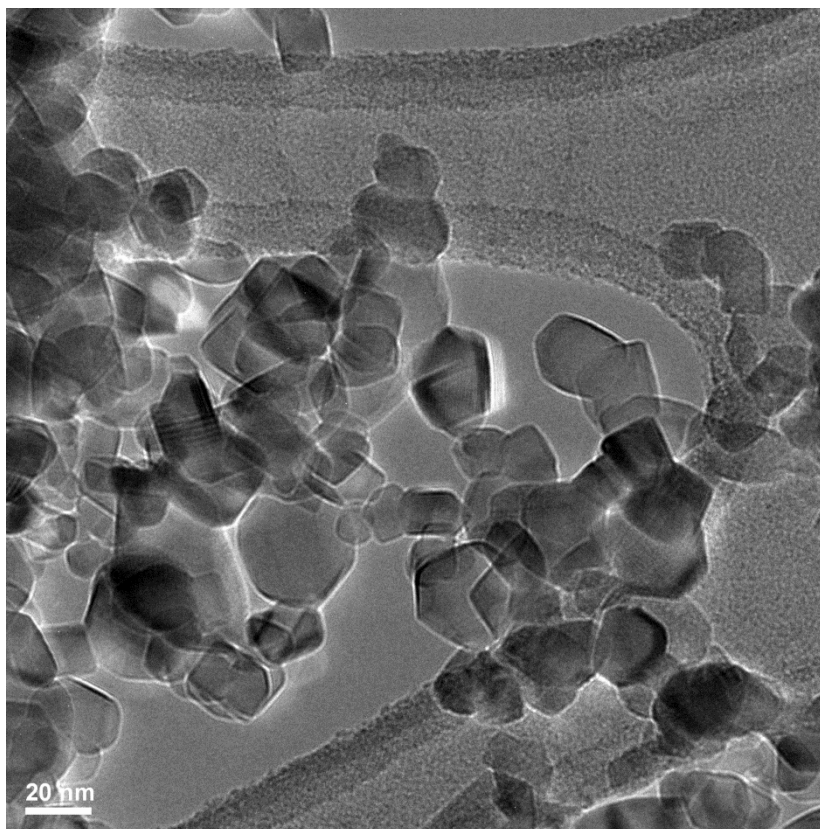


Figure S1. *TEM image of the TiO<sub>2</sub> powder*

## S2. Overview of dry fly ash properties

**Table S1.** *Overview of dry fly ash properties collected from waste incineration plants in Switzerland with the input materials including waste and sludge mixture (WaS), waste (Wa) and wood (Wo).*

| Sample Name | Incinerated Material | Intrinsic density<br>(g/cm <sup>3</sup> ) | Apparent density<br>(g/cm <sup>3</sup> ) |
|-------------|----------------------|---|--|
| WaS         | Waste & Sludge       | 2.75                                      | 0.31                                     |
| Wa          | Waste                | 2.78                                      | 0.29                                     |
| Wo          | Wood                 | 2.80                                      | 0.25                                     |

The intrinsic density is based on the mass and the true volume of the ashes with the pores excluded and the apparent density bases on the powder volume including the voids. More details about the physical and chemical characteristics of the fly ash samples can be found in (Buha et al ., 2014).

**S3: representativeness of the leachates (MOD)**

To test the representativeness of (MOD), three individual samples were prepared by the same method for each type of the fly ash. The pH and conductivity of every individual sample were shown below. The generally constant values indicated the meaningful representativeness and the reproducibility of the leaching procedures.

**Table S2.** *pH and conductivity of three replicated samples of leachates (MOD)*

|          | pH   |      |      | Conductivity( $\mu\text{S}/\text{cm}$ ) |      |      |
|----------|------|------|------|---|------|------|
|          | 1st  | 2nd  | 3rd  | 1st                                     | 2nd  | 3rd  |
| WaS(MOD) | 7.2  | 6.7  | 7.3  | 1251                                    | 1180 | 1353 |
| Wa(MOD)  | 9.9  | 9.9  | 8.9  | 990                                     | 958  | 1018 |
| Wo(MOD)  | 11.2 | 11.1 | 11.2 | 1016                                    | 922  | 942  |

#### S4: SEM-EDX images

Samples for SEM-EDX were created by depositing a few droplets of the leachate onto a silicon wafer, then evaporation of water by resting in oven at 70 °C. Based on the sample preparation procedures, the tested particles by SEM-EDX contained both the natural particles remaining in the leachates after filtration and the particles formed by the originally dissolved components during the drying procedure.

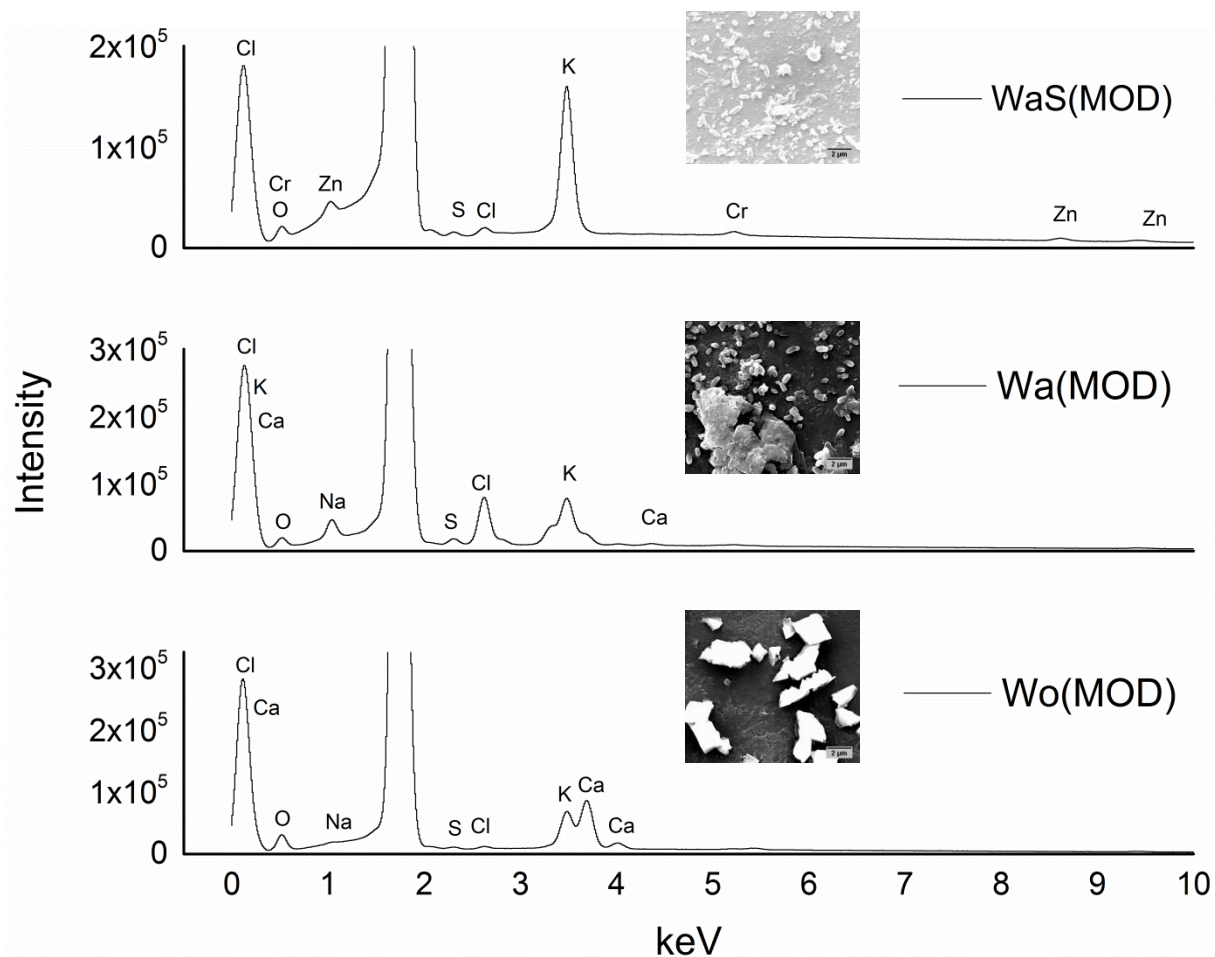


**Figure S2.** Results of SEM-EDX for particles in fly ash leachates (MOD). Note that the peaks of Si and Pt between 1 keV and 2 keV were cut off as they were the main elements from the sample holder and coating agent, respectively.

## S5: Analysis of the elemental compositions of the leachates

The metal compositions in the leachates of the fly ash are significantly different from those in the corresponding dry fly ash. From the study of Buha et al, Al, Ca, Na, Pb, S, Zn are all detectable in dry fly ashes used to make the synthetic leachates<sup>1</sup>, whereas the major metallic elements in the (N) and (MOD) leachates are Na and Ca. Al was detected in Wa(MOD) and Wo(MOD) even though the concentrations are much less than those of Na and Ca. However, Al did not exist in leachate Wo(N). This is possibly due to the high pH value of Wo(N) resulting in the formation of precipitates such as Al(OH)<sub>3</sub>. The main anions detected in (N) and (MOD) are Cl<sup>-</sup> and SO<sub>4</sub><sup>2-</sup>. A small amount of Br<sup>-</sup> is detected in all leachates tested. The result is generally consistent with previous studies where Cl<sup>-</sup>, SO<sub>4</sub><sup>2-</sup>, and HCO<sub>3</sub><sup>-</sup> are the dominant anions in landfill leachates (Kjeldsen et al., 2002). The charge balance is calculated based on the results shown in Table 1, the ratios of positive to negative charges for the leachates are generally between 0.6 and 0.8. The biases of charge balance are possibly due to the existence of NH<sub>4</sub><sup>+</sup> in the leachates which was not measured in the experiments. Consistent with the ICP-OES and IC results, the SEM-EDX results shown in Figure S2 also gave an overview of the major elements in the leachates WaS(MOD), Wa(MOD) and Wo(MOD). Different from the natural landfill leachate which always contained different compositions of heavy metals such as Fe, Mn and Pb (Baun et al., 2004), only Zn was detected in the fly ash leachates. Compared with the elemental composition of the dry fly ash (Buha et al., 2014), the heavy metals in the dry fly ash such as Fe and Pb are removed by filtration due to the formation of large particles and not detected in the leachates. Zn was the most concentrated metal in the dry fly ash of WaS (Buha et al., 2014), but in the corresponding filtrate WaS(N) and WaS(MOD), the concentration of Zn was only half of Na (the metallic element with highest concentration in the obtained leachates), indicating that most of the Zn were insoluble and forming the large particles removed by filtration. Elements such as Na, K, and Cl are detected in the synthetic leachates revealing that they exist in water as free ions or form residue particles which can pass the sequential filtration.

### References

Buha, J.; Mueller, N.; Nowack, B.; Ulrich, A.; Losert, S.; Wang, J., Physical and chemical characterization of fly ashes from Swiss waste incineration plants and determination of the ash fraction in the nanometer range. *Environmental science & technology* 2014, 48, (9), 4765-73.

Baun, D. L.; Christensen, T. H., Speciation of heavy metals in landfill leachate: a review. *Waste management & research* 2004, 22, (1), 3-23.

Kjeldsen, P.; Barlaz, M. A.; Rooker, A. P.; Baun, A.; Ledin, A.; Christensen, T. H., Present and long-term composition of MSW landfill leachate: a review. *Critical reviews in environmental science and technology* 2002, 32, (4), 297-336.